The Milky Way, Coming into Focus: Precision Astrometry Probes its Evolution and its Dark Matter

Susan Gardner[1], Samuel D. McDermott[2], and Brian Yanny[2]

[1]Department of Physics and Astronomy, University of Kentucky,
Lexington, KY 40506-0055, USA
[2]Fermi National Accelerator Laboratory,
Batavia, IL 60510, USA

September 17, 2021

Abstract

The growing trove of precision astrometric observations from the *Gaia* space telescope and other surveys is revealing the structure and dynamics of the Milky Way in ever more exquisite detail. We summarize the current status of our understanding of the structure and the characteristics of the Milky Way, and we review the emerging picture: the Milky Way is evolving through interactions with the massive satellite galaxies that stud its volume, with evidence pointing to a cataclysmic past. It is also woven with stellar streams, and observations of streams, satellites, and field stars offer new constraints on its dark matter, both on its spatial distribution and its fundamental nature. The recent years have brought much focus to the study of dwarf galaxies found within our Galaxy's halo and their internal matter distributions. In this review, we focus on the predictions of the cold dark matter paradigm at small mass scales through precision astrometric measurements, and we summarize the modern consensus on the extent to which small-scale probes are consistent with this paradigm. We note the discovery prospects of these studies, and also how they intertwine with probes of the dynamics and evolution of the Milky Way in various and distinct ways.

Contents

1 Introduction

It has long been recognized that detailed observations of our Milky Way (MW) galaxy and its stars could lead to a *near-field* cosmology. This is distinct from far-field studies of the large-scale structure of the Universe [1], which are realized through observations of the cosmic microwave background (CMB) [2, 3] or of the clustering of galaxies [4, 5]. Although small-scale structure probes can also be made at far field,
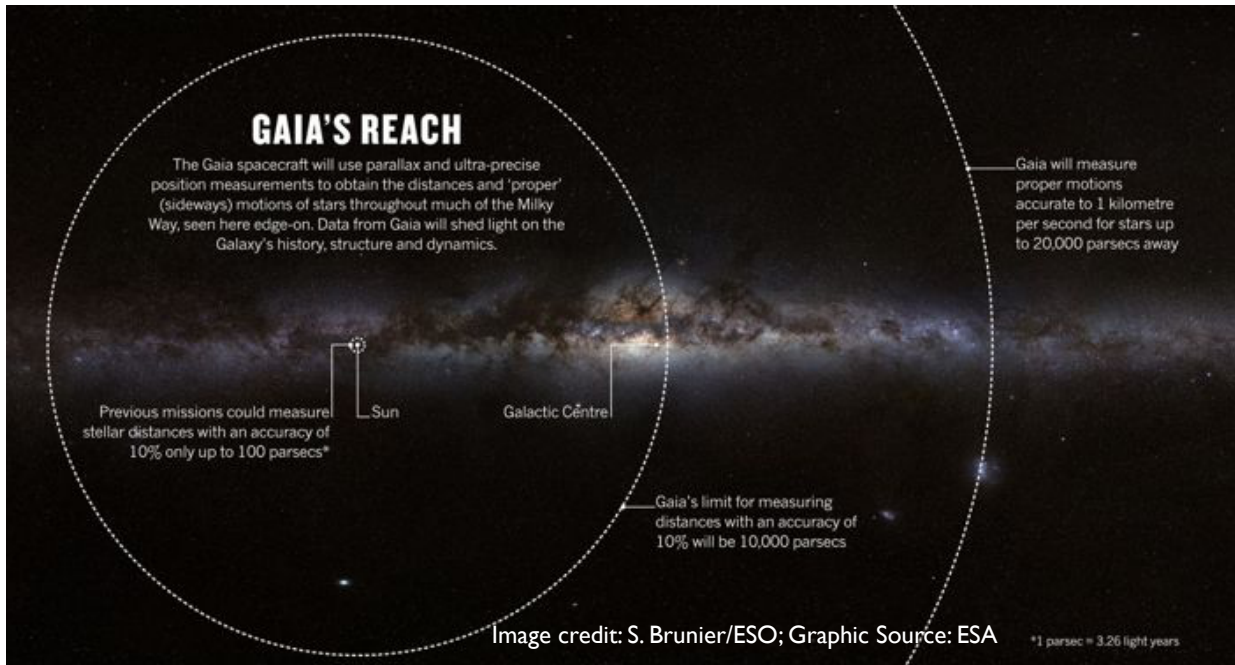
Figure 1: An illustration of *Gaia*'s reach — note that "previous missions" refer to Hipparcos [18]. From [19], reprinted by permission from Springer Nature.

through, e.g., gravitational lensing [6, 7] or from the imprint of neutral hydrogen in the intergalactic medium on the spectra of distant quasars [8, 9], in this review we focus on the small-scale tests possible in the nearest of fields: the MW itself. Studies within the MW offer probes of dark matter with a precision not currently possible through any other means. In contrast, all terrestrial experiments in particle, nuclear, or atomic physics that search for dark matter (DM) require that the DM particles have non-gravitational interactions with the particles of the Standard Model (SM). This may change — advances in sensing beyond the quantum limit [10], stimulated by the sensitivity needs of the LIGO gravitational wave detector [11], have spurred other DM studies [12, 13, 14, 15] — and gravitational detection of a DM candidate may yet be realized [14]. Nevertheless, the unique precision with which we are able to probe the structure and dynamics of our own galaxy extends our ability to hunt for DM beyond the reach of terrestrial experiments. In this review we consider how sharpening observations of MW stars drive new and reinvigorate old investigations of the Galaxy, to probe its structure and evolution, including all of its DM and its own matter distribution and the fundamental properties of its constitutive elements. Probes of MW structure are hence probes of the nature of dark matter. This follows a long tradition: all of the positive evidence for DM thus far comes from astronomical observations within and beyond our own Galaxy [16, 17].

All of this has been made possible through the rise of large-scale astronomical surveys over the last decades, beginning with the Sloan Digital Sky Survey (SDSS) [20], and continuing with 2MASS [21], Pan-Starrs1 [22], and DES [23]. The sensitivity and reach of these studies have been greatly enhanced through the advent of data releases from the *Gaia* space telescope [24, 25, 26]. We show an estimated footprint of the *Gaia* data in Fig. 1. The *Gaia* mission enormously extends the reach and precision of the astrometry from the Hipparcos mission of the early 1990's. *Gaia* data account for the parallaxes of more than 1.3 billion objects[1] within 10 kpc in *Gaia* Data Release 2 (DR2) [27, 25]. This is roughly 1% of the MW's stars, and this trove greatly expands on our knowledge of the MW compared to the parallaxes for

---

[1]More precisely, the *Gaia* data enable a 5-parameter astrometric solution corresponding to the sky location, parallax and proper motions of each object.
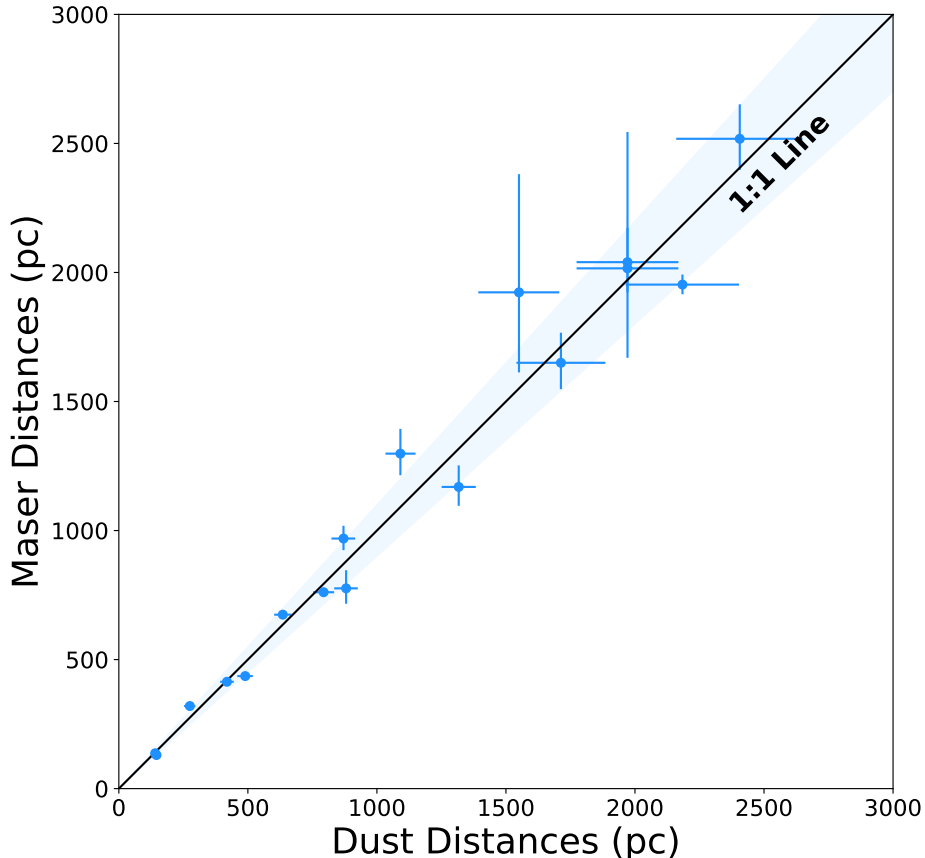
Figure 2: Two methods of assessing distances to nearby dust clumps compared: one method uses VLBI parallaxes, mainly to masers, and the other employs *Gaia* DR2 data. The distance assessments for the two methods agree within $\leq 10\%$ for distances ranging from 100 pc to 2.5 kpc with a negligible offset. From [30], reproduced with permission ©ESO.

2.5 million objects within 200 pc measured by Hipparcos [18]. Astrometric parallaxes give an enormous improvement in the quality of distance assessments over ground-based surveys, which are largely forced to rely on photometric methods, and the precision of the distance assessments [25], and the completeness of the stellar samples [28], with *Gaia* DR2 are extremely high. It is possible, e.g., to select a data sample of some 14 million stars within 3 kpc of the Sun's location with an average relative parallax error of less than 10% [29]. As a separate example, we compare two distance assessment methods to local dust clouds — one uses *Gaia* parallaxes and the other uses parallaxes of masers measured by the VLBI — and show the result in Fig. 2.

Through these studies our perspective of the MW has shifted: its mass distribution is neither that of an isolated system, nor is it in steady state. These outcomes are at odds with long-standing theoretical assumptions. Although the time scales associated with these changes are long, their impacts are appreciable nonetheless, giving us the opportunity to study the MW as it responds to external forces, and yielding new probes of its particle dark matter. To set the stage for later discussions, we open in Sec. 2 with a perspective on the theoretical framework for the matter distribution in our Galaxy prior to these discoveries. We review the distribution function formalism for both visible and dark matter, noting the so-called standard halo model (SHM) [31] employed in dark matter direct detection experiments and observational evidence for its limitations, before turning to recap the cold dark matter (CDM) paradigm, noting its long-standing small scale problems [32, 33, 17] and limited relaxation mechanisms.

We then turn, in Sec. 3, to a brief summary of the gross features of the MW as they are known thus far. We provide current best values of the MW mass, size and shape; and we list important components of the MW, survey its known rotation curve, and provide insights into the environment in which it is situated. We refer the interested reader to earlier, extensive reviews [1, 34] for extended discussion of earlier results and historical context.

Beginning in Sec. 4 we turn to smaller scale features of the MW. We describe the Magellanic clouds, satellite galaxies, stellar streams, and patterns in MW stars and how they probe the structure of the MW. The purpose of Sec. 4 is to give a current inventory of the constituent parts of the MW, and to describe how to harness their unique characters to extract information about the nature of the MW halo. In Sec. 5 we describe how, and in what manner, such systems constrain DM particle properties. We start this section with an overview of the implications of the hierarchical nature of the assembly of DM halos for the MW. We use this as an entry point to discuss specific models of dark matter in more detail. We start with dark sectors that are characterized by their kinematics rather than by other microphysical aspects. We then move to a handful of other dark sectors, each of which has a qualitatively different galactic-scale phenomenology. Finally in Sec. 6 we look at these same systems for the manner in which they reveal non-isolating and non-steady-state effects. In Sec. 7, we consider how these newly established effects impact the assessment of the local DM density and velocity distribution, important to DM direct detection experiments, and we conclude our review in Sec. 8, offering an assessment of future discovery prospects.

2   Past as Prologue

In this section we note how the theory of the matter distribution in the MW emerges from kinetic theory, along with its commonly employed assumptions, to set the stage for our discussion of recent discoveries and their implications. The one-body density of a system of N particles in six-dimensional phase space is determined by [35]

$$f_1(\mathbf{p}, \mathbf{q}, t) = \left\langle \sum_{i=1}^{N} \delta^{(3)}(\mathbf{p} - \mathbf{p}_i)\delta^{(3)}(\mathbf{q} - \mathbf{q}_i) \right\rangle, \tag{1}$$

where the average is over the full phase space density $\rho(\mathbf{p}_1, \mathbf{p}_2, \ldots, \mathbf{p}_N, \mathbf{q}_1, \mathbf{q}_2, \ldots, \mathbf{q}_N, t)$. Liouville's theorem tells us that the full phase-space density behaves as an incompressible fluid, so that

$$\frac{d\rho}{dt} = \frac{\partial \rho}{\partial t} + \{\rho, \mathcal{H}\} = 0, \tag{2}$$

where the curly brackets denote a Poisson bracket. Upon adopting a Hamiltonian $\mathcal{H}$ with pairwise forces, this yields the Bogoliubov, Born, Green, Kirkwood, and Yvon (BBGKY) hierarchy, relating the time-evolution of the s-body density to the $(s+1)$-body density. If a is the range of the two-body force and $n = N/V$, the BBGKY hierarchy collapses to a equation in f_1 only if either the system is dilute and/or has short-range forces, $na^3 \ll 1$, or it is dense and/or has long-range forces, $na^3 \gg 1$. The former limit yields the Boltzmann equation and can be used to model nuclear heavy-ion collisions [36, 37]. The latter limit, if we let $f_s \propto (f_1)^s$ so that the particles are uncorrelated, yields the Vlasov, or collisionless Boltzmann, equation

$$\left[\frac{\partial}{\partial t} + \frac{\mathbf{p}}{m} \cdot \frac{\partial}{\partial \mathbf{q}} - \frac{\partial \mathcal{U}_{\text{eff}}}{\partial \mathbf{q}} \cdot \frac{\partial}{\partial \mathbf{p}} \right] f_1(\mathbf{p}, \mathbf{q}, t) = 0, \tag{3}$$

where $\mathcal{U}_{\text{eff}}$ is the effective potential, and is apropos to galactic dynamics [38].

In this review we focus on the mass distribution of the MW, considering both its visible and dark matter. We particularly focus on the component of its visible matter in stars, its dominant component

away from the Galactic midplane[2]. To go from $f_1(\mathbf{p}, \mathbf{q}, t)$ for a N particle system in the $na^3 \gg 1$ limit to a description of the Galactic matter distribution requires further assumptions [38]: (i) that the long-range nature of the gravitational forces allows us to segue from a N-particle system to a fluid with some total mass and (ii) that the birth and death of stars have negligible impact. We have already neglected both collisions, which is supported by estimated stellar relaxation times that exceed the age of the Universe, and correlations. Neglecting the finite stellar lifetime also incurs some errors, because the force on a star from neighboring stars is attractive, but this force is far less than that from a distant but much more massive matter distribution, because of the long-range nature of the gravitational force: in a system of uniform mass density the most distant members of an ensemble dominates the gravitational force on any given point [38]. Thus the physics that allows us to replace a collection of stars with a smooth mass distribution also allows us to neglect correlations. With this we replace $f_1(\mathbf{p}, \mathbf{q}, t)$ with the smooth distribution function $f(\mathbf{v}, \mathbf{x}, t)$. Introducing Φ as the gravitational potential per unit mass, the Vlasov equation takes the form [38]

$$\left[\frac{\partial}{\partial t} + \mathbf{v} \cdot \frac{\partial}{\partial \mathbf{x}} - \frac{\partial \Phi}{\partial \mathbf{x}} \cdot \frac{\partial}{\partial \mathbf{v}} \right] f(\mathbf{v}, \mathbf{x}, t) = 0 \,. \tag{4}$$

This is to be solved simultaneously with Poisson's equation, relating the gravitational potential per mass to the mass density:

$$\nabla^2 \Phi = 4\pi G \rho \,, \tag{5}$$

where $\rho(\mathbf{x}, t) = M \int d^3 \mathbf{v} f(\mathbf{v}, \mathbf{x}, t)$ and M is the total mass of the system. Isolated, steady-state systems have distribution functions that correspond to equilibrium solutions of this system of equations. In what follows we develop this connection explicitly.

We emphasize that we have chosen a nonrelativistic normalization such that $f(\mathbf{v}, \mathbf{x}, t)$ has mass dimension 3 in the "natural units" familiar to a high-energy particle physicist. At risk of ambiguity, but following convention, we will use a similar notation for the distribution function after we have projected out the spatial component, such that $f(\mathbf{v}, t) = \int d^3 \mathbf{x} f(\mathbf{v}, \mathbf{x}, t)$ is dimensionless in natural units, or has units $(\text{velocity})^{-3}$ more generally. We show explicit examples of steady-state $f(\mathbf{v})$ in the MW in Sec. 7.

2.1   Mass Distribution of a Static, Isolated Galaxy — and its Symmetries

We expect an isolated system in steady state to be characterized by integrals of motion; we also suppose it to be self-gravitating and of finite mass. An integral of motion I of interest to us is referenced to stellar orbits, so that $I(\mathbf{x}(t), \mathbf{v}(t))$ is constant for a given orbit. We thus focus on *isolating* integrals [38]. As long established, if I is such an integral of motion, it is also a solution of the steady-state Vlasov equation, and indeed — as per Jeans theorem — any steady-state solution of that equation can be expressed in terms of the system's integrals of motion, or functions thereof [39]. The particular integrals that appear depend on the symmetries of the system. Noether's theorem guarantees the existence of a conserved quantity for each continuous symmetry [40]. For example, if $\mathcal{H}$ is time-independent, making it invariant under translations in time, then the system's energy E will be an integral of motion and $f(E)$. Similarly if the system is also spherically symmetric, so that it is invariant under rotations, then the orbital angular momentum $\mathbf{L}$ is also an integral of motion and $f(E, \mathbf{L})$; if it is axially symmetric about the $\hat{z}$-axis, L_z is an integral of motion and $f(E, L_z)$ instead.

There has been much discussion of whether the converse of Noether's theorem could also hold, with explicit counterexamples in well-known textbooks of classical mechanics [41, 42] showing that it does not. These counterexamples concern systems in which invariant quantities exist for which there are

---

[2]At the Galactic midplane, the volume density of the interstellar medium, comprised of atomic and molecular hydrogen, ionized gas, and dust, is thought to exceed that of stars by about 50% [38], but gas and dust are very much localized to the mid-plane region.

no associated continuous symmetries. Our interest here, however, is in integrals of motions that are invariant along stellar orbits. In this case, Noether's theorem and its converse are both guaranteed, where we refer to Theorem 5.58 of Olver [43]. Thus if L_z is an integral of motion, then the associated matter distribution is axially symmetric; also if $\mathbf{L}$ is an integral of motion, then the associated matter distribution is spherically symmetric. Thus a failure of axial symmetry speaks to failure of L_z as an integral of motion [44]. Along related lines, we note that, as an extension of Lichtenstein's theorem [45] in fluid mechanics, an isolated, static, self-gravitating, ergodic[3] stellar systems has been shown to be spherically symmetric [38], though this can also be shown without reference to fluid mechanics, where we refer to [46] for an extended discussion and further references. If the density distribution associated with $f(E)$ is spherical, then $f(E)$ is non-negative as well, as expected on physical grounds, though the Eddington formula for $f(E)$ does not in itself guarantee it [38]. As a further consequence, Noether's theorem says that $\mathbf{L}$ must be an integral of motion as well, yielding $f(E, \mathbf{L})$. Consequently $f(E, \mathbf{L})$ is non-negative as well. Finally, if the distribution function of an isolated, static system is axially symmetric, so that it takes the form $f(E, L_z)$, then it is also reflection or north-south symmetric [46], where we note [47] as well for a slightly less general proof, so that it is symmetric under $z \to 2z_0 - z$ with z_0 the center of the galactic mid-plane. We discuss observational probes of these symmetries and the implications of the pattern of their breaking in Sec. 6.

The modeling of the Galaxy is commonly realized through a superposition of its disk, bulge, bar, and halo components [48, 49], with each component modelled by a distribution function f_i [38] in steady state. Although E is an integral of motion, it is more useful to choose the action integrals J_R, J_ϕ, and J_z as its arguments [50], where R, ϕ, and z are the (in-plane) radial, azimuthal, and vertical coordinates with respect to the plane of the Galactic disk. For reference J_ϕ is the angular momentum about the symmetry axis $\hat{z}$ of an axisymmetric disk. We note that $f(\mathbf{J})$ modeling gives a very good description of the velocity distributions observed by the RAVE survey [51, 52], and we show the comparison of data versus model in Fig. 3. Although we see that $f(\mathbf{J})$ modeling can work very well, it is a Jeans-theorem-based analysis, and it contains all of the underlying assumptions we have noted. We discuss evidence for the breaking of these assumptions, noting the context in which they occur, in Sec. 6.

2.2 The Galactic Dark Matter Halo

A galactic dark matter halo can be described within the distribution function framework we have just detailed. Its distribution function is poorly known, even in our own Galaxy, simply because the only established dark matter interactions are gravitational. Yet the possibility of the direct detection of particle dark matter through its elastic scattering with nuclear targets [53] in highly sensitive, low-background underground experiments [54, 55] has stimulated keen interest in the physics and characteristics of the Galactic data matter halo. Indeed, such information is essential to translating the outcomes of a dark matter direct detection experiment to limits on a dark matter candidate's mass and nuclear cross section [56, 57]. In what follows we consider the particular Galactic inputs needed at the Sun's location, noting that the local effects from dark matter capture on the solar system have been determined to be small [58, 59].

In a typical dark matter direct detection experiment the nuclear recoil energy E and possibly its direction $\mathbf{\Omega}$, in some coordinate system, would be detected. This is possible if the candidate particle's mass is in the range of roughly 10-100 GeV, as expected for the long popular weakly-interacting massive particle, or WIMP, dark matter candidate [60]. More recently, the idea of measuring electronic recoils to probe dark matter candidates in the sub-GeV mass range [61, 62, 63, 64, 65, 66, 67, 68, 69, 70, 71, 72, 73] in scattering experiments has been developed; the interpretation of such experiments also requires astrophysical information on dark matter [74]. In what follows we focus on dark matter-nuclear

---

[3]An ergodic distribution function $f(E)$ uniformly samples its energy surface in phase space [38].
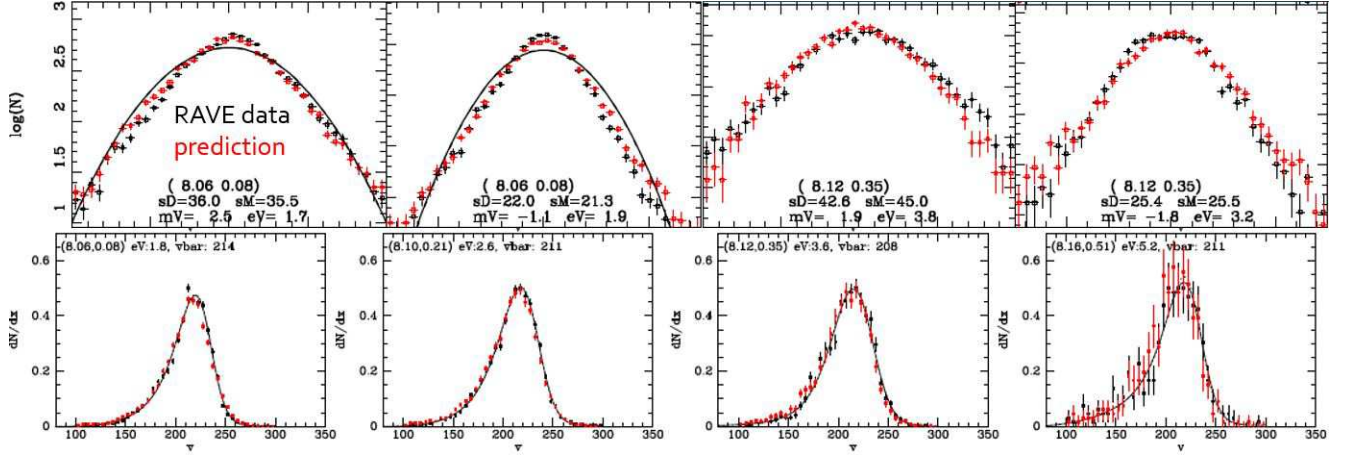
Figure 3: Comparisons of the velocity distributions from $f(\mathbf{J})$ modeling fitted to data from the CGS survey (red points) with those of red dwarfs from the RAVE survey (black points). The top row shows velocity components V_R, V_z near the Sun's location and the Galactic mid-plane (left two panels) and at $|z| \sim 0.35\,\text{kpc}$. The lower row shows V_ϕ distributions at increasing heights from the plane, from left to right, with the furthest bin centered on $0.51\,\text{kpc}$. From [52].

interactions, though our considerations largely generalize to the case of electronic recoils as well — we refer to [75] for a discussion of new features resulting from atomic excitations. We also note [76] for a review of nuclear and hadron physics issues in the evaluation of the cross section for dark-matter-nuclear scattering and to [77] for a review of how these experiments, taken en masse, constrain dark matter models. We also note [78] for a discussion of astrophysical issues pertinent to the interpretation of an annual modulation signal.

If the scattering of dark matter and nuclear target were simply elastic, as usually assumed, then information on the local dark matter density and velocity distribution would suffice to interpret the results [57]. In particular, an integral over the *lab frame* dark-matter velocity distribution $f_{\text{lab}}(\mathbf{v}, t)$ involving

$$v_{\min} = \left(\frac{E M_A}{2\mu_{\chi A}^2} \right)^{1/2} \tag{6}$$

would be required, where M_A and $\mu_{\chi A}$ are the nuclear and reduced masses, respectively; and the integral is computed up to the escape velocity. Potentially, too, the directional information such an experiment can provide is not only a sensitive discriminant of dark matter models [79], but it can also yield constraints on the dark matter velocity distribution [80]. In the event that the recoil direction is not detected, the integral is simply some function of $v_{\min}$, but it is also time dependent, because the Earth's velocity with respect to the Galactic rest frame is time dependent. This last velocity is relatively well-known, and, assuming that the local standard of rest coincides with the rotational standard of rest, it is fixed by the vector sum of the local circular speed, the peculiar velocity of the Sun with respect to the rest frame of Galactic rotation, and the velocity of the Earth about the Sun. Nevertheless, the underlying dark matter velocity distribution is not well-known, nor is its needed integral, which we term $g(v_{\min}, t)$. We note in passing if the scattering were *inelastic* [81, 82], as possible if the particle were composite [83, 84, 85, 86], though this is not required, then the nuclear response to the dark matter probe is also involved [87, 88], complicating the connection between the experimental outcomes,

the dark matter astrophysical inputs, and the desired dark matter constraints. The use of effective field theory for dark matter-nuclear scattering shows that additional currents could also mediate the effect [89, 87, 88], impacting the determination of DM parameters [90].

There has been much discussion of strategies to eliminate the ill-known function $g(v_{\min})$, given studies with different nuclear targets and an assumption of elastic scattering [91], or simply of how a combined analysis could be made [92], though the former appears to require that a signal is observed in one nuclear target first [91].

Given these uncertainties, all direct detection experiments assume the SHM [31] in order to put their results on the same footing. Thus the assumed distribution function is in steady-state and is that of an isotropic, isothermal sphere, so that its velocity distribution is of Maxwell-Boltzmann form[4]

$$f(v) \propto \exp\left(-\frac{v^2}{\sigma_v^2}\right). \tag{7}$$

If the DM density has a radial profile $\rho(r) \propto 1/r^2$, then the circular speed of the DM has a radial dependence $v_c \sim 1/\sqrt{r}$[38]. Extensive evidence now exists to suggest that the SHM is not realistic on several counts. Chief among the ways that the DM halo is believed to depart from isotropy and isothermality are that: (i) its shape is not spherical; (ii) its velocity-distribution is somewhat modified by these shape effects, and its high velocity tail, pertinent to searches for lighter mass WIMP candidates, may be modified by Galactic evolution, such as debris flow effects [94, 95]; (iii) its mass distribution, particularly in smaller mass halos, is a matter of debate; and (iv) the Galaxy itself is not in steady state. We address the first two points briefly here, consider point (iii) in the next section, and reserve that of (iv) and its broader consequences to Sec. 6. We delve into the implications of these refinements for the local dark matter density and velocity distribution in Sec. 7.

Fully accounting for all of these noted effects would take us beyond the framework we have outlined in Sec. 2.1, though it is worth emphasizing that the SHM can already be probed and refined within its scope in a data-driven way. It has, after all, a number of simplifying assumptions. We refer to Green [57] for an extended discussion. For example, if spherical symmetry is assumed, the structure of the dark halo can be determined from the stars alone [96], in that the circular speed with Galactocentric radius r inferred from the effective Galactic potential, reconstructed from astrometric measurements of stars with *Gaia* DR2 data, is compatible with the circular speed directly measured with Cepheids [97].

We now turn to a discussion of the points we have outlined. The shape of the Galactic halo is not well-known, but it can be constrained though observations of stars and/or HI gas [98]. There is considerable evidence, of long standing, for distortions in the Galactic disk, as it is both warped and flared in HI gas [99, 100] and in stars [101, 102]. Striking evidence for the latter has emerged recently from three-dimensional maps of samples of 1339 and 2431 Cepheids, respectively [103, 104]. Galactic warps have been thought to have a dynamical origin, appearing and disappearing on time scales short compared to the age of the universe, due to interactions with the halo and its satellites [105, 106], though it has also been suggested that the warp in HI gas is due to the presence of the Large Magellanic Cloud (LMC) [107]. We refer to Sec. 3.2 for further discussion of the current status and to Sec. 6 for a broader discussion of non-steady-state effects in the MW and its origins.

The velocity ellipsoid [108] and DM distribution [109] are not spherical either, with the evidence favoring a prolate matter distribution. Studies of flaring HI gas in the outer galaxy also support a prolate DM distribution [110]; these authors note that a prolate halo can support long-lived warps [111], which would help to explain why they are commonly seen [110]. It has also been suggested that some of these features could arise from a dynamically active disk [112] in isolation.

The Galactic velocity distribution can also be impacted by the tidal disruption of dark matter

---

[4]In a galaxy, a velocity distribution may be of Maxwell-Boltzmann form, but this does *not* imply that equipartition (or the usual results of equilibrium statistical mechanics) apply [93].

subhaloes[5], and the resulting debris flow can also impact the high velocity tail of the dark matter distribution, as studied in the context of the via Lactea II simulation [94, 95]. A broader issue is the impact of Galactic evolution on the survival and evolution of CDM substructure [113] itself, and we turn to this in the next section.

2.3 The Cold Dark Matter Paradigm

The extreme uniformity of the observed cosmic microwave background suggests that the early universe was nearly homogeneous and isotropic. This initial state can be realized through a yet earlier inflationary epoch [114]. The quantum field sourcing this inflationary epoch was beset by fluctuations, as all such fields are [115, 116, 117]. These fluctuations manifested as perturbations to the overall density field $\rho(\mathbf{x})$, which grew with time into large-scale structures, such as galaxies.

Defining the overdensity $\delta(\mathbf{x})$ as the fractional density difference from the mean ρ_0, determined over a volume for which the universe appears homogeneous, it is apparent that the overdensities at two nearby points may be correlated. The power spectrum $\mathcal{P}(\mathbf{k})$ of these correlations is the Fourier transform of that correlation function. With $\delta_{\mathbf{k}} = \int_V d^3\mathbf{x}\,\delta(\mathbf{x})\exp(-i\mathbf{k}\cdot\mathbf{x})$, we have $\mathcal{P}(\mathbf{k}) \equiv \langle|\delta_{\mathbf{k}}|^2\rangle/V$. Then $\mathcal{P}$ depends only on the scalar wavenumber k, because the universe is isotropic. In the CDM model [118], the supposed power spectrum $\mathcal{P}(k) \propto k$, due to Harrison [119] and Zeldovich [120], is scale invariant, meaning that the gravitational potential associated with a root-mean-square (RMS) fluctuation at scale k is independent of k [38], thus sidestepping the problem that the fluctuations might prove to be too large at either large *or* small scales [120].

It was quickly realized that this model would engender an inside-out growth of structure [121, 122], as consistent with the observation of galaxies at large z, with interesting implications at galactic scales [123]. It had also been realized that the size and mass of spiral galaxies should be much larger than once thought [124, 125, 126] and that the bulk of that mass would be dark. Thus, N-body numerical simulations should prove powerful probes of the CDM distribution and evolution [127]. Moreover, in order to test the CDM paradigm, it is essential to test whether this supposed scale-free hierarchy is actually reflected in the data. The evolution of structure with scale k and redshift z is encapsulated by the transfer function

$$T^2(k) \equiv \frac{\mathcal{R}(k, z=0)}{\mathcal{R}(0, z=0)}, \tag{8}$$

where $\mathcal{R}(k, z) \equiv \langle\delta_k^2\rangle|_z / \langle\delta_k^2\rangle|_{z\to\infty}$ and the power spectrum in the linear regime is given by

$$\mathcal{P}(k) \propto T^2(k)\mathcal{P}_{\mathrm{prim}}(k) \tag{9}$$

where the primordial power spectrum $\mathcal{P}_{\mathrm{prim}}(k)$ is also taken to be scale invariant, and thus of Harrison-Zeldovich form.

A comparison across a wide range of physical scales between the linear structure formation prediction assuming a CDM model with inflation and recent observational data is shown in Fig. 4. The data in this figure is evidently well-described by the linear theory prediction derived from the best-fit Planck 2018 parameters [3]. This is true even at high-k, corresponding to (relatively) small length scales, since even the low-z, high-k measurements of the Ly-α forest probe the possibility of overdensities in underdensities [8]. However, a departure from linearity is necessarily anticipated at high matter densities and large wavenumbers [118, 129, 130, 131]. *Ab initio* cosmological calculations in the effective theory of large scale structure can probe mildly nonlinear scales [132], but remain limited to scales larger than roughly 20 Mpc [133, 134]. Thus, the MW is part of the small-scale frontier in which we hunt departures from

---

[5]A halo that orbits inside a larger halo is a *subhalo*. Subhalos are a qualitative prediction of the hierarchical nature of galaxy formation, as we discuss in more detail in Sec. 4.
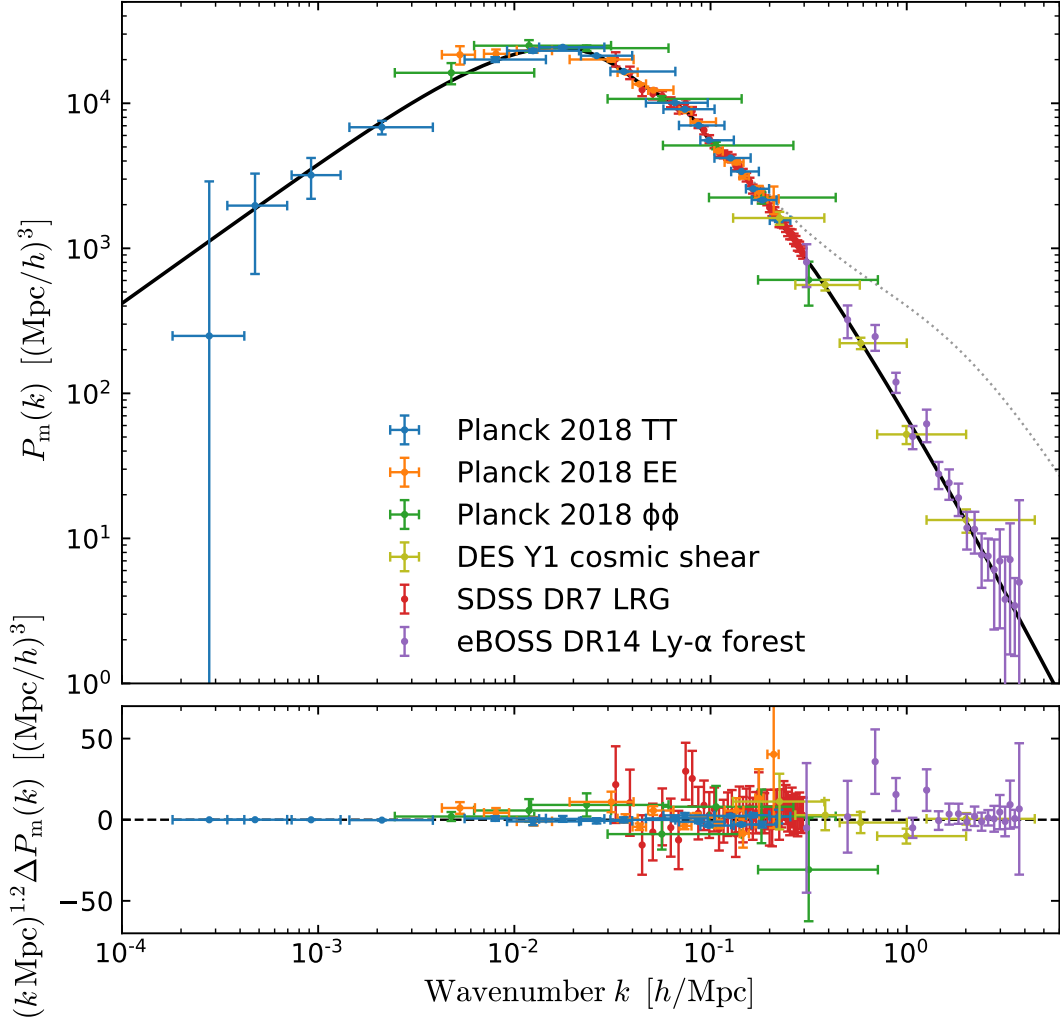
Figure 4: Upper panel: The measured matter power spectrum compared to the prediction of the best-fit Planck 2018 cosmology [3] (solid) and an example prediction of a nonlinear power spectrum (dashed). Large wavenumbers correspond to small physical distances, $L \simeq 2\pi/k$. Lower panel: Deviation of the matter power spectrum ΔP from the Planck model, scaled by $k^{1.2}$. The MW probes the nonlinear, high-k regime. From [128].

the CDM paradigm. Studies of the MW are squarely in the nonlinear regime, and comparisons to numerical simulations of cosmological structure necessarily play a key role.

For this reason, we turn to the study of the cold matter structure from N-body simulations, and comparison to observations, to determine whether indeed there is small scale structure without end. This issue has incurred much discussion. Some N-body numerical simulations show that large fractions of dark matter subhaloes undergo complete disruption, prompting the question as to whether the origin of this effect is physical, arising from tidal heating and stripping, or is a numerical artifact. This issue has been recently been studied carefully by van den Bosch and collaborators [113, 135], and they find that the destruction of CDM subhaloes in the absence of baryonic effects is extremely rare. They identify a number of numerical effects that could yield numerical overmerging, driven by resolution limitations and finite system size. Moreover, it appears that dark matter substructure survives Galactic evolution up to the current epoch [136, 137]. This puts in context the current lack of consensus as to why subhalo destruction happens at all. Certainly, however, some measure of disruption, from tidal

interactions, generating gravitational heating, is expected, and this should be revealed by the formation of tidal tails in self-gravitating subhaloes and in their perturbations.

A separate point of interest is the matter distribution, which reflects $d^3\mathbf{v}\, f$ in the DF framework. Thus we are considering a steady-state configuration — the result of the relaxation processes we describe later in this section — and we term this a halo. Studies of the luminosity distribution of elliptical galaxies are well-described by a two-power density model [38], and it is natural to consider a similar model of the DM distribution as well. Indeed, the well-known Navarro, Frenk, and White (NFW) model [138]

$$\rho(r) = \frac{\rho_0}{(r/a)(1 + r/a)^2} \tag{10}$$

is a specific case of just such a form. Although ρ_0 and a would appear to be free parameters, the numerical simulations of [139] reveal them to be strongly correlated, so that Eq. (10) can be regarded as a one-parameter family of shapes. That remaining parameter can be fixed by choosing a maximum radius. A conventional choice is r_{200}, the radius at which the mean density is 200 times the *critical density* ρ_c[6], where $\rho_c(t) = 3H^2(t)/8\pi G$; we discuss this choice in more detail below. The concentration c of the halo is given by $c = r_{200}/a$, and the simulations of [139] show little sensitivity to its value — the total mass enclosed within r_{200} can vary by powers of ten, yet c changes by no more than a factor of a few. The NFW model is "cuspy" because $\rho(r)$ diverges in the $r \to 0$; it also potentially suffers from a logarithmic divergence of its total mass at large radii, though this divergence is in practice cutoff by choice of a maximum radius such as r_{200} mentioned above. Remarkably, Navarro, Frenk, and White have determined that the form of Eq. (10), if applied to a primary halo, appears to be universal [140, 141], with few exceptions [142], describing systems differing by over 20 orders of magnitude in mass [143].

The density profiles of subhaloes, in contrast, are more typically described by a single-power-law form, with a cutoff at larger distance, engendered by tidal effects from the host halo [144]. A diversity of subhalo profiles have been observed, as reviewed by [145], with evidence for both cuspy and cored profiles and much corresponding debate as to their differing origin.

Returning to the profiles of primary haloes, we note that the origin of the observed universal behavior is not well understood. For example, numerical studies have shown that NFW profiles emerge even if the initial power spectrum $\mathcal{P}(k)$ is set to zero above some $k = K$ [146, 147]. Thus a cuspy profile in this case cannot arise as a relic of an initial condition; rather, dynamics must insure the effect. A halo is the outcome of the violent relaxation of a phase of initial gravitational collapse, to yield a system to which the virial theorem applies; this process is sometimes called virialization — and thus this is what must act, regardless of initial condition, to yield the NFW form. We note that a virial analysis suggests that r_{200} is crudely the radius over which the halo is in virial equilibrium, making it the *virial radius*[7], with the mass beyond that radius being apparently in first infall [38]. This rationalizes its two power-law form. We refer to [148] for further thoughts on its origin.

2.3.1 Small-Scale Challenges

Although the CDM paradigm has been enormously successful in explaining the large-scale structure of the Universe, small-scale challenges to it have slowly emerged as well [32, 33]. These are potentially entrained with numerical challenges in simulating the number and structure of CDM subhaloes [113, 135, 136, 137]. There are observational challenges as well, though the ability to identify faint subhaloes in the MW has greatly improved in recent years. In addition, the role of baryons in determining the structure of subhaloes is still being clarified. Nevertheless, we may yet establish the limits of the CDM paradigm by (i) determining whether there is indeed a deficient number of observed satellites with

---

[6]So-called because in a flat universe, $\Omega(t) \equiv \rho(t)/\rho_c(t) = 1 \,\forall\, t$.

[7]The mass associated with the volume enclosed by the virial radius is the *halo mass*. It is apparent that only a rough assessment of a halo mass is possible.

respect to the number expected, (ii) determining whether the structure of subhaloes is consistent with their intrinsic luminosity, or by (iii) resolving whether the cores of subhaloes are cored or cusped. These are known as the "missing satellites", "too big to fail", and "core-versus-cusp" problems, respectively. It has been suggested that the missing satellites problem has been solved [149], yet a complete consensus has not been reached — see, e.g., the "Dark Matter" review of [150] — and we refer to the review of [17] for a detailed discussion. In Sec. 4 we consider small-scale DM probes that would seem less sensitive to baryon effects.

2.3.2 Relaxation Mechanisms

"Relaxation" encompasses the processes by which a system can approach equilibrium — that is, how it can approach a steady state. We emphasize that a galaxy can attain dynamical equilibrium, but not thermodynamic equilibrium, because there is no maximum entropy state in this case [38]. We have already noted how the collisionless Boltzmann equation, along with the Poisson equation, governs the construction of the static galactic distribution function. This is possible, in part, because the stellar relaxation time, mediated by the diffusion of a star through two-body collisions — in contrast to its evolution in the smooth mass field of the Galaxy — is exceptionally long. That is, the time scale for the star to change its speed v by that same amount is estimated to be [38]

$$t_{\text{relax}} \sim \frac{0.1\,N}{\ln N} t_{\text{cross}}\,, \tag{11}$$

where the time for a star of speed v to cross the Galaxy is $t_{\text{cross}} \sim R_G/v$, and R_G is its radius. Thus in our Galaxy with $N \sim 10^{11}$ and of a few hundred t_{cross} in age [38], the two-body relaxation time is absurdly long, as noted long ago by Zwicky [151, 93], and we must look to other processes to determine how a system with gravitational interactions can evolve with time. Otherwise we would have the conundrum of having to explain how a galaxy might form very close to the state in which we observe it today.

We note three basic mechanisms by which a N-body gravitational system can evolve to a steady state [38, 152, 153, 38]: phase mixing, violent relaxation, and chaotic mixing. Only the last leads to irreversibility, through its extreme sensitivity to the system's initial conditions. In all cases the collisionless Boltzmann equation applies, so that Liouville's theorem holds — but only if we resolve the fine-grained phase-space structure and consider populated orbits. In violent relaxation, the potential is time-dependent, as in the example of gravitational collapse, so that the energy is not a constant of motion. Thus the distribution function is not static, but $df/dt = 0$ still applies. We contrast chaotic mixing and phase mixing in that the orbits in the former case are stochastic rather than regular, so that over time two orbits that were initially close in phase space separate exponentially with time. Nevertheless, the mechanism by which the N-body gravitational system can relax is common in all cases. That is, the population of orbits in phase space spreads out with time, even if Liouville's theorem requires that the total volume of phase space remains constant. Viewed broadly, after some time, a fixed region of phase space will contain both occupied and unoccupied regions. If we define a coarse-grained distribution function, $\bar{f}$, blurring the occupied and unoccupied regions, we can realize $\bar{f} < f$ and thus relax to a higher entropy state. Even in the case of regular orbits, the time scale of this process can be rather smaller than the age of the Galaxy, allowing it to evolve from its initial state. Whether visible and dark matter evolve to a similarly coarse-grained distribution function is a matter of assumption [153].

We conclude this section by emphasizing that the paths by which a N-body gravitational system can achieve steady-state are limited. This stands in stark contrast to systems in which inelastic or dissipative processes are present. We refer to [154] for just such an exemplar dark matter study. More generally, studies of the global population of dark matter in phase space, to identify, e.g., a dark disk in the MW [155, 156], can serve to anchor novel features of the dark universe. We consider this in greater detail in Sec. 5.

3 Targeted Review of Parameters of the Milky Way

Early parameterizations of our home MW were simplified due to the limitations of the available data. Infrared and microwave studies able to penetrate the dust obscuration at low latitudes in the disk and toward the Galactic center in the 1990s improved our overview significantly [157]. Most recently, the *Gaia* dataset with accurate parallax-based distance and proper motion information has again enormously improved the breadth and depth of our knowledge of the MW. Studies of motions and densities of stellar streams, satellite dwarf galaxies and globular clusters in the Galactic halo have served as probes of the Galactic potential, presumably dominated by a DM component.

The overall picture of our MW remains one of a pair of stellar disks, thin and thick [158], surrounded by a massive dark halo of uncertain extent, shape, orientation, and clumpiness. Many details, however, are beginning to be filled in: as one looks more closely, these reveal more structure on many scales [159]. Moreover, systematic studies of the spatial distribution of stellar metallicities, i.e., a chemical cartography, particularly in the ratio of the alpha chain elements to Fe [160, 161], shows dissection by chemistry to be key to distinguishing the two disk components [161]. We discuss small-scale structures in the ensuing sections, and focus here on the gross properties of the MW itself.

3.1 Milky Way Mass

The total mass of the MW, including its dark halo, is roughly 10^{12} times the mass of the Sun, denoted $M_\odot$, enclosed within a virial radius of ≈ 200 kpc [162]. Our best measures come from studies of the orbits of satellites such as the LMC/SMC system [163] as well as studies of the distribution of standard candles such as blue horizontal branch (BHB) stars and assuming they have come into approximate equilibrium under the Jeans approximation [164]. That assumption of relaxed equilibrium is not true in detail, and so overall the estimates for mass still come with rather hefty error bars of 30% to 50% [162].

There are models for the distribution of non-dispersive DM on many scales from N-body simulations. These generally find DM halos of galaxies well fit by a NFW [140] profile with inner slope $\rho(r) \sim r^{-1}$ and outer slope $\rho(r) \sim r^{-3}$, plus a central density and a concentration scale indicating a transition from inner to outer slope, as in Eq. (10). Even simpler isothermal models of DM density $\rho(r) \sim r^{-2}$ are reasonable fits to many halo simulations over a wide range of scales, but, of course, the total integrated mass of an isothermal halo tends to infinity at large radius and so must be cut off by a steeper falloff at large r. Studies of the stellar distribution in the outer parts of the Galaxy show a steeper-than-NFW outer slope falloff, with $\rho(r) \sim r^{-4.5}$ for stars [165], and it is possible that the DM falls off more quickly than the NFW profile predicts as well. In the inner parts of galaxies, while the NFW model and all non-dissipative models of DM predict cuspy ($\alpha < 0$) density spikes at small r where $\rho(r) \sim r^\alpha$, in fact, there is little observational evidence for any central cusps with slope as steep as $\alpha = -1$ in stellar density or in DM. Studies of velocities and densities of stars in the central regions of the MW's largest nearby satellites Fornax and Sculptor [166] show $0 > \alpha > -0.5$. Researchers [167] have shown how baryonic dissipation can flatten out cuspy spikes in the center of galaxies and help understand the relative paucity of observed satellites compared to numbers of DM clumps predicted in computer simulations [168]. We note that the observations of the centers of galaxies and clusters to determine the profile slope remains an exceedingly difficult measurement. In clusters with a central black hole, [169] showed that the expected density profile near a central black hole would approach $\alpha \sim -1.75$. In the dense cluster M15, thought to have an intermediate mass black hole, [170] have shown evidence for some cuspiness in the stellar profile, though we stress that the number of stars in the very central region is extremely small leading to large Poisson error on the inner density slope.

3.2 Size and Shape

Where does the MW end? To a large extent, the answer to this question is a matter of definition. Various proposals for the end of a dark matter halo include: comparisons against the background density at the time that the halo separated from the Hubble flow [171], comparisons against the background density at a floating redshift [172], and dynamical measures, such as the splashback radius [173]. The total mass of a virialized NFW halo depends logarithmically with the maximum distance, noting Eq. (10), is

$$M_{\rm NFW} = \int_0^{R_{\rm max}} d^3 r \rho_{\rm NFW} = 4\pi\rho_0 a^3 \left[\ln(1 + R_{\rm max}/a) - \frac{R_{\rm max}}{a + R_{\rm max}} \right]. \tag{12}$$

Thus, $dM_{\rm NFW}/dR_{\rm max} \propto R_{\rm max}/(R_{\rm max} + a)^2$, so that for $R_{\rm max} \simeq 10a$ choices of how to truncate the Milky Way halo can affect its estimated mass at the $\sim \mathcal{O}(10)\%$ level.

The DM halo of our MW extends to at least 50 kpc as the orbits of the LMC/SMC are clearly strongly affected by it. The stars and gas of the LMC/SMC and its associated DM appear to be on their first orbital pass around the MW [174, 175]. The details of the orbit and distribution of gaseous and stellar tidal tails shows strong evidence for tidal friction and an alteration in the semi-major axis of the combined MW — LMC/SMC system orbit, which provides evidence for drag from the DM halos of the two systems slowly drawing closer together [174]. Beyond 50 kpc, tracers are rare, though the dwarf galaxy Draco at 80 kpc from the MW does show a flattened stellar distribution, which could be a sign of either tidal influence of the MW at 80 kpc or evidence for having its own DM halo. Recent work suggests the latter, as no evidence of tidal stripping of Draco stars is seen [176]. In contrast, nearly every dwarf satellite companion that approaches within 20 kpc of the MW center appears to have strong evidence for tidal distortion and in many cases stars from the satellite object are stretched into an elongated stream by tidal interaction with the MW and its DM halo [177].

We conclude that the influence of DM is strong in the halo of the MW out to at least 50 kpc, but appears to diminish significantly at radii greater than 80 to 100 kpc. Our nearest large spiral neighbor, Andromeda, which is $\gtrsim 700$ kpc distant from the MW [178], has its own complex system of tidal streams and associated dwarfs, and has its own dark halo of uncertain extent [179]. Both the MW and Andromeda's dark halos likely extend out to beyond 200 kpc from their respective centers with density decreasing at the NFW outer slope of -3 or steeper. The extent to which the halos overlap in between or can be said to be a common halo is uncertain. The currently favored CDM hierarchical structure formation scenario — with build up of structure from smaller clumps densities to larger — suggests that the halos began well separated. Their overlap is increasing over time and they will completely merge a few billion years in the future. There are no known sufficiently luminous stars or other tracers in between the two large spiral systems to map the DM distribution between them in detail. A problem with using luminous tracers far out in the halo of the MW, beyond 100 kpc, is that the timescales for completing an orbit or responding to dynamical friction effects approach or exceed the Hubble time, $\tau_H \equiv cH_0^{-1} \simeq T_{\rm Univ} \simeq 10^{10}$ yr. For this reason it becomes difficult to distinguish systems in equilibrium or which have relaxed from those that are just forming or interacting for the first time.

3.3 Components

The shape of the MW thin and thick stellar disks is clear. The more massive thin disk has an exponential distribution in radius with scale length of over 3 kpc and an exponential falloff in vertical ($|Z|$) scale height of 300 pc. These quantities refer to the $1/e$ fall-off in the directions parallel and perpendicular to the plane of the disk, respectively. It is strongly dissipated and rotates at about 220 km/s at a radius of about 8kpc from the Galactic Center, the radius at which the Sun orbits (another estimate of mass). We discuss precision determinations of these parameters later. Such thin disks are unstable to clumping and strong bar formation [152], and thus the existence of only a weak bar in the MW (and

other so-called Grand Design spiral galaxies) was early evidence for a supporting massive dark halo [180] surrounding each spiral galaxy. In addition to the thin disk, the MW has a chemically distinct thick disk, which consists of stars with alpha peak element metallicity about 2x higher ($[\alpha/\text{Fe}] \approx 0.3$ on a log base 10 scale) than in the thin disk [181]. This population of stars presumably comes from an environment that has been enriched by the debris of remnants of exploded high-mass progenitor (type II) supernovae.

Recent findings made possible in large part by *Gaia* satellite measurements point to a major, approximately face-on (as opposed to a prograde or retrograde infalling) merger of a massive ($> 20\%$ of the MW's mass) dwarf galaxy. This has been called the *Gaia*-Enceladus/Sausage event, and is estimated to have occurred between 10 and 12 Gyr in the past [182, 183]. This event was gas rich and is thought to have provided impetus for a significant epoch of higher-mass star formation. This may have led to the high abundance of alpha-element rich stars of the thick disk. In addition, that event disturbed and dynamically heated, primarily vertically, an existing proto-thin disk, explaining both the larger scale height (0.8 kpc) and shorter scale length (2 kpc) of the thick disk compared with today's thin disk [184, 185]. Recent studies of the $[\alpha/\text{Fe}]$ composition of stars at a variety of Galactocentric radii confirm the picture of a short scale length for the high-$[\alpha/\text{Fe}]$ thick disk, essentially ending just beyond R_0, and additionally find support for an extended, low-$[\alpha/\text{Fe}]$ thin disk, flared beyond R_0, with on-going star formation [186, 161].

The so-called asymmetric drift or lag of thick disk stars, which complete a rotation around the galaxy at a slower pace than thin disk stars at similar radii from the Galactic center, can also be understood as the result of this ancient massive merger. Mergers can lead to a partial cancellation of the existing disk angular momentum, with some of the circular velocity of rotation of the thick disk becoming an up-and-down vertical component of motion [38].

While the *Gaia*-Enceladus/Sausage event is accepted as the most significant merger that our Galaxy has had in the past 10 Gyr, there is evidence for other substantial merger events, possibly in the much more recent past [187], and for on-going interactions with our satellite neighbors. Determining the predicted kinematic signature in the Galaxy's disk or halo resulting from a close interaction with a massive satellite such as Sagittarius [188, 189] is a subject of ongoing theoretical study, even if Sagittarius is less massive [190] than once suggested [191]. Moreover, the LMC [192, 44, 193], with or without Sagittarius [194], can influence the Milky Way, and studying their impacts remains an active area of research. Also see Section 6.4 below.

In the outer reaches of the thin disk, beyond the solar radius at 8 kpc and extending to as far as 30 kpc, there is considerable evidence for warping, flaring, or more complex, corrugated disturbances in the stars and gas as portrayed in Fig. 5 [195, 101, 196]. This is seen in both gas, via radio observations, and in the visible motion of stars. As discussed below, this is indicative of a non-static potential [44], which may be caused by recent interactions of our MW, in particular within the last Gyr, and ongoing. The primary culprits behind these perturbations are the LMC/SMC system as well as the massive Sagittarius dwarf system and its associated DM overdensities.

Until recently the shape of the halo was assumed to be spherical or slightly oblate or prolate, with the halo axes lined up with the disk axes. Recent observations have updated this picture and provided substantial additional detail. Though the outer **stellar** halo of the MW is oblate, flattened with $c/a = 0.8$ [199] or flatter along the vertical axis, [200] found evidence for a prolate rather than oblate DM dominated potential. N-body simulations of [201] found prolateness of dark halos to be a common feature of large scale structure. Detailed fits to the Sagittarius stream data, however, found that rotational symmetry about the $\hat{z}$axis did not hold [202] and in fact a triaxial halo, slightly misaligned, was necessary to fit the data. More recent refinements to these fits by [192] found that the LMC/SMC system and its accompanying DM was a major perturber of the MW's disk and halo system. In fact, the mass of the LMC/SMC system may approach 25% that of the MW, as reviewed in more detail below. This renders a perturbative expansion to the dynamics poorly behaved, and requires more detailed 3-D
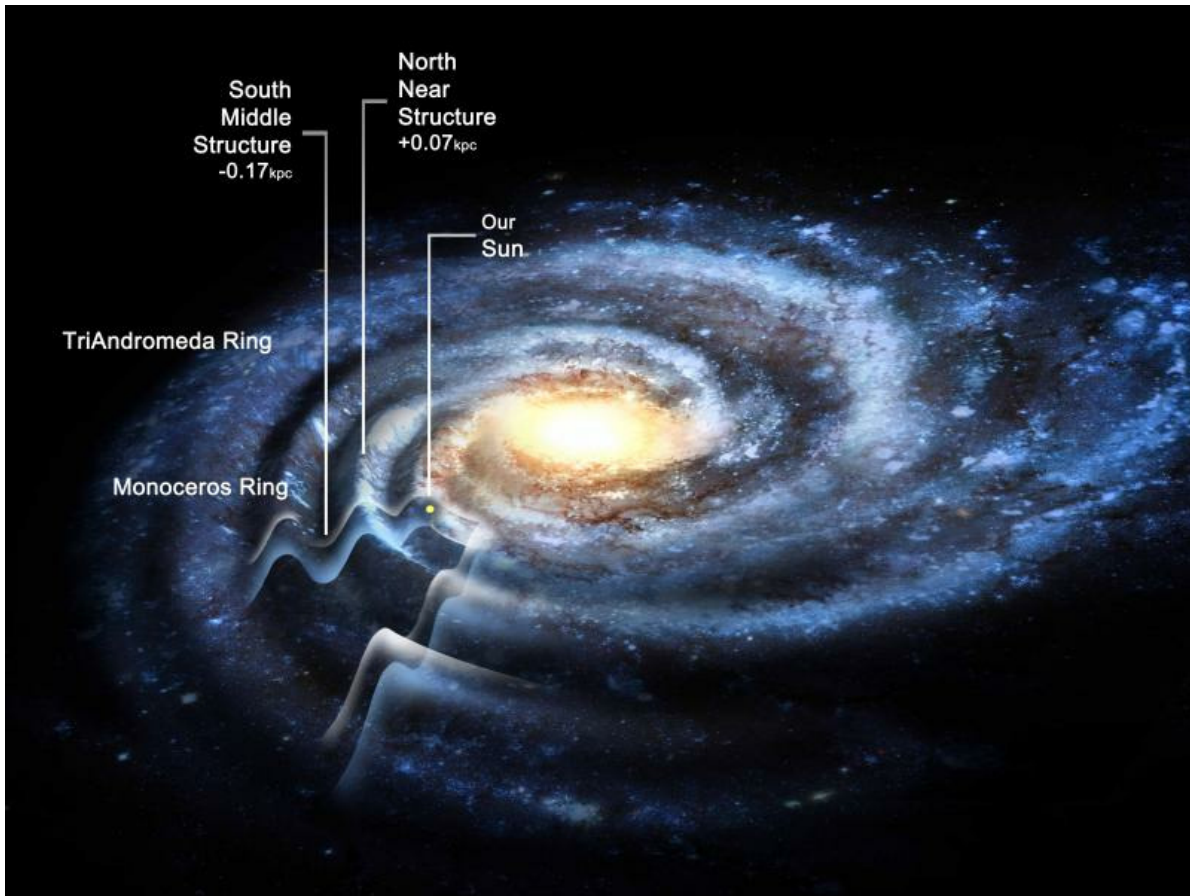
Figure 5: Artist's conception showing corrugated ripples in the MW's disk [195, 101, 196]. The vertical structure of the MW's disk is not well characterized except quite close to the Sun, with evidence for dynamical processes that couple vertical and planar motions [197, 198]. Credit: Dana Berry/Rensselaer Polytechnic Institute

.

N-body simulations. A current view of the shape and orientation of our MW dark matter halo is of a tri-axial or tilted axisymmetric MW DM halo. This halo is mis-aligned with the stellar disk and has its long axis oriented in the direction of the LMC/SMC as shown in Fig. 6 [192, 44].

The "clumpiness" of the halo DM is very uncertain, and may be closely tied to the nature of DM itself. Exploring the evidence for DM clustering on all scales from a few pc to a few kpc is an observational endeavor of much current focus. Globular clusters on 10-50 pc scales and the solar system on scales of 10^{-4}pc do not appear to have any significant DM and have measured mass-to-light ratios near unity (e.g. [203]) suggesting that all mass is accounted for by the visible starlight (or the Sun in the case of the solar system, though evidence for dark matter may yet come from the outer reaches of the solar system [204]). This is in contrast to dwarf galaxies on 500-1000 pc scales which clearly show evidence for very significant DM halos and mass-to-light ratios that exceed 100 in the most extreme cases [205]. The smallest scale on which DM is clumped may then lie somewhere in this $10 - 1000$ pc range.

3.4 Rotation Curve

More insight can be gained into the distribution of DM in and around the stellar disks by examining our Galaxy's rotation curve; namely, the velocity at which a star on a circular orbit in the plane of the
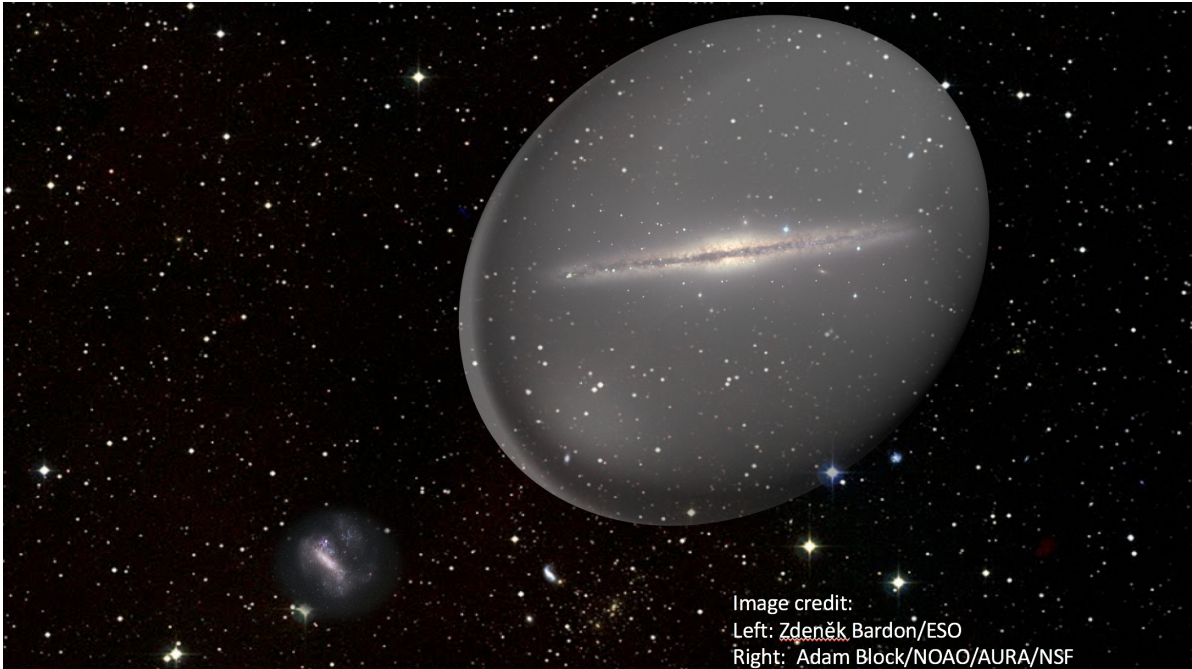
Figure 6: Artist's conception showing the relative tilt of the dark halo surrounding the MW in the direction of the Large Magellanic Cloud system (lower left). The MW and Magellanic clouds are separated by 50 kpc. Note that the halo actually extends well past 200 kpc in extent and is composed of clumps of unknown lumpiness. The MW's halo also completely envelopes the LMC/SMC and their own smaller dark matter halo. Credit: Austin Hinkel/University of Kentucky.

thin disk a given distance from the Galactic center rotates. The GRAVITY collaboration's observations of the Galactic center have greatly improved the determination of the Sun-center distance [209]. This information, in concert with *Gaia* DR2 data, as well as with other optical and infrared surveys, has refined the rotation curve over the distance range $5 < R < 25$ kpc, and yields $V_c = 229.0 \pm 0.2 \, \text{km s}^{-1}$, with a systematic uncertainty of 3% [206], at the distance of the Sun to the Galactic Center of $R_0 = 8.122 \pm 0.0.031$ kpc [209]. Recent improvement in the treatment of optical aberrations have improved the agreement between their earlier results [209, 210] to yield $R_0 = 8.275 \pm 0.034$ kpc [211], where we have combined statistical and systematic errors in quadrature throughout. For reference, various other recent measurements and fits at R_0 give $V_c = 242 \, \text{km s}^{-1}$ [52], $V_c = 233.6 \pm 2.6 \, \text{km s}^{-1}$ [97], and $V_c = 243 \pm 8 \, \text{km s}^{-1}$ [207].

We compare in Fig. 7 the circular velocity curves obtained from the DF analysis based on $f(\mathbf{J})$ modeling and fits to data from the CGS survey, which also yields the comparison with RAVE data shown in Fig. 3 [52], with direct determinations from observational data. In particular, we compare with analyses using observations of red-clump giants with *Gaia* DR2 and APOGEE [206], which jointly fits these data to the parameters of an NFW DM halo under the assumption of axial symmetry, and observations of nearby Cepheid variable stars [97]. We also compare to a direct measurement of the local acceleration of the solar system using the apparent proper motion of quasars from *Gaia* Early Data Release 3 (EDR3) data [207], which yields fundamental Galactic parameters at the Sun's location. For the results of [206], we apply a 3% error bar at all radii. For the result of [97] we depict their linear model including a prior on the Sun-center distance from [210], simultaneously varying within 1σ the local value of V_c, the value of R_0, and the value of dV_c/dR. It is worth noting that the slopes of the two observational analyses, over the region that they compare, are in good agreement with each other, yielding $-1.7 \pm 0.1 \pm 0.46 \, \text{km s}^{-1}\text{kpc}^{-1}$ [206] and $-1.41 \pm 0.11 \, \text{km s}^{-1}\text{kpc}^{-1}$ [97]. Each of these
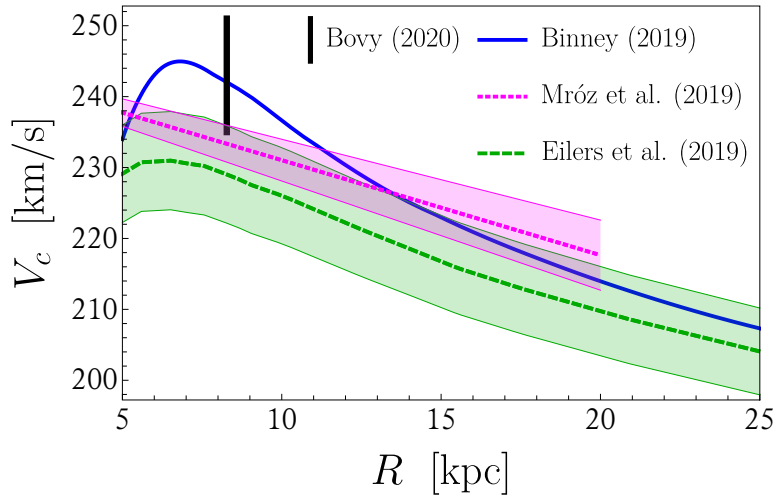
Figure 7: Circular speed V_c as a function of radius from the center of the MW, as determined from $f(\mathbf{J})$ modeling [52] and fits to measurements reported by [206, 97], as well as a value inferred from the measurement of the solar system's acceleration [207]. We include a constant 3% error bar on the entire V_c curve of Eilers et al. [206], consistent with their systematic error assessment, and we simultaneously vary the best fit parameters of the linear model of Mróz et al. [97] by 1σ. The spherically-aligned Jeans Anisotropic Method of [208] gives a result intermediate to that of [97, 206].

assessments is at odds with older results that suggested the rotation curve would be flat, see, e.g., [212]; the local acceleration analysis of [207] finds a comparable value to the most recent results, but with a much larger error, $-2 \pm 9 \, \mathrm{km \, s^{-1} kpc^{-1}}$ [207].

An accurate rotation curve is important to constraining the amount and distribution of DM at these same radii near the Sun and in the outer parts of the disk. It is also pertinent to the assessment of other parameters, such as the pattern speed of the Galactic bar. For example, using the assessment of the Outer Lindblad Resonance (OLR) location from a distinct *Gaia* DR2 data sample [29], the rotation curve information determines the bar pattern speed [213]. It is worth comparing the pattern speeds that result from different rotation curve information. The rotation curve result to which we have referred is much more precise than older studies [206]; for reference, we note earlier work which also employs HI data [214], making it quite distinct. Here, although $v_c = 240 \pm 6 \, \mathrm{km \, s^{-1}}$ [214] is a bit bigger, the determined local radial derivative is also more negative, so that although the Eilers et al. result [206] gives $49.3 \pm 2.2 \, \mathrm{km \, s^{-1} kpc^{-1}}$ for the pattern speed [213], the central value of the Huang et al. result [214] evaluates to $50.7 \, \mathrm{km \, s^{-1} kpc^{-1}}$, within 1σ of the more precise determination. Thus reasonable consistency between the different rotation curve assessments exists.

The slope of the Galactic potential at a given radius translates directly to an estimate of the circular speed of the disk at that radius and thus, by inverting the relation, the MW's rotation curve is a sensitive probe of changes in the Galactic potential and ultimately of the underlying mass distribution. Recent estimates of the rotation curve from [206] can be closely compared with other data-based and theoretically driven estimates [52] to challenge models containing such components as dark disks [215]. We shall have more to say about the implications of the interpretation of the rotation curve for our understanding of the local density of dark matter in Sec. 7.

3.5 Environment

Within the local group of our MW, the LMC/SMC and Andromeda, many authors have remarked on a plane of satellites which appears to defy random infall of gas and dwarf galaxy satellites over cosmic

time [216]. One explanation for this is that the alignment is guided by a DM filament, a component of a large scale structure [217]. Structures on the largest scales ($> 50\text{Mpc}$) of the so-called cosmic web consist of filaments of DM extending between large vertices of DM (where baryon-rich galaxy clusters collect). Individual field galaxies align along these filaments with a prolate dark halo configuration. All these early simulations, however, assumed axisymmetry of the halo and alignment between the stellar disk axes and the dark halo axes. Whether of not the existence of these coherent planes of satellites — some of which also appear to show kinematic coherence — are fully compatible with the predictions of CDM theory that predicts a more random or thermal build up of structure from smaller to larger scales remains uncertain [218].

On even larger scales, Galaxy clusters do appear to have common extended intra-cluster DM envelopes punctuated by sharp spikes of DM around each large cluster member galaxy, but the models are subject to some degeneracies [219].

4   Probing the Milky Way at the Small-Scale Frontier

Dark matter astrophysics has long been concerned with observational probes of the CDM paradigm. Studies of largest-scale structures are inevitably cosmological in nature. These cosmic tests range from the cosmic microwave background (CMB) radiation, which encompasses the entire visible Universe, to the baryon acoustic oscillation scale, which is visible in both the CMB and the distribution of galaxies from surveys of the low-redshift universe, to the behavior of galaxies in the immediate vicinity of the MW. Each of these is remarkably consistent with the CDM paradigm, which predicts that DM is organized in gravitationally self-bound structures termed "halos". The CDM prediction is that such structures are formed "hierarchically": small structures separate from the Hubble flow and collapse first, and larger halos are formed from successive collisions and mergers of these small initial objects. Partially merged subhalos that are at least partially self-gravitating may persist within a larger host halo for many orbits before being tidally disrupted and joining the larger virial distribution.

Notwithstanding the success of the CDM paradigm at cosmic scales, concerns at galactic and sub-galactic scales have existed for decades. These are commonly discussed as belonging to one of four particular problems: (i) the missing satellites problem, (ii) the too big to fail problem, (iii) the baryonic Tully-Fisher relation, and (iv) the core-cusp controversy. We will address the first of these in the context of the MW, and refer to other recent reviews on the remaining topics [33, 17].

Probes of DM halos currently span the approximate range $10^8 - 10^{15}$ M$_\odot$. In this section, we will give an inventory of CDM structures within the MW, and briefly overview how they are affected by and arranged within the MW's gravitational potential. We will order this section roughly by size, beginning with the largest, most obviously apparent substructures of the MW with masses $\sim \mathcal{O}(10^{11})$ M$_\odot$ and proceeding to lower masses and less prominent subsystems of mass $\lesssim \mathcal{O}(10^8)$ M$_\odot$.

4.1   The Large Magellanic Cloud

Our understanding of the LMC has evolved substantially in recent years [220, 175, 174, 221, 222]. Using data from the *Gaia* satellite [27], we have also gained significant insight into the influence of the LMC on the MW: the reflex motion of the MW in response to the gravitational influence of the LMC has now been detected [223, 192, 224, 225]. Detailed studies of the interactions of the LMC with the MW halo and its satellites suggest that the LMC is relatively heavy, with a mass $M_{\text{LMC}} \gtrsim 0.1 \times M_{\text{MW}}$ [163, 192, 226, 225, 227]. This is compatible with the results of a comparison of a census of LMC satellite members to N-body simulations [228, 229, 230].

Of direct concern for improving our understanding of the MW is the growing appreciation that the LMC can directly and significantly influence the local phase space of DM particles [231]. This is
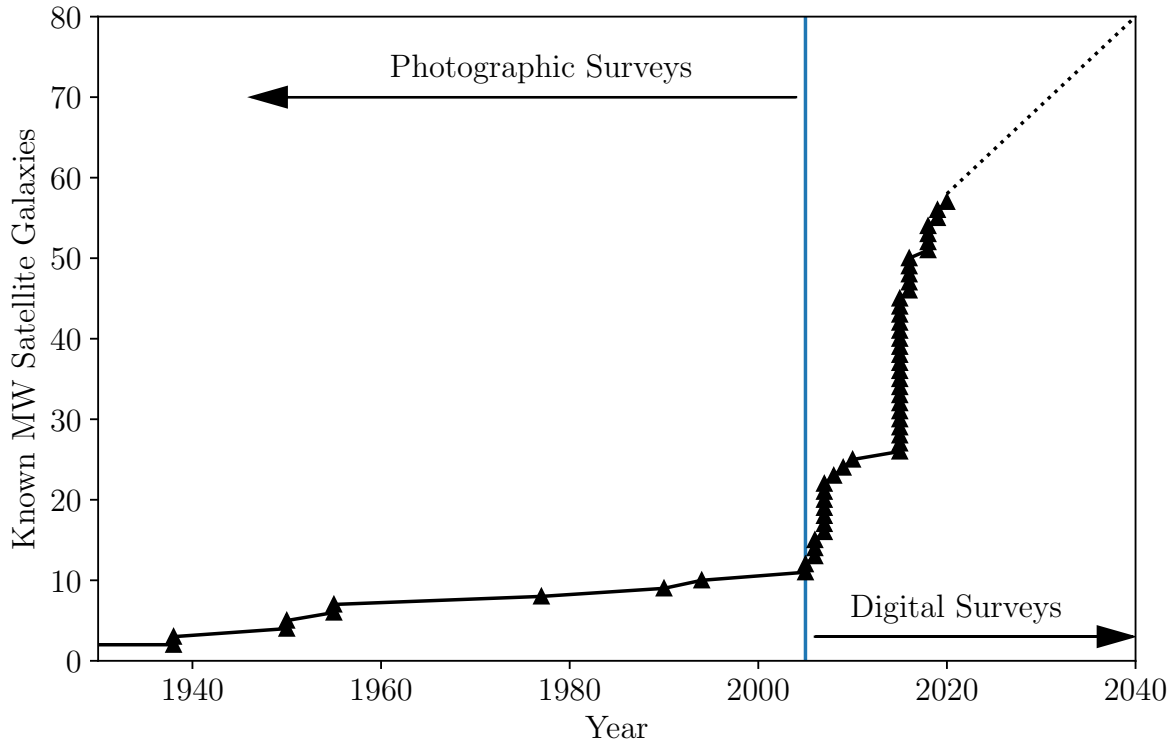
Figure 8: Known MW satellite galaxies as a function of time. The dotted line is a schematic projection for future surveys. Data courtesy of Joshua D. Simon.

possible due to both the high relative velocity of the centers of mass of the MW and the LMC as well as the reflex motion of particles in the solar neighborhood to the influence of the LMC, as can be probed through studies of axial symmetry breaking in the MW [44, 29]. Thus, our understanding of the MW is now sufficiently precise that further refining this understanding necessarily requires accounting for our largest satellites.

4.2   Milky Way Satellite Galaxies

The possibility that distant clusters of visible stars were island universes with their own history and identity independent of our immediate environment was originally suggested by Kant [232, 233]. Almost a century ago, this hypothesis (and, by extension, the Copernican principle) was confirmed by Hubble [234]. Some of these other galaxies of stars are now understood to be gravitationally bound to the MW. These smaller galaxies that are gravitationally bound to the MW are known as satellite galaxies.

The essential foundation of any substantive understanding of these satellite galaxies is their enumeration. Small self-gravitating astronomical structures are classified in a variety of ways. One useful binary classifier of different such systems is whether or not their dynamics are determined by a significant DM component. Those with a large DM density and evidence of multiple epochs of star formation are commonly referred to as dwarf galaxies. In the early years of this century, as numerical simulations improved, an apparent tension between the number of observed and predicted dwarf galaxies was noted by a number of authors (see *e.g.* [33]). However, it is now believed that there is no missing satellites problem [149, 235]. The problem has been resolved by a number of factors. Chief among these have been recent discoveries of satellite galaxies around the MW [236, 237, 238]. Currently, almost 60 dwarf galaxies are known, a number that has changed by almost an order of magnitude in the past decade. For a recent review on the status of known satellites of the MW, see [239], whose Fig. 1 we capture in
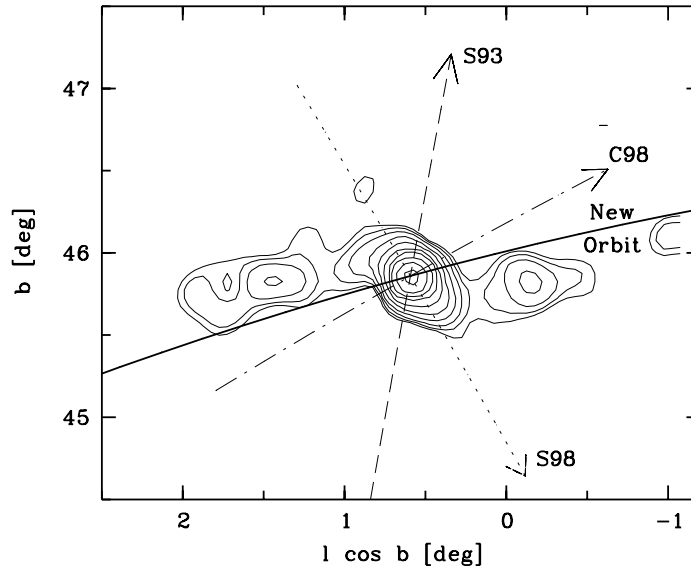
Figure 9: The initial detection of tidal tails of the Pal5 stream. From [253]©AAS. Reproduced with permission.

Fig. 8. This reveals the dramatic increase in known satellite galaxies as a function of time and technology. Predictions for the star-formation efficiency of these same small host environments have also been updated and improved [240, 241, 242, 243, 149], which has also helped to ameliorate the discrepancy. Upcoming facilities such as the Rubin Observatory will extend the sensitivity to faint satellites even further [244], which will extend our ability to test the CDM paradigm to the frontier of fainter and smaller objects.

In a cosmic context, the number of small satellite galaxies probes the high-wavenumber tail of the matter power spectrum [245, 246, 247, 248, 249, 250, 251], where we note [17, 33] for reviews. The power spectrum of matter at these large wavenumbers (corresponding to cosmologically small physical sizes) is in turn determined by the details of the DM of the universe. We make the connection between DM microphysics and galactic dynamics more explicit in Sec. 5.

4.3   Stellar Streams

Stellar streams are extended distributions of stars with similar kinematics and chemical composition. They are presumably formed from disruption of globular clusters and dwarf galaxies as those objects fall into the gravitational potential well of and virialize with their host halo. See [252] for a recent and comprehensive historical and methodological overview of stream finding in and around the MW.

The discovery of tidal tails around Palomar-5 (Pal5), shown in Fig. 9 [253], was a landmark occasion for the study of stellar streams. The extended tidal tails of streams are in fact their essential distinguishing feature for tracing the interesting features of their host halo, including its assembly history [254, 255, 256, 257, 258] and its steady-state structure [259, 260, 261, 202, 262, 263, 264, 265, 266, 267, 268, 269, 270, 271, 272]. The tidal tails trace the trajectory of the disrupted progenitor along its original orbit, while in transverse directions the stream remains kinematically cold (unless perturbed by a massive satellite [192]). The phase space of the stream remains coherent, and the original characteristics of the progenitor can be inferred [254] as long as the stream is on a regular orbit [273, 274].

There were 26 known streams circa 2016 [275], with 11 more discovered in DES data [177]. We show a recent collection of streams observed in the DES footprint in Fig. 10 [177]. At least three more streams have been discovered so far in *Gaia* data [276, 277, 278]. Spectroscopic follow-up from the S^5 survey
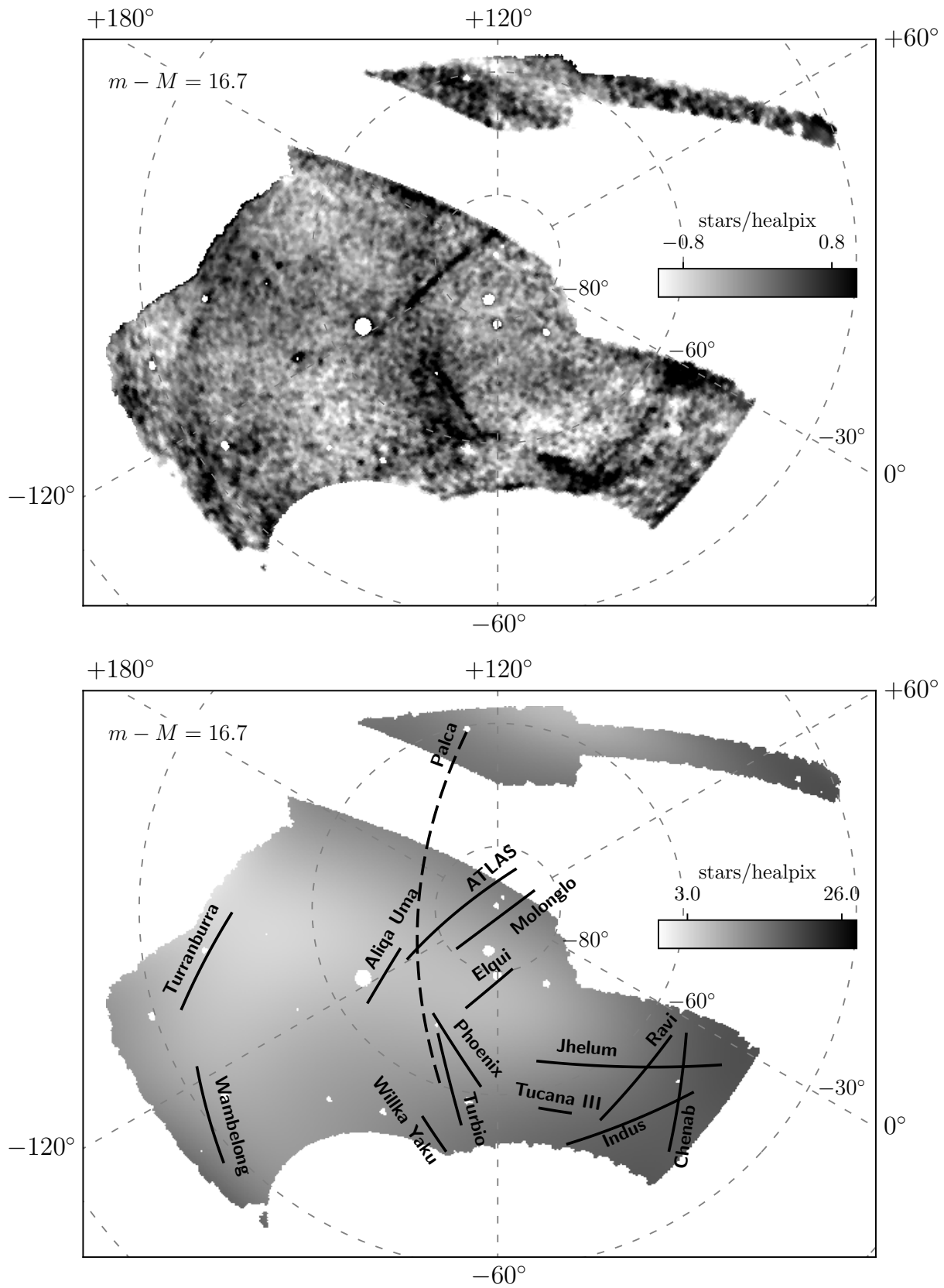
Figure 10: Stellar streams of the MW as observed in the DES observational footprint. From [177]©AAS. Reproduced with permission.

[279] will further characterize these populations and provide additional clues as to their evolutionary history, as will complementary future surveys [280].

Streams carry with them a historical record of their gravitational interactions. The scars of this history will be particularly visible if the stream has been perturbed along its kinematically cold transverse directions by the influence of a massive perturber. Gaps and lumps transverse to the leading and trailing arms are entirely absent in a smooth background potential, but are induced by overdensities within the halo. For this reason, streams provide particular sensitivity to otherwise dark satellite members of their host halo [281, 282, 283, 284, 285, 286]. Such substructures are predicted by the hierarchical assembly mechanism of DM halo formation, as discussed in Sec. 5.1. In Sec. 5 we shall have much more to say about how different theories of DM lead to different predictions for the structure and frequency of these perturbations.

4.4   Patterns in Milky Way Field Stars

All of astronomy hinges on the search for regularity in observations of different subsets of the Universe. Yet the detection of anomalies in the known positions of stars due to the gravitational influence of known objects is only one hundred years old. Finding *statistical* correlations in the positions, velocities, or accelerations of nearby stars are data- and computation-intensive challenges and thus particularly modern versions of this very old type of search.

Photometric gravitational lensing is a prominent example of this type of statistical observational effort. Lensing detections of DM are thus far largely confined to extragalactic contexts, beyond the purview of this study, but we give a brief summary of aspects of the field here. We then extend some of the concepts from photometric gravitational lensing to related families of searches.

First, we define photometric gravitational lensing to be the study of shear distortions in single images of background light from stars, quasars, and galaxies. This requires large photometric data sets and precise images. The lensing distortions are termed "strong" or "weak", depending on how severe the lensing is and over what angular range and across how many distant sources the lensing signal is correlated. Strong lensing is exemplified by the Einstein ring formed when a source, lens, and observer are exactly aligned. It is also possible to detect multiple images of the same object without seeing the extended arc of the Einstein ring. Anomalies in strongly lensed images can provide evidence of substructure in the lens [288, 289]. Such studies have a number of exciting successes, as shown in Fig. 11, but are so far limited to cosmological distances [290, 287]. (Recently, it has been suggested that such lensing events are more numerous than expected in CDM [291].) Weak lensing in contrast is detected by statistical methods on large image sets [292, 293]. Transient effects like flux ratio anomalies and apparent magnification, which rely on relatively high cadence photometric observations, are termed "weaker than weak" lensing, because they do not lead to a change in the apparent position of the object, and are sometimes referred to as "microlensing" [294, 293]. (The even more subtle effect of a phase lag on the wavefront of a gamma ray burst, the so-called femtolensing, is unlikely to be observable after accounting for finite-source-size effects [295].) Microlensing studies offer opportunities for measuring populations of particularly dense objects like planets and the very dense DM halos predicted in non-CDM cosmologies. Gravitational lenses have been detected from radio to gamma-ray energies [296, 297, 298, 299, 300], using techniques spanning all of these methods. Due to the large, fluffy nature of halos in the CDM picture, a complete understanding of the building blocks of the MW halo is not likely to be completed in this way should the CDM hypothesis be correct. At this time, however, we can say that lensing provides evidence that is entirely compatible with the CDM picture of the MW halo. We defer to Sec. 5 the implications of lensing analyses for DM particle candidates in CDM and beyond.

Photometric lensing is but one technique to discover otherwise-invisible small-scale DM substructure. With the advent of extremely precise position (and thus parallax and proper motion) information from
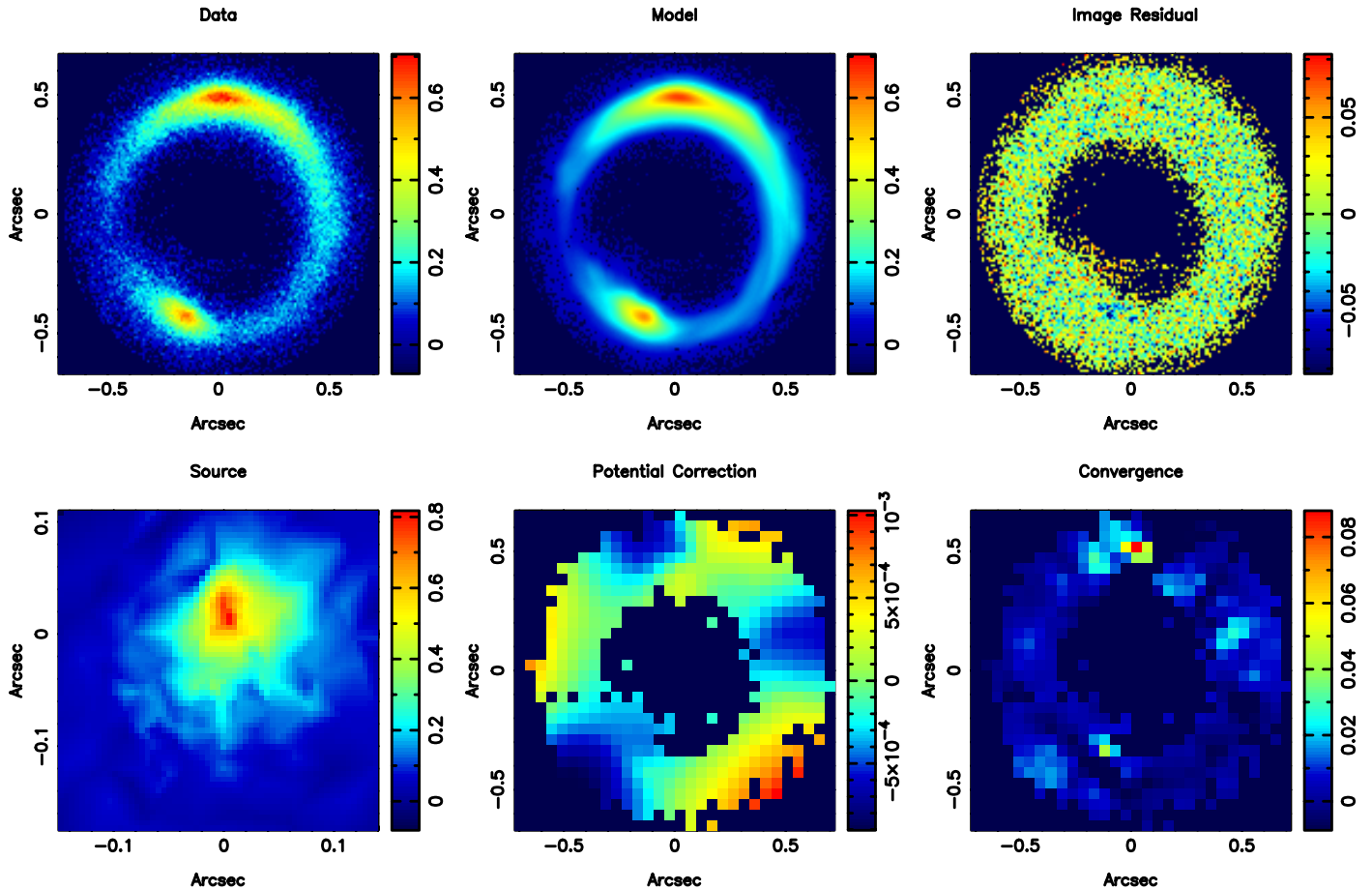
Figure 11: A detection of dark matter substructure in a strongly gravitationally lensed image. Substructure is revealed in the lower right-hand panel. From [287], reprinted by permission from Springer Nature.

the *Gaia* satellite [301], studies of patterns in MW stars are no longer necessarily confined to photometric anomalies. For instance, these precise velocity data can be turned directly into a map of the overall halo potential [302, 303]. Alternately, astrometric or velocity-based lensing has recently been proposed. This requires studying perturbations to the precise *Gaia* astrometric solution. As with the photometric case, these perturbations can arise in the time-domain [304, 305, 306] or may be revealed through higher-point correlations across a broader statistical sample [307]. The hope is that these methods of astrometry can provide a census of dark compact objects. Similar to the case of photometric lensing, astrometric lensing is most promising for very dense subhalos.

In addition to measures of position- and velocity-space distortions, another frontier in the study of the halo of the MW is acceleration measurements [308, 309, 310, 311, 312, 313, 314]. Following the trend identified in the case of velocity measurements, acceleration measurements can probe the local acceleration due to the overall DM halo, and thus finely map the local gravitational potential. Alternately, pulsar timing arrays that look for correlated phase lags in pulsar signals will be another important tool for understanding the substructure of the MW halo [315, 316, 317, 318, 319]. These probes provide very exciting prospects for the next generation of studies of the immediate DM halo.

5   Probes of Dark Matter Candidates via Milky Way Observations

In general, the number of small DM halos is determined by the *primordial* distribution of DM at all distance scales. One convenient summary of the nature of the DM (but, as discussed below, not the unique one) is to characterize it as "hot" or "cold" depending on a single parameter: the *free-streaming scale* in the epochs when cosmic structures begin to form. Below this distance scale (or, equivalently, at larger wavenumber), density perturbations do not grow. A hot DM candidate is generally recognized as having been relativistic at the time of the formation of the density perturbations that characterize the CMB, with a characteristic free-streaming scale much larger than 10 kpc. A cold DM candidate will have a free-streaming scale much smaller than 10 kpc. (Naturally, warm DM interpolates between hot and cold DM and has a free-streaming scale of order 10 kpc.) This is often quantified by calculating the so-called DM transfer function, which is the ratio of the power spectrum of a given DM candidate to a cold DM particle with the same energy density. This transfer function will abruptly go to zero above the wavenumber of the free-streaming scale k_{fs}. The vanishing of the transfer function implies the vanishing of the power spectrum, which in physical terms means the absence of structures with physical sizes below $\sim k_{\mathrm{fs}}^{-1}$.

Beyond the "warmth" of the DM, a full description of the small-scale distribution of DM requires knowledge of its power spectrum on all physical scales. However, calculating this quantity requires detailed knowledge of the DM microphysics. For this reason, a precise treatment of the compatibility of DM candidates with cosmic and astrophysical observations requires a complete model of DM genesis and its interactions with itself and with the SM.

In this section, we first give a brief overview of structure formation in CDM and non-CDM cosmologies. Then we summarize the status of several DM models that deviate from the CDM paradigm at small scales. We draw concrete conclusions about the properties of various DM particle candidates by connecting to the various observational probes discussed in Sec. 4. We begin with a general discussion of structure formation in the conventional CDM paradigm and how this can be used to draw broad inferences about the nature of the DM. Then we extend our discussion by focusing on a handful of concrete models of DM-SM interactions.

5.1   Hierarchical Structure Formation in the Milky Way and Beyond

Observational diagnostics of the amount of DM in small scale structure come in many forms. At late cosmological times, these are often summarized in the halo mass function (HMF), or, in the case of a particular host galaxy such as the MW, the subhalo mass function (SHMF), which is the number of subhalos as a function of their mass, $dN_{\mathrm{sh}}/dM_{\mathrm{sh}}$. These functions are intimately related to the primordial DM density perturbations, but also encapsulate all the nonlinear gravitational, plasma, and potentially rich dark sector physics experienced by the structures after they are formed. Thus, the SHMF is a complicated function of inherent DM properties as well as of primordial cosmological information and more quotidian data like the host mass and environment.

By "primordial" we mean the data that set the initial boundary conditions for the era of linear structure growth. At the present time, our knowledge of the primordial characteristics of the Universe is limited to the information we can extract from the cosmic microwave background (CMB) radiation and indirect measurements of the era of Big Bang nucleosynthesis (BBN). Large-wavenumber perturbations in the CMB are relevant for structures of galactic size. By "large-wavenumber", we mean that these scales correspond to inverse length scales that are of order 10 kpc or shorter. These perturbations grow during the cosmic dark ages of the early universe into structures of a great range of density and a remarkable range of diversity. However, the number and the gross features of small DM halos
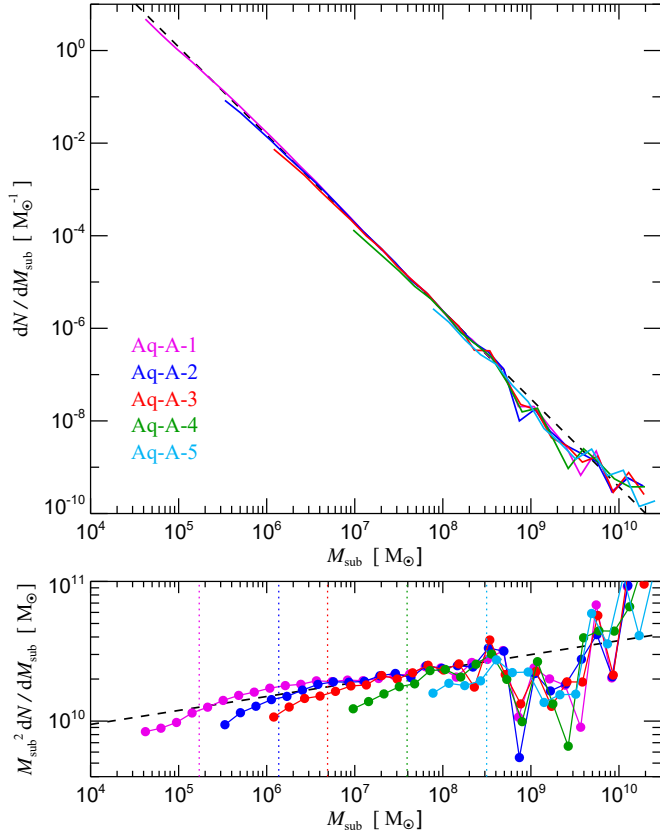
Figure 12: The halo mass function in a cosmological CDM simulation. From [326].

ultimately depend on the distribution of the primordial DM density perturbations at large wavenumber [248, 320, 321, 322, 323].

The DM density perturbations at high wavenumber are in turn determined by the precise phase space distribution of the DM. This determines how the DM overdensities (and, eventually, the baryonic overdensities captured within) grow as a function of cosmic time [324]. The DM phase space distribution is itself determined by the DM particle properties: when and how it was produced and attained an appreciable cosmic abundance, what interactions it had after that time, and how and when it decoupled from those interactions [17, 325]. For this reason, specific DM particle physics properties need to be specified in order to predict a particular distribution of DM on specific scales.

The baseline model adopted for most simulations of cosmic structure evolution is that of cold and collisionless dark matter, the CDM paradigm. Roughly speaking, CDM is expected to have a hierarchical distribution of structures, wherein small structures form first and merge to form large structures at lower redshift. Cosmological simulations reveal a HMF $dN_{\rm h}/dM_{\rm h} \propto M_{\rm h}^{-\alpha}$ for some positive constant $\alpha \lesssim 2$ [326]; this is illustrated in Fig. 12, where the dashed line compares simulation results against the model $dN_{\rm h}/dM_{\rm h} \propto M_{\rm h}^{-1.9}$. This scaling with halo mass appears to be largely robust against tidal effects from interactions with the host halo, aside from an increased scatter in the number of halos [327], which we provide an example of in Fig. 13. As discussed in more detail in this section, any deviation from the cold, collisionless, low-density, weakly coupled paradigm will result in a departure from (and generally a suppression of [328]) the HMF expected within CDM. Often, these departures will have characteristic features that reveal further details of the DM. In this way, an understanding of the SHMF of the MW is a sensitive method for investigating the essential characteristics of the DM.

A direct probe of the SHMF for halo masses above $\sim 10^8$ $M_\odot$ comes from counting dwarf galaxies within the MW. Above this characteristic mass scale, halos are expected to become efficient at en-
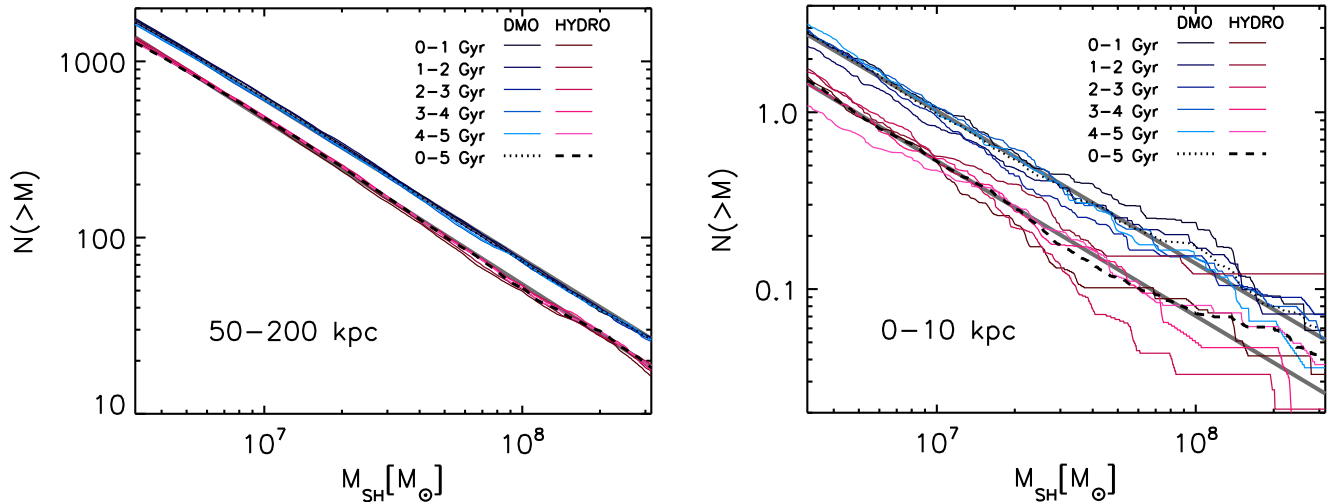
Figure 13: The subhalo mass function in a cosmological CDM simulation. **Left:** subhalos with large pericenter from their host halo. **Right:** subhalos with small pericenter from their host halo. There is an increased scatter when tidal interactions are more important. From [327].

couraging star formation [329, 330, 331, 332, 333]. Critically, it is the *peak* halo mass, rather than the present-day mass, which may have decreased due to disruption effects during infall, that controls this efficiency [332, 333]. The efficiency of star formation is the key parameter making such halos detectable, so we illustrate the correlation between the stellar mass and the halo mass in Fig. 14. We conclude that halos are amenable to searches for visible self-gravitating structures if they have masses $M \gtrsim 10^8$ $M_\odot$ or a characteristic velocity dispersion greater than $\sigma_v \sim \sqrt{2GM/R} \sim 10$ km/s, assuming that $R \sim 10$ kpc defines the size of small subhalos. (Smaller, denser, structures that are dominated by their baryonic gravitational potential such as globular clusters, nuclear star clusters, and giant molecular clouds are therefore not as informative as to the nature of the DM.) As discussed above in Sec. 4.2, our census of satellite galaxies of the MW has undergone a substantial growth in the recent past. The consensus is now that the MW resides in a DM halo with a typical population of subhalos [149]. This constrains major deviations from the CDM paradigm.

Because of these recent advances, the frontier of the search for the DM is now in the search for dark structures below the characteristic mass scale of star formation, $M \lesssim 10^8$ $M_\odot$. This requires new searches that extend observations from the direct search for luminous satellites to indirect methods that are sensitive to entirely dark substructures of the MW.

One method for looking for dark substructures are studies of lensing, as discussed in Sec. 4.4. This is a promising route for determining the mass function of cosmological CDM halos [334]. The amount of anomalous flux ratios observed in samples of gravitational lenses is consistent with the amount of substructure predicted in CDM cosmologies [335, 290]. Direct searches for microlensing of stars in the MW and Andromeda galaxies and the Magellanic Clouds by the OGLE [336, 337], MACHO [338], EROS [339], and Subaru HSC [340] collaborations confirm the CDM halo picture. The low rate of lensing events observed by these collaborations are compatible with the expectation of fluffy and low density CDM subhalos, and thus are primarily used to rule out other candidates [341, 342, 343]. Combining lensing with complementary information allows for even stronger constraints on all models [344].

Searches for patterns in other measurements of MW stars provide another handle for studying the particle nature of DM. The prospects for a positive detection of local substructure with pulsar timing arrays depends on the DM theory. Though the possibility of finding the dense subhalos predicted in non-CDM cosmologies is promising on the timescale of decades [317, 318], it is less promising in the case of fluffy CDM halos [345]. So far, other pattern-based studies mentioned in Sec. 4.4 are also not
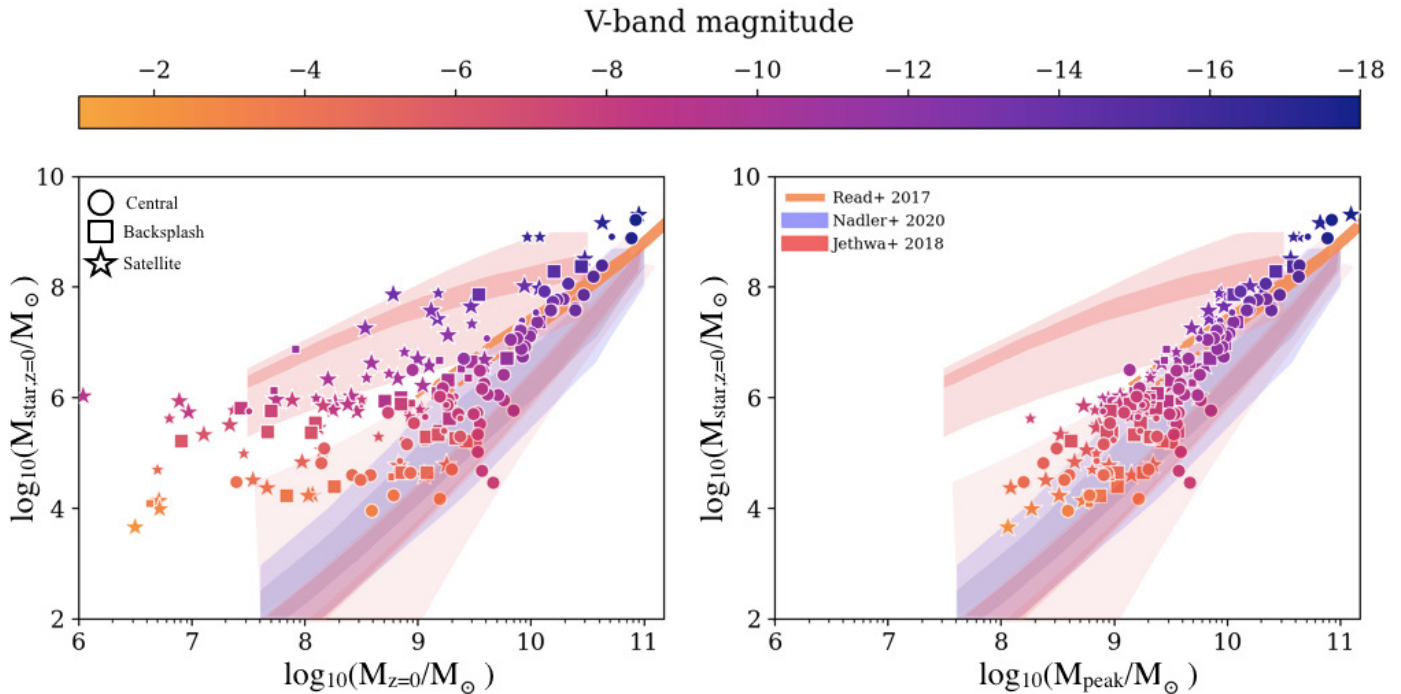
Figure 14: The stellar-mass/halo-mass relation as a function of subhalo mass at **(left)** $z = 0$ and **(right)** at peak mass before infall. Subhalos with peak mass before infall of $\gtrsim 10^8$ $M_\odot$ efficiently form stars. Shaded bands are theoretical predictions without tidal mass loss. Points are simulated galaxies. From [333].

competitive with lensing probes.

Stellar streams, surveyed in Sec. 4.3, offer another promising probe of the structure of the MW. Of particular interest is their ability to probe the nature of the smallest building blocks of the MW dark matter halo [347, 283]. Because of the small number and the unique nature of these streams, they are studied on an individual (rather than an ensemble) basis. We discuss two particularly well-known streams here.

The "poster child" stream Palomar 5 (Pal5) [270] is known to have a significant interaction with the MW bar [348, 349], presenting an irreducible background to searches for DM substructure in this system. We show updated observations of Pal5 compared with a set of simulated versions of a Pal5-like stream with and without simulated perturbers in Fig. 15 [346]: observations are reproduced at the top of the figure in blue; a simulation of an unperturbed, or "regular", stream which has undergone tidal disruption by its host galaxy, but has experienced no other external perturbative interactions, is shown in green; and a simulated stream with two interactions, evidenced by two gaps on the left (leading) and right (trailing) arm, is shown in red. We note that very recent simulations have also raised the possibility that mass segregation, which concentrates many black holes each of 3 $M_\odot$ or more in the central regions of Pal 5, can have a significant effect on its evolution [350].

The GD-1 stream is expected to be more robust against these confounding baryonic effects [351, 286] due to its large pericenter, retrograde orbit, and large inferred separation from known baryonic substructure [352], and is thus a promising target for detecting DM substructure [353]. Recently, observations of GD-1 have been used to probe the SHMF of the DM of the MW [352, 354, 355]. These studies indicate that the GD-1 stream most likely was perturbed by at least one dense, massive object — and it is unlikely to have been the Sagittarius dwarf remnant [354]. The rate of encounters of a stream on a GD-1-like orbit with a substructure of the virialized MW dark matter halo is expected to
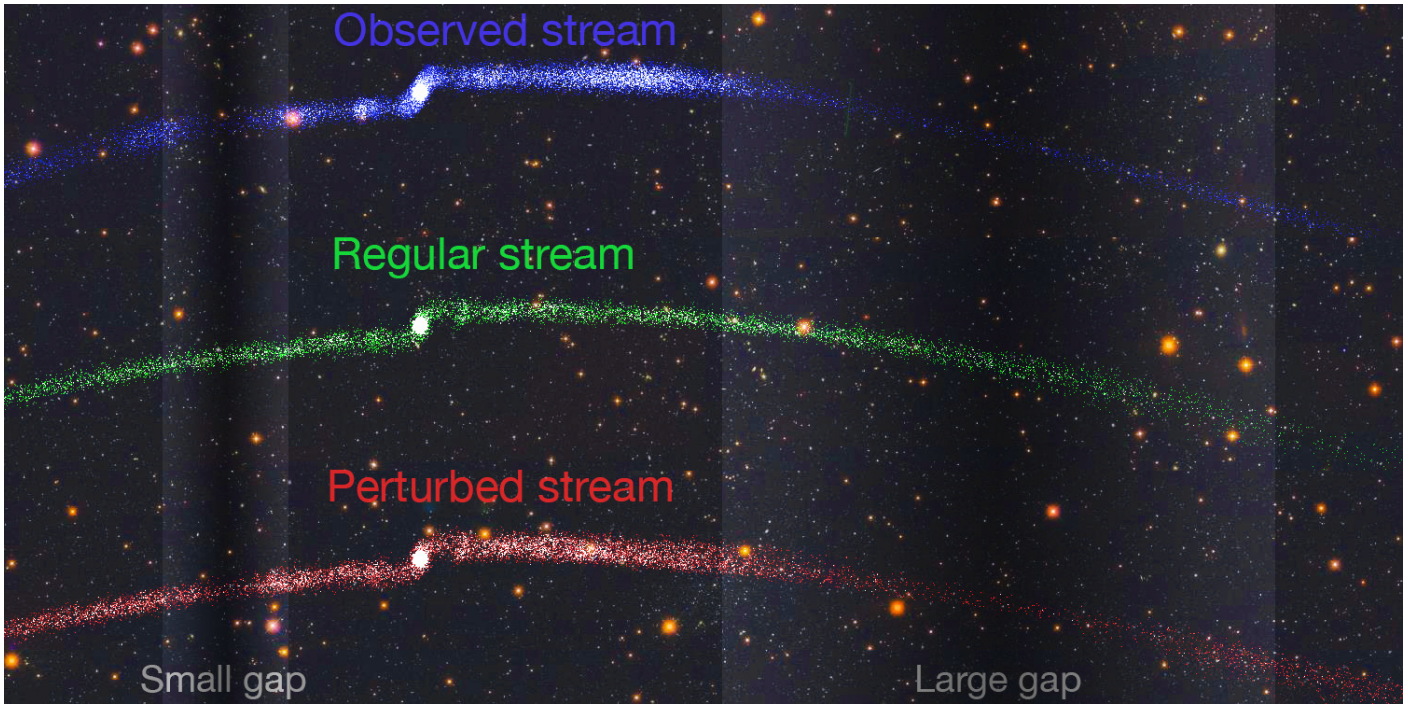
Figure 15: Comparison of observation and simulations of the Pal 5 stream with and without the gravitational influence of massive satellites of the simulated host. The body of the remaining Pal 5 progenitor is the white oval, left of center in each panel. Tidal stream stars escape the progenitor at two Roche-lobe overflow points, leading to a kink in the complete stream. From [346].

be large enough to account for the observed perturbation of GD-1 [286, 352]. Following the logic laid out above, this rate is evidence that the subhalo mass function must not overly be suppressed in the mass range $10^6 - 10^8$ M$_\odot$ [354, 355]. This provides evidence in favor of cold, rather than warm, DM, and has been used to constrain the mass of thermal DM to be larger than 4.6 keV [355]. On the other hand, the perturber may be somewhat more dense than expected in a conventional CDM-like scenario [352], potentially pointing the way to new physics, as shown in Fig. 16. However, if the interaction with the subhalo remnant is taken into account, N-body simulations suggest that a kinematically warm DM population may actually be preferred [356]. Studies of streams are still a relatively young subject, and will benefit from further exploration of potentially confounding physical effects.

In conclusion, studies of MW satellites and their invisible brethren are powerful but still-developing probes of the nature of the hierarchical structure formation paradigm. Counts of visible satellites match qualitative expectations from simulations, thus providing compelling evidence that the DM in our galaxy is formed roughly hierarchically at least down to subhalo masses $M \sim 10^8$ M$_\odot$. The stellar stream GD-1 provides further suggestive hints that hierarchical structure formation continues at least one order of magnitude lower in halo mass, and streams in general will be a compelling testbed for future advances in understanding the nature of the MW's assembly and current constitution.

5.2 Nearly Thermal Dark Matter

In the classification scheme adopted above, DM is characterized as being either cold, warm, or hot. This scheme relies fundamentally on the assumption that DM has reached thermal equilibrium at some point in its cosmological evolution. A stronger assumption that is often implicitly adopted is that the DM was in fact in *chemical* equilibrium *with the SM thermal bath*, as in the canonical weakly interacting massive particle (WIMP) scenario, where we use chemical equilibrium to refer to the equilibration of
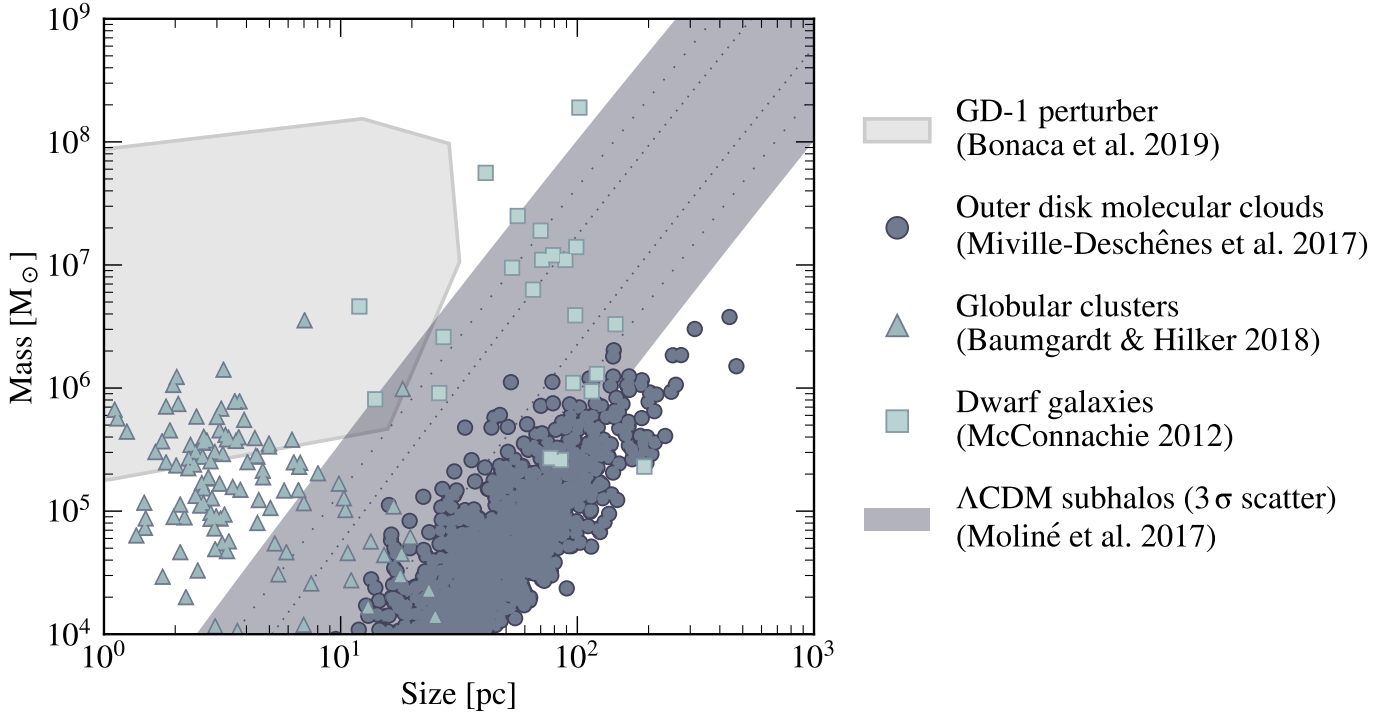
Figure 16: Inferred mass and size of the perturber of GD-1 compared to known constituents of the MW, both dark and luminous. From [352]©AAS. Reproduced with permission.

annihilation processes. We explore departures from both of these assumptions in this subsection, though for now we will still find it useful to compare the DM phase space distribution to the thermal SM phase space.

One possible departure from the conventional scenario is that DM could have attained thermal equilibrium and have a thermal phase space distribution $f_{\rm DM}(\mathbf{v}, z) \propto \exp(-3m_{\rm DM}v^2/2T_{\rm DM}(z))$, but the equilibrium temperature $T_{\rm DM}(z)$ describes only its own "dark sector". In order for the DM particles to shed their energy and entropy, they must be able to annihilate away some of its equilibrium abundance, except for a one-parameter family of particles with a temperature $\xi = T_{\rm DM}/T_{\rm SM} \simeq (T_{\rm mr}/m_{\rm DM})^{1/3}$, and with the requirement $m \gtrsim 530$ eV in order to become nonrelativistic at sufficiently high temperatures to match the high-wavenumber modes of the CMB. Suffice to say, such a scenario is sufficiently fine-tuned as to be unappealing. Instead, it is conventional to assume that a secluded dark sector has a light partner particle into which the DM particle can annihilate, thereby satisfying constraints on the relic density.

A related alternative is that the dark sector has a secluded number-changing self interaction. Such a DM candidate cannibalizes itself to keep warm [357]. This extra self-generated warmth slows the redshifting of energy and suppresses the growth rate of density perturbations [357, 358] to a degree that is ruled out by current observations [359] unless the interactions couple very late and change the density negligibly [360].

A DM candidate that differs in certain key respects from a simple thermal relic is sterile neutrino DM [320, 361]. This particle never reaches full thermal equilibrium with the SM bath. Rather than freeze out like a canonical WIMP, so that its relic density is determined once its interactions are no longer strong enough to maintain thermal equilibrium, such particles may "freeze in" over a long period of time or may attain the correct energy density during a brief period of resonance production (due, e.g., to a large lepton asymmetry). The sterile neutrino is constrained by MW satellite counts in much the same way as in the strongly interacting scenario discussed below in the context of dark matter with
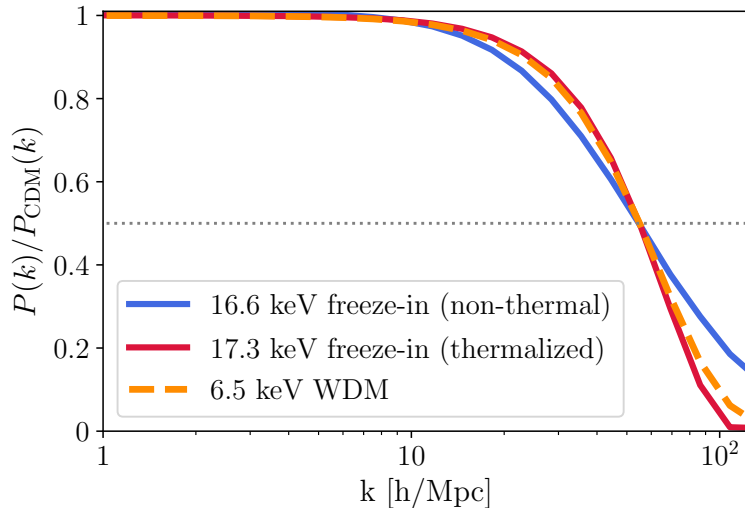
31

Figure 17: Transfer function for density perturbations of a dark matter particle that is "frozen-in" through a coupling with a light kinetically mixed dark photon compared to thermalized dark matter of different masses, from [366].

a large scattering cross section with SM material: too light of a sterile neutrino will have too large of a free-streaming length, and will suppress the formation of MW satellites below a characteristic mass scale [325]. We show these bounds in Fig. 19.

The sterile neutrino freeze-in process has been generalized in a number of ways since [362, 363, 364]. Recently, the calculation of the necessary parameters to achieve the correct DM energy density has been performed in the context of DM that interacts with the SM through a very light kinetically mixed dark photon [365, 366]. This model, like the sterile neutrino, is kinematically colder than a completely thermalized particle of the same mass, but with a very long high-velocity tail. Both of these novel features must be accounted for when calculating the expected subhalo abundance. We show the transfer function of this DM candidate in Fig. 17.

5.3 Extremely Massive and Ultralight Dark Matter Candidates

Extremely massive and ultralight DM candidates differ from the preceding cases by having no notion of temperature. Instead, these candidates are completely athermal, and derive their energy density from a novel mechanism unrelated to the thermal energy of the SM or dark sector bath. See [367] for a recent overview of model possibilities.

By extremely heavy DM candidates, we mean DM composed of particles that are so massive that their individual nature becomes apparent. In some sense, the particulate nature of DM structures is then probed directly, instead of the averaged thermodynamic quantities that we typically consider, such as the local and cosmic density. The archetypal heavy DM candidate is the primordial black hole (PBH) [368], but composite extended structures such as nuclear-like dark many body states can also grow to become extremely massive in the early universe [369, 370, 371, 372, 373, 374, 375], with unique observational signatures [376, 377, 378].

On the other hand, ultralight DM candidates are those whose mass is so low that they form extremely high-occupancy states, and thus behave more like a classical wave than like a classical particle: their de Broglie wavelength λ_{dB}, which is inversely proportional to their mass and their characteristic velocity dispersion, exceeds their interparticle spacing in the MW and its satellites when $m_{DM} \lesssim 100$ eV. For a recent review, see [379]. Such particles will induce a diminished dark matter transfer function
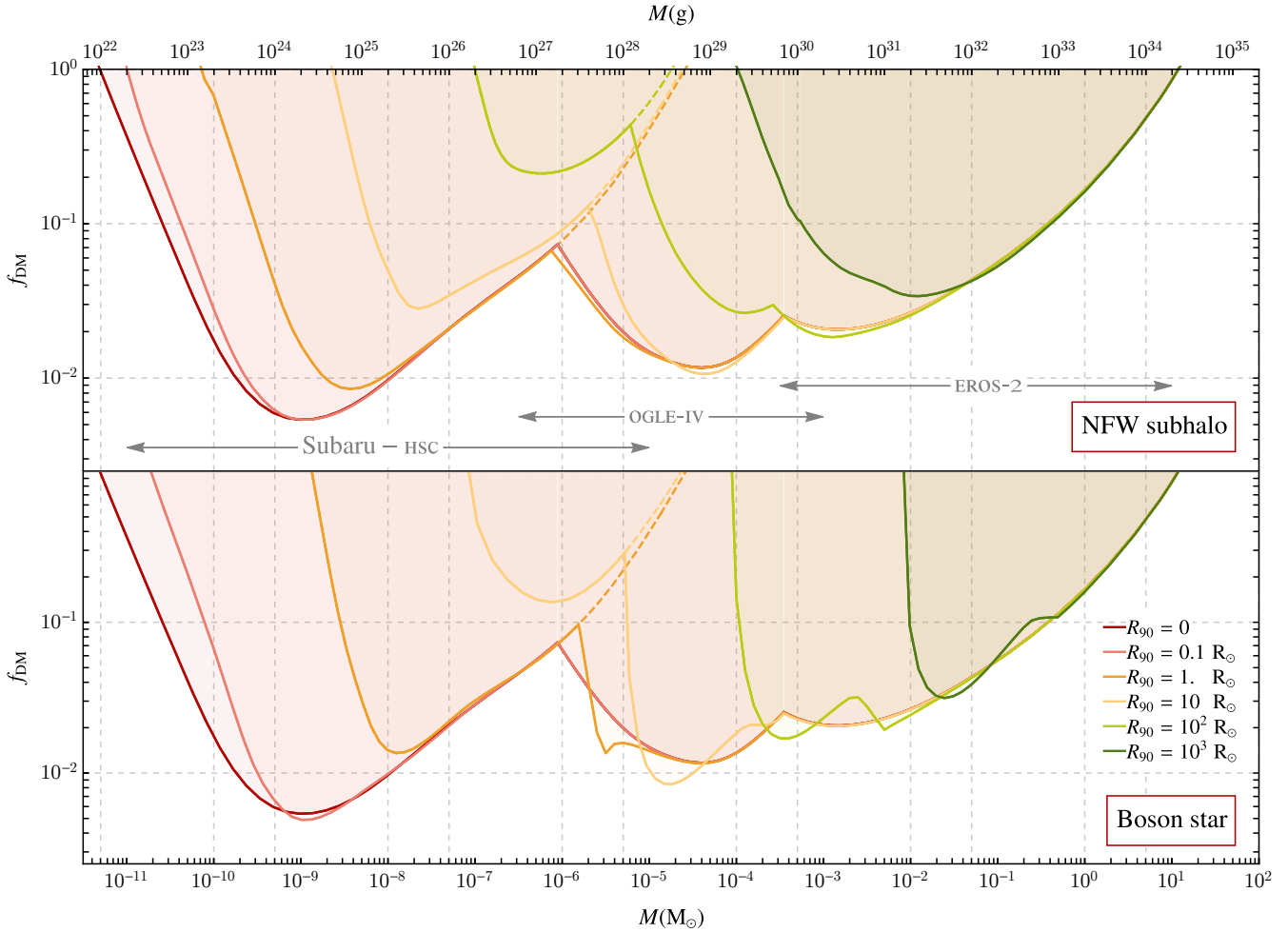
Figure 18: Constraints on dense halo objects formed from extremely massive or ultralight dark matter candidates. Reprinted with permission from [342, 343]. Copyright 2020 by the American Physical Society.

above a characteristic wavenumber set by their mass because their quantum nature prevents them from collapsing on scales smaller than their de Broglie wavelength. This is macroscopically important when that wavelength matches the ~ 10 kpc dwarf galaxy length scale mentioned above. By assuming a characteristic velocity dispersion of $\bar{v} \sim 10$km/s, one can calculate that ultralight DM will match the dwarf galaxy length scale at currently probed sizes of $\gtrsim 10$ kpc if the dark matter mass is less than $m_{\mathrm{DM}} \sim 10^{-22}$ eV, since $\lambda_{\mathrm{dB}} = (m_{\mathrm{DM}}\bar{v})^{-1} \simeq 10$kpc $\times (m_{\mathrm{DM}}/10^{-22}\mathrm{eV})^{-1}$ [380]. Dark matter of mass well below this value will not "fit" into dwarf galaxies, inhibiting their growth and unacceptably suppressing the subhalo mass function in conflict with observations [381, 382, 383]. This may be extended to larger and smaller systems with current and future data [384, 385].

In the context of the MW, there is an interesting and perhaps surprising convergence between ultralight and extremely massive DM particles. This happens because ultralight particles typically have attractive self-interactions that cause them to form ultra-dense agglomerations over cosmic timescales [386, 387, 388, 389, 390, 391]. Thus in both cases, these DM candidates are probed by lensing searches. Treating the heavy objects as point lenses [341] (as appropriate for a PBH) or extended lenses [342, 343] (as appropriate for a composite object of self-interacting particles) changes the constraints somewhat. We show results assuming either an NFW or a boson-star-like density profile in Fig. 18.

Compact objects such as PBHs also have the ability to dynamically disrupt observed stellar systems

33

Figure 19: Constraints on non-CDM dark matter candidates reproduced from [325]. **Left:** constraint on the mass and elastic scattering cross section between a dark matter particle and the proton. **Right:** constraint on the mass and mixing angle of a sterile neutrino.
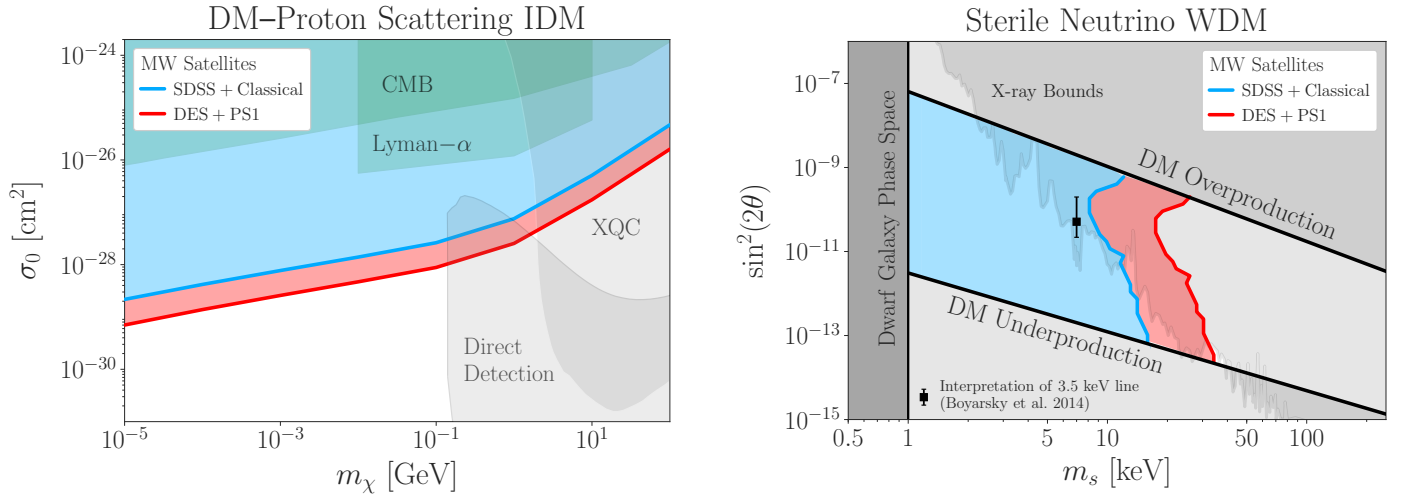
[392, 393, 394]. Fokker-Planck simulations of dwarf galaxies exclude compact objects of mass M_{CO} from constituting a fraction $f \simeq (M_{CO}/10 \ \mathrm{M_\odot})^{-1}$ of the total DM in the MW [395, 396]. Simulations of wide binaries in the MW stellar halo lead to similar bounds with slightly lower masses [397]. See [398] for a more detailed discussion and for additional non-dynamical constraints on compact objects. The convergence in physical effects noted above in the case of lensing also carries over to dynamical considerations, and has been used to place strong constraints on ultralight DM [399].

5.4 Interactions of Dark Matter with Standard Model Matter

Dark matter that interacts so strongly with the SM that it cannot penetrate the Earth and reach underground DM direct detection experiments (sometimes referred to as IDM) is probed in a multitude of ways. We set aside cosmological and direct probes of such DM models, and focus here on the implications for the subhalo abundance of the MW.

These strong interactions will couple the DM fluid to the baryon fluid at the time of the formation of the CMB, at a time when the baryons are being prevented from falling into overdense halos by the pressure of the hot and abundant photons. This means that the subhalo abundance is suppressed in these scenarios [400, 325, 401]. The severity of the suppression depends on the temperature of the decoupling of the DM and SM fluids. The scattering cross section of such a DM candidate with baryons is constrained by comparing calculations against the current measurements of the SHMF, in analogy with the SIDM case above. We show recent constraints on this type of model in Fig. 19. In addition, much of the parameter space of these models are subject to stringent constraints from their contributions to the energy density of the Universe during the epoch of BBN [402].

5.5 Self-Interacting Dark Matter

Self-interacting DM (SIDM) was initially proposed as a solution to both the core-cusp problem and a seeming dearth of small MW satellites [403]. We will not further address the inner profiles of MW satellites except to say that in SIDM scenarios these problems and their resolutions are inherently linked.

The SIDM power spectrum features a high-k cutoff that is similar to that of warm DM [404, 405], although SIDM can additionally feature dark acoustic oscillations [406, 407, 408] that can serve as a powerful distinguishing marker of additional model complexity. However, the additional complexity of the self-interacting dark sector means that any prediction of high-k power is dependent on a large number of model parameters. These can be summarized in terms of a dark kinetic decoupling temperature, analogous to the temperature at which the SM particles decouple from the photon bath and begin to form structures [404, 405, 408]. If this temperature happens to be close to the corresponding temperature at which high-k SM modes decouple from the photon bath, $z_{\rm kd,\,SM}^{\rm (high-k)} \simeq 4$ keV as discussed above, then the deviation from the CDM power spectrum can be visible in field galaxy counts.

Understanding the SHMF of SIDM involves physics that is both unique to the subhalo and physics that connects the subhalo to its host. For instance, the gravothermal evolution of the self-gravitating SIDM halo, and the eventual gravothermal catastrophe befalling all self-gravitating systems [409, 410, 411, 412], is a necessary ingredient for drawing conclusions about the nature and the density of observed SIDM halos [413, 414, 415]. When considering SIDM subhalos in the MW, tidal interactions can play a critical role in interpreting the SHMF [416, 413, 414]. These factors, sometimes mitigating and sometimes compounding the effects of the self-interactions, must be taken into account when drawing inference about DM self interactions.

5.6 Dark Matter with Inelastic Transitions

Dark matter that can interact via inelastic transitions, either through internal excitation [81] or light-particle emission [82], has a very different phenomenology than DM that only interacts elastically. This type of DM can form structures very similar to those formed by the SM, ranging from the length scales of acoustic oscillations in the early universe [407] to structures of the size of the MW disk [155, 156] and below [408, 417, 418, 419]. In fact, such dissipation can be the key to forming the extremely massive composite DM candidates discussed in the previous subsection [369, 370, 371, 372, 373, 374, 375].

Most interesting for studies of galactic dynamics is DM equipped with a dissipative force. This can form a dark disk, which may be coincident with or at least concentric with the MW stellar disk. This impacts the matter surface density observed by stars in the local neighborhood, and can thus have an observable effect on their phase space distribution [155, 156, 420, 421]. Inferences on the dark disk density using observations from the *Gaia* satellite have thus far been limited to the equilibrium case [422], which, as argued above, needs to be improved upon given our updated knowledge of the dynamics of the MW. We discuss inference of the local DM energy density more below in Sec. 7.1.

6 Probes of Change

Our ability to ascertain *change* in the MW — beyond the birth and death of single stars — has come as quite a surprise. Certainly, the DF formalism we have outlined in Sec. 2 is constructed to address a system in steady state. Although the existence of the MW's spiral arms and the discovery of the Galactic bar speak to non-steady-state effects, it has been thought that these effects could be accommodated with only small adjustments of the DF formalism, despite the fact that the spiral arms signal a spiral distortion in the Galaxy's gravitational field. This engenders radial mixing of the gas and stellar disks, with stellar distributions in metallicity and age giving observational support to such effects — yet the overall angular momentum distribution may be largely undisturbed [423]. Considerable evidence for imperfections throughout the Galactic disk also exists, however: it is warped and flared in HI gas [99, 100] and in stars [101, 102], and we have already noted the striking evidence for the latter from three-dimensional maps of Cepheids [103, 104]. Rings [424, 425] and ripples [426, 196] in regions farther from the Sun, where the disk is relatively thin, have also been noted.
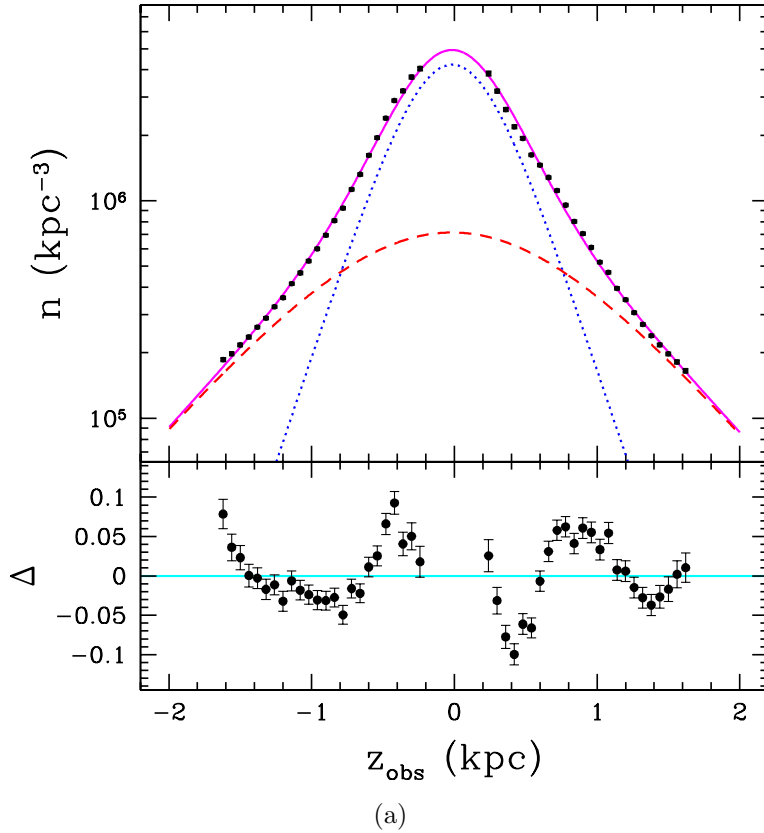
Figure 20: Estimated number density n as a function of observed distance z_{obs} from the Sun (top), using photometric parallaxes and SDSS observations of K and M dwarfs within an in-plane distance of 1 kpc, with the black points showing the observed star counts, including an overall normalization factor. The magenta curve is a model fit to those points, assuming no North-South breaking, and the contributions from the thin (blue dots) and thick (red dashes) disks as well. The bottom panel shows $\Delta \equiv (\mathrm{data} - \mathrm{model})/\mathrm{model}$, revealing a wave-like vertical asymmetry, north and south. From [427]©AAS. Reproduced with permission.

We believe that observations of wave-like asymmetries near the Sun's location in main-sequence stars from the SDSS [427, 428], in vertical velocities of red-clump stars from the RAVE survey [429], as well as from *Gaia* DR2 [430], speak to a sea change, revealing the existence of non-steady-state effects in the solar neighborhood. Evidence for axial-symmetry breaking of out-of-plane main-sequence stars in the north with SDSS has also been observed [102]. The astrometry of *Gaia* DR2 [24, 27] has greatly enriched these studies. For example, the striking snail shell and ridge correlations within the position and velocity components of the DF [197] have also been discovered, revealing axially asymmetric and presumably non-steady-state behavior. This, as they note [197], is attributable to the existence of the Galactic bar, spiral arms, as well as of other, external perturbations.

In what follows we discuss probes of non-steady-state effects broadly, considering first evidence from north-south symmetry breaking and phase-space correlations, before turning to the study of broken stellar streams and intruder stellar populations. The latter two — and probably the last three — probes are of such complexity that they serve as *prima facie* evidence for non-steady-state effects. In the case of north-south symmetry breaking, we note that a study of north-south and axial symmetry breaking can framed to show concretely that the MW is not in steady state, following the theorems we have discussed in Sec. 2 [44, 29]. The particular origins of these various symmetry-breaking and phase-space correlation effects are not well-established, but we review various proposed explanations —
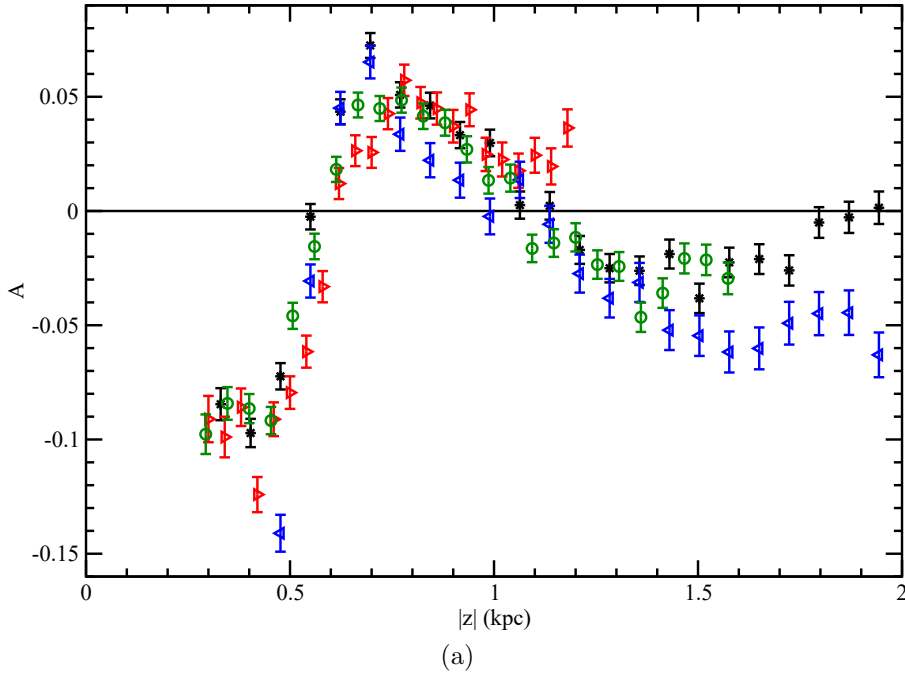
Figure 21: The asymmetry in star counts, north and south, with height $|z|$ from the Galactic mid-plane, for different bands in $(g - i)_0$ color. Note $1.8 < (g - i)_0 < 2.4$ (black), $0.95 < (g - i)_0 < 1.8$ (blue), $0.95 < (g - i)_0 < 1.8$ (red), and the green points employ a distance relationship based on $(r - i)_0$ color. From [428]©AAS. Reproduced with permission.

all of which involve external perturbations.

6.1 North-South Symmetry Breaking

We show the first observation of a vertical asymmetry in stellar number counts, from [427], in Fig. 20, with distances computed using a photometric parallax relation. A follow-up analysis confirms this result, as shown in Fig. 21 [428]. The north-south *asymmetry* is defined as

$$A(|z|) \equiv \frac{n(z > 0) - n(z < 0)}{n(z > 0) + n(z < 0)}, \tag{13}$$

where $n(z)$ are the stellar number counts north ($z > 0$) and south ($z < 0$), measured from the Galactic mid-plane. The insensitivity of the observed vertical asymmetry to stellar selection suggests that it is indeed a density wave. We also note results from the RAVE velocity survey that show evidence for vertical ringing in V_z of stars [429] at similar distances to those studied in [428], as well as an observed vertical wave in mean metallicity [431], inferred from SDSS photometry, with features similar to the observed density wave.

To probe the possible origin of the vertical symmetries we have noted, we turn to a combined analysis of axial and north/south symmetry breaking [44], using a sample of 14 million *Gaia* DR2 stars within 3 kpc of the Sun's location, carefully selected for sensitive studies of symmetry breaking [29]. The axial asymmetry $A(\phi)$ is determined by counting stars on either side of the anti-center line in the Galactocentric longitude $\phi = 180°$, computing

$$A(\phi) = \frac{n_L(\phi) - n_R(\phi)}{n_L(\phi) + n_R(\phi)}, \tag{14}$$

Figure 22: The axial asymmetry $A(\phi)$ with ϕ, for selections north (N) and south (S), (a) red (S), black (N), and blue (N+S), (b) we compare $A(\phi)$ in the N+S sample with the difference of $A(\phi)$ in the north and $A(\phi)$ in the south (N-S) (squares). From [44]©AAS. Reproduced with permission.

where $n_L(\phi)$ and $n_R(\phi)$ are defined as the number of stars, left and right, of the anti-center line. This observable probes the vertical component 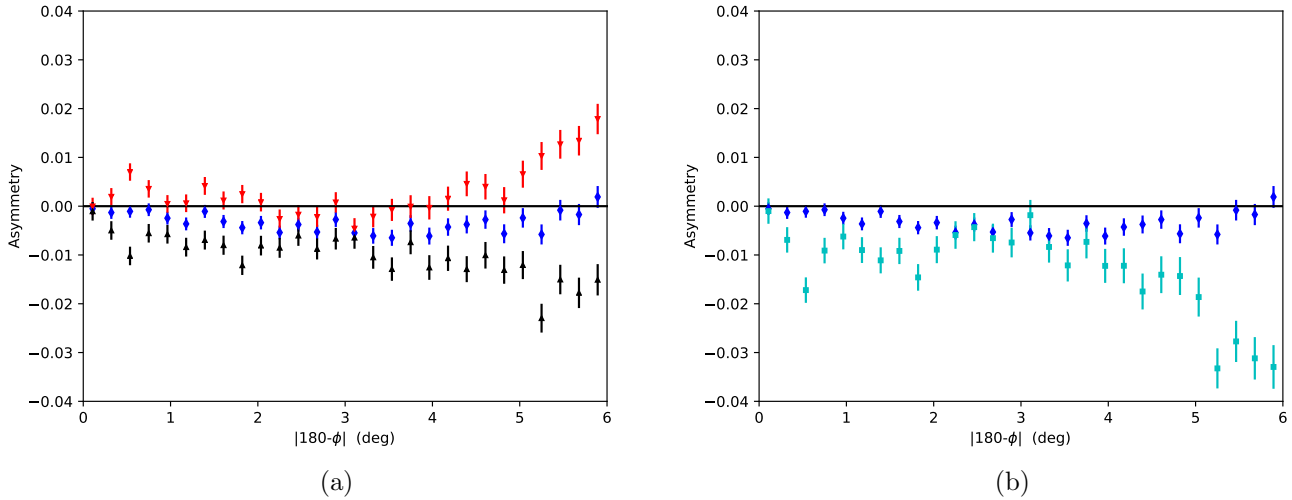of the angular momentum as an integral of motion; that is, if $A(\phi) = 0$, it is conserved, as per our discussion of Noether's theorem [40] in Sec. 2. The result of this evaluation for stars with $z > 0$ (north N), $z < 0$ (south S), and for all z (N+S) is shown in Fig. 22. Since $A(\phi) \neq 0$ in all cases, axial symmetry is broken, but it is also apparent that $A(\phi)|_N - A(\phi)|_S \gg A(\phi)|_{N+S}$. This pattern of symmetry breaking, as per our discussion of [46] in Sec. 2, can only result if our large sample of stars is not in steady state. Ergo the Galaxy near the Sun's location is not in gravitational equilibrium. This outcome supports an external perturbation origin for the vertical asymmetries, and for the novel phase space structures we consider in the next subsection.

We first pause to consider the north and south pattern of the asymmetries shown in Fig. 22a. These results in the solar neighborhood can be compared to the axial asymmetries expected from the distorted halo shapes determined from the analysis of peculiar velocities of stars in the Orphan stream [192]. The outcome suggests that the halo of the MW is prolate in shape and tilted in the direction of the LMC/SMC system [44], as illustrated in Fig. 6. The prolateness of the halo is distinguished by comparing subtle differences in star counts in the northern vs. southern hemispheres, building on the result of [192]. Including the effects of the Sagittarius dwarf as well appears to adjust the picture to favor an oblate and possibly radius-dependent geometry [194], and their results also support a large mass for the LMC, in agreement with [192]. On the other hand, earlier studies of flaring HI gas in the outer galaxy support a prolate DM distribution [110]; these authors note that a prolate halo can support long-lived warps [111], which would help to explain why they are commonly seen [110].

In other galaxies, [432] shows that one can determine whether external galaxies are more prolate or oblate in their stellar distributions by observing their stellar density profiles as another check on N-body models of DM if the DM DF reflects that of light. Whether or not this is so has not yet been established.
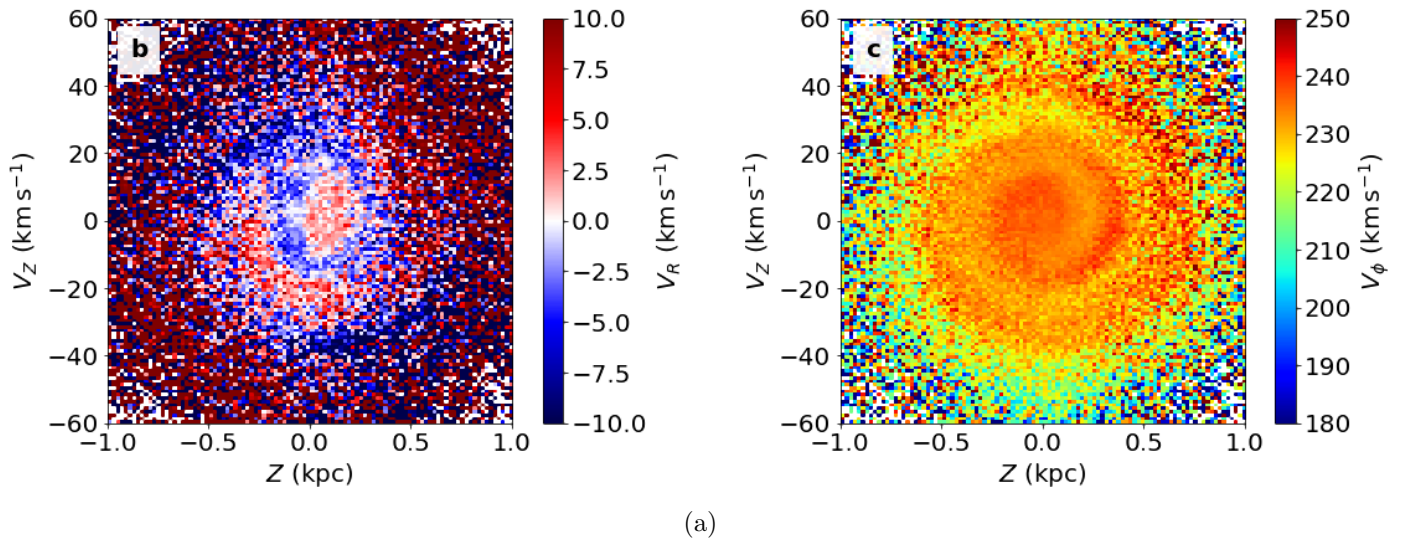
Figure 23: Distribution of stars located $8.24 < R < 8.44$ kpc from *Gaia* DR2 data in the vertical position-velocity $(Z - V_Z)$ plane colored as a function of median V_R (left) and V_ϕ (right) in bins of $\Delta Z = 0.02$ kpc and $\Delta V_Z = 1$ km s^{-1}. From [197], reprinted by permission from Springer Nature.

6.2 Phase-Space Correlations

We show the novel phase-space correlations of the so-called *Gaia* snail in Fig. 23. This structure is apparent in a vertical velocity-position phase space diagram. It indicates strong evidence for recent and on-going disturbances of the disk of the MW by interloper structures such as the Sagittarius dwarf or other massive structures with a significant vertical component to their motion.

Thus it would seem that the vertical asymmetries in the stellar density may indeed be due to an ancient impact, possibly by the Sagittarius dwarf galaxy [427]. Support for the impact hypothesis comes from numerical simulations [191, 433]. The novel phase-space structures noted by [197, 434] also offer support to the impact hypothesis, as such features had been predicted as a consequence [191, 435, 436, 437]. We refer to [438, 190] for a review of the state of observations of phase-space correlations and the theory behind the *Gaia* snail. Note that assigning responsibility for the snail to one particular dwarf such as Sagittarius may be problematic [439], and that models continue to evolve and benefit from additional data.

Recently, too, the discovery of stars with non-prograde kinematics in the disk has led to determination of a previously unidentified ancient impact, from *Gaia*-Enceladus (or the *Gaia*-Sausage) in the inner halo [182, 183], which we discuss further later. Finally, [440] have noted significant merger debris, and streams, in the halo, which are also an expected consequence of ancient impacts.

6.3 Fitting Broken streams and the Galactic potential shape

Detailed observations of tidal stellar streams in the halo of our MW are potentially strong probes of the distribution of matter, including the DM, on scales of 20-100 kpc, as overviewed in Sec. 4.3. Combining observations of stellar position, proper motion, radial velocity, distance estimates and density of stars along halo stellar streams is potentially an extremely strong probe of the Galactic potential at radii inside the streams' orbit. There are at least two known cases where segments of streams originally identified as independent are now thought to be originate from the same stellar cluster. The Orphan stream (above the Galactic plane) and the Chenab stellar stream (below the plane) have been observed to share close orbital parameters and in fact may have a common origin [441]. Models are being

undertaken to show how an interaction with the LMC at some time in the past can explain a prominent feature in the stream [192]. More recently the ATLAS and Aliqa Uma stream segments appear to share a common origin [442]. The nearby halo streams of GD-1 and Khir also potentially share a common origin [443]. The full potential of using broken streams to constrain the mass of the LMC are still limited by the precision of the available data, with error on distances being the limiting factor. A stream which covers a wide range in distance between its apo- and peri-galacticons can be used to put a constraint on the mass within — such as has been done with the Orphan stream [444].

Aside from broken streams, at least one stream is observed to have a kink along its length. This is thought to be evidence of an interaction with an otherwise unseen massive perturber [352, 355]. The implications of this interaction for theories of DM have been discussed in more detail in Sec. 5. A calculation by [286] shows how the presence or absence of gaps in the density of stars along a stellar stream may be used in a more general way to constrain the mass and number density of DM blobs floating through the halo.

6.4   Intruder Stellar Populations

Gaia has contributed to our understanding of the history of how the Galaxy has built up over time, as recently reviewed by [445]. The largest past merger has been that of the *Gaia*-Enceladus-Sausage, though recent work suggests that this is in fact two separate mergers. The smaller of these nearly simultaneous mergers, dubbed the Sequoia merger [446], is distinguished by having released stars on kinematically distinct retrograde orbits. The Sequoia merger may possibly have left a dwarf galaxy nucleus remnant today in the form of the so-called ω-Cen globular cluster, though it is likely not a true globular cluster due to its multiple stellar populations. The case for two ancient mergers has also been made by [447]. The metallicities and kinematics of these merger remnants are present today in the disk of the MW.

Whether or not smaller merger remnants in the disk can be isolated is an on-going topic of research with an ever-growing list of techniques. For instance, [448, 449, 278] find evidence for stars in a nearby stream, Nyx, using, in part, machine learning techniques, and [450] are able to disentangle populations of stream stars embedded within the disk of relatively low contrast, again taking advantage of the excellent *Gaia* dataset. Determining the limits of sensitivity of these new techniques is the subject of ongoing work, and caution is advised in identifying intruder populations via any single technique. If possible, using multiple methods, such as chemical signatures and kinematic markers, is necessary to draw inference on the nature of the possible merger remnants, as carried out by a recent analysis of Nyx candidate stars with the GALAH survey [451].

7   Implications for the Local Dark Matter Phase Space Distribution

The local DM phase space distribution, namely, the distribution function, $f_{\rm DM}(\mathbf{x}, \mathbf{v}, t|R_\odot)$, at the Sun's location, reflects all of the environmental and evolutionary factors we have discussed thus far. This object is defined as the one-body distribution function, and is well-posed regardless of whether the assumptions that would lead it to be a solution of the collisionless Boltzmann equation, as we discuss in Sec. 2, are fulfilled. Here we provide a summary of what is known about this elusive object, noting first that it is the local DM mass density, $\rho_{\rm DM}(R_\odot) = M_{\rm MW} \int d^3\mathbf{v} f_{\rm DM}(\mathbf{x}, \mathbf{v}, t|R_\odot)$, where $M_{\rm MW}$ is the total mass of the MW, and the local DM velocity distribution, $f_{\rm DM}(\vec{v}|R_\odot) = \int d^3\mathbf{x} f_{\rm DM}(\mathbf{x}, \mathbf{v}, t|R_\odot)$, that are of greatest interest to DM direction detection searches, as we have highlighted in Sec. 2. We will first treat the total local DM density, $\rho_{\rm DM}(R_\odot)$. Then we will discuss the local DM velocity distribution, $f_{\rm DM}(\mathbf{v}|R_\odot)$, including possible contributions from partially mixed phase-space structures.
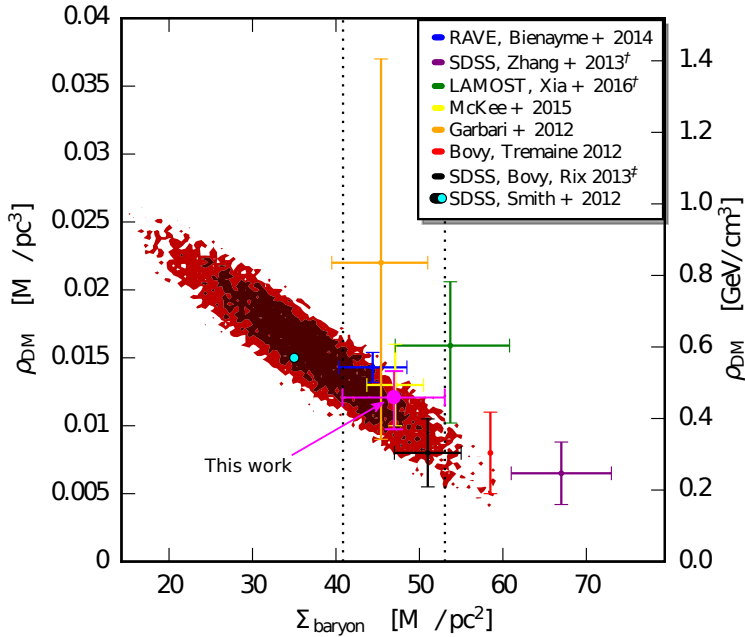
Figure 24: Illustration of the degeneracy in the determination of the local dark matter density and the baryonic surface density, comparing the two-dimensional marginalised posterior of [452], with the results of particular groups. From [452], and we refer to that reference for all details.

7.1 The Local Dark Matter Density

A long-standing problem has been the determination of the matter density in the vicinity of the Sun [453], as inferred from the measured kinematics of the local stars [454]. In this so-called Oort problem, a sample of stars, assumed to be in a gravitationally relaxed, or steady, state is used to trace the local gravitational potential and to infer the local matter density. We note Refs. [38, 455] for a detailed account of earlier work. Since such dynamical methods yield the total matter density, a careful accounting of ordinary, or baryonic, matter must be made simultaneously, because it is their difference that gives the local dark matter density. A local census of baryonic matter in the solar neighborhood, including stars, brown dwarfs, and gas, gives $0.0889 \pm 0.007 M_\odot \, \mathrm{pc}^{-3} = 3.4 \pm 0.3 \, \mathrm{GeV \, cm}^{-3}$ [420], consistent with the assessment of $0.09 \pm 0.01 M_\odot \, \mathrm{pc}^{-3}$ in [38], even if their detailed contents differ. The dynamical mass estimate has been assessed to exceed this by 10% [38], and indeed $0.3 \, \mathrm{GeV \, cm}^{-3}$ has traditionally been estimated to be the local dark matter density in the SHM [31], which we have reviewed in Sec. 2. Recently, progress has been made through the simultaneous, but separate, analysis of the baryonic and dark matter contributions in an integrated Jeans equation analysis [452]. Although the stellar tracers of the gravitational potential are certainly blind to the distinction between visible and dark matter, the degeneracy between these two forms of matter is broken if one works a few vertical scale heights above the Galactic plane [456], because there the contribution would be mostly dark matter. The outcome of this analysis is shown in Fig. 24; it can be seen that the apparent discrepancies between groups are ameliorated once the baryonic-dark matter degeneracy is taken into account [452]. We also note the outcome from a Jeans analysis of *Gaia* EDR3 and APOGEE data, $\rho_{\mathrm{DM}}(R_\odot) = (8.92 \pm 0.56 \, (\mathrm{sys})) \times 10^{-3} M_\odot \mathrm{pc}^{-3} \, (0.339 \pm 0.022 \, (\mathrm{sys}) \, \mathrm{GeV cm}^{-3})$ [208], as well as a determination from precision binary pulsar timing measurements, $\rho_{\mathrm{DM}}(R_\odot) = -0.004^{+0.05}_{-0.02} M_\odot \mathrm{pc}^{-3}$ [313], once the baryon density is removed [457], with a Jeans analysis of *Gaia* DR1 data finding local DM densities compatible with either result depending on the stellar tracer population chosen [420].

The appearance of vertical oscillations in the stellar number counts and velocity distributions of the

MW [427, 428] and variations in the effective vertical height of the Sun across the Galactic plane [102], speaking to warping in the disk, strongly suggests the existence of non-steady-state effects, for which we have reviewed definitive evidence in Sec. 6. Thus the explicit time-dependence of the DF must be taken into account, as in Refs. [458, 452]. It is important to emphasize that suitable DFs have to be simultaneous solutions of the collisionless Boltzmann and Poisson equations, as discussed in Sec. 2. This work was completed before the release of the *Gaia* DR2 data, and with the discovery of striking axial symmetry breaking features, such as the *Gaia* Sausage [197], it is apparent that terms neglected in previous analyses can be significant. Indeed, larger variations in the dark matter density have been found, even varying up to a factor of 2 larger than the SHM result [459]. For reviews of systematic uncertainties and different approaches to this problem, see [455, 460].

We note that increasing the local dark matter density should not shift the normalization of the rotation curve (i.e., the plot of V_c versus galactocentric distance, as shown in Fig. 7 and discussed in Sec. 3.4) by a large amount. This is true because most of the enclosed mass at the solar circle, and thus the largest contribution to the circular velocity at $R \approx R_\odot$, is due to the density of baryonic matter (stars). This latter mass density is not perfectly known, and extractions of its value are anticorrelated with the local DM density [452], as shown in Fig. 24. On the other hand, if the density of luminous stars is well constrained, then small dips and wiggles in the rotation curve can be used to map out a residual dark component with some accuracy. Certainly any axial asymmetries there, or in the local stars [44, 29] could be used to constrain the axial-symmetry-breaking terms in a Jeans analysis, leading to improved assessments of $\rho_{\rm DM}(R_\odot)$.

While data so far have focused nearly entirely on stellar positions and velocities (i.e., the 0th and 1st derivatives of motion), over time, *Gaia* data and upcoming data from pulsar timing arrays are of sufficient accuracy that accelerations in star motions may be eventually be able to be used to constrain the MW's potential [312, 314], as discussed in Sec. 4.4.

7.2   The Local Dark Matter Velocity Distribution

The local DM velocity distribution $f_{\rm DM}(\mathbf{v}|R_\odot)$ is important chiefly for interpreting experimental results related to the direct detection (DD) of DM, although we note that *comparisons* between such experiments are nevertheless possible without knowledge of this distribution [91, 461]. Our knowledge of $f_{\rm DM}(\mathbf{v}|R_\odot)$ is informed by our knowledge of global properties of the MW, which allow simulators to identify MW analogues in cosmological N-body simulations of DM structure formation [462, 463, 464, 465, 466, 467]. These global properties have been discussed in Sec. 3.

When constructing a semi-empirical dark matter velocity distribution suitable for interpreting dark matter direct detection data, it is particularly important to account for known local structures, such as the Sagittarius dwarf [468]. In the limit of a large number of DM events in a near-future DD experiment, it may conversely be possible to extract this information from the recoil spectra [80, 469].

The task of identifying kinematically distinct components of the stellar halo and converting these to weighted contributions to the DM halo has undergone a rapid and substantial evolution in the last several years [470, 470, 471, 472, 459, 473, 474, 475]. A consensus has roughly emerged that distinct phase-space substructures can account for at most $\lesssim 20\%$ of the DM velocity distribution [476, 459, 475], and departures from the SHM given in Eq. (7), which assumes a Maxwellian velocity distribution for 100% of the DM halo, as we have discussed in Sec. 2, are correspondingly small [459, 471, 477, 475, 478].

The fact that these departures are small does not mean they cannot be quantified. A velocity distribution that is more realistic than the SHM has been developed recently. The SHM^{++} [459] is not strictly isotropic and isothermal. It accounts for the *Gaia*-Enceladus merger by adding to the SHM a new anisotropic component governed by a single parameter $\beta = 1 - (\sigma_\theta^2 + \sigma_\phi^2)/2\sigma_r^2$, where σ_i are the
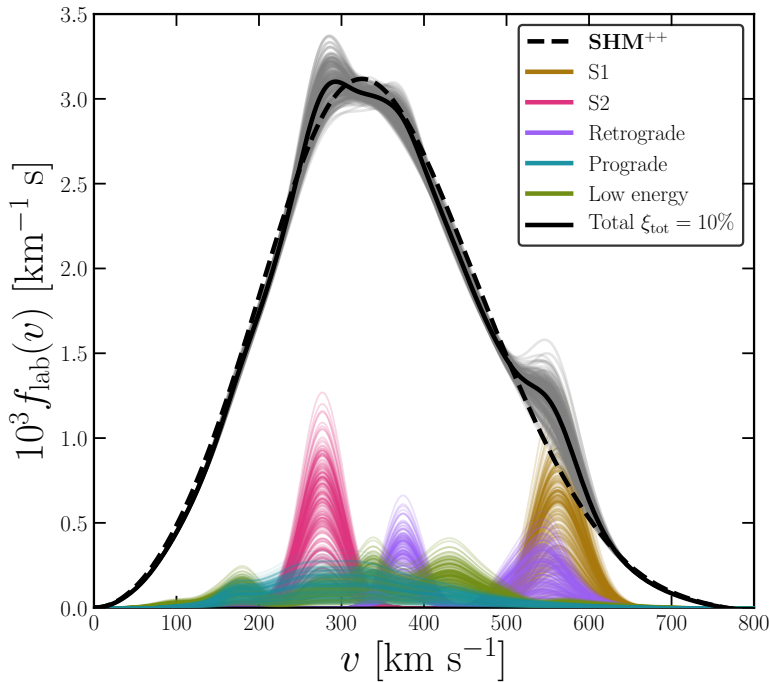
Figure 25: Possible MW velocity distributions as inferred from substructures in *Gaia* data consistent with other global constraints on the MW DM halo [475]. Reprinted with permission from [475]. Copyright 2020 by the American Physical Society.

velocity dispersions in the spherical galactocentric reference frame:

$$f_a(\mathbf{v}) \propto \exp\left(-\frac{v_r^2}{2\sigma_r^2} - \frac{v_\theta^2}{2\sigma_\theta^2} - \frac{v_\phi^2}{2\sigma_\phi^2}\right), \quad \sigma_r = \frac{3v_0^2}{2(3-2\beta)}, \quad \sigma_\theta = \sigma_\phi = \frac{3(1-\beta)v_0^2}{2(3-2\beta)}. \quad (15)$$

The parameter $v_0 = \sqrt{2}\sigma_v$ is the speed of local standard of rest, mentioned above, which determines the characteristics of the bulk halo in the SHM^{++}, $f_{\text{SHM}} \propto \exp(-v^2/v_0^2)$. The total velocity distribution according to the SHM^{++} also requires a relative normalization η to relate the relative contribution of the anisotropic component: $f(\mathbf{v}) = (1-\eta)f_{\text{SHM}}(\mathbf{v}) + \eta f_a(\mathbf{v})$ [459]. The parameter $\eta \sim 20\%$ ensures that the contributions from this anisotropic, phase-space unmixed, component are not dominant [475].

The SHM^{++} does not account for smaller structures, which may yet be energetically important. For example, counter-rotating structures can have noticeable effects for dark matter particles with kinetic energies near experimental thresholds, and thus these structures are especially important for the original goal of interpreting DM DD experiments [459, 479, 475]. Such small counter-rotating structures have been identified using a number of methods [448, 449, 278, 475]. We show in Fig. 25 a range of possible MW velocity distributions including these yet smaller structures as cataloged by [475]. We compare these semi-empirical $f(\mathbf{v})$ distributions to the SHM^{++}, which itself differs from the SHM.

8   Summary and Future Prospects

In this review we have considered how precision astrometry, particularly from the *Gaia* space telescope, has enriched our ability to study the MW, particularly in regards to its dynamical and DM aspects. In particular, we have reviewed our current understanding of the DM phenomenon as illuminated by the stellar halo of the Milky Way. Starting from very general principles, we have discussed the structure and contents of the MW and how the DM is distributed within it.

We have discussed what we know observationally about the MW halo and the subhalos within it. We have considered concrete models covering the range from a weakly (or sub-weakly) interacting fermion (WIMP), to an ultralight boson with a super-saturated phase space density, to a non-luminous massive compact object, such as a rock, planet, or black hole (MACHO). We have recapped studies of the impacts of such DM candidates on a variety of stellar systems spanning a huge range of masses.

Cosmological data, primarily astrophysical in nature, show that DM has an overall mass content within the observable universe of about five times that of the known baryonic matter (stars, gas, and dust). This DM is largely cold and collisionless (unlike a gas with collisions) and is non-luminous (does not interact electromagnetically). No clear resolution to the question of the fundamental nature of the DM has manifested itself despite nearly 90 years of observations since the existence of DM was first proposed. Here, we have emphasized the essential features of what we consider to be a promising route to identifying the DM: using observations of motions and distributions of stars in and around the MW to constrain what we know about how DM is clumped. A minimum clumping scale, if observed, is inversely related to the mass scale of a DM particle. Studies of star kinematics in globular clusters and dwarf galaxies suggest a minimum clumping scale could exist at the threshold of our experimental and theoretical sensitivity, in the range $10 - 1000$ pc, and future work should be able to search for and refine such a scale, if it exists uniquely.

Studying stellar motions, especially the dispersions of motions, illuminate the total mass distribution of the MW, because the virial theorem dictates that these motions are determined by the entire mass enclosed by their orbit, including the invisible DM. In this review, we have reviewed the theoretical foundation of such searches, and we have gone beyond studies of stellar motion to consider the study of number counts of stars in balanced volumes of space. We have shown that such counts are a powerful probe of the symmetry of the underlying matter distribution. Any observed breaking of such symmetries, even at the 1% level, can lead to important insights about the distribution and extent of unseen DM on sub-galactic scales. Upcoming refinements to the already essential *Gaia* data on MW stellar kinematics, combined with photometric stellar population information from optical surveys at the Rubin observatory and from other complementary surveys, and even multimessenger studies of compact astrophysical objects, will continue to provide datasets capable of further constraining DM properties. The future of the study of the DM halo of the MW promises to continue to grow ever more illuminated by these studies.

Acknowledgments

References

[1] Ken Freeman and Joss Bland-Hawthorn. The New Galaxy: Signatures of Its Formation. ARA&A, 40:487–537, January 2002, doi:10.1146/annurev.astro.40.060401.093840, astro-ph/0208106.

[2] Wayne Hu and Scott Dodelson. Cosmic Microwave Background Anisotropies. ARA&A, 40:171–216, January 2002, doi:10.1146/annurev.astro.40.060401.093926, astro-ph/0110414.

[3] N. Aghanim et al., Planck Collaboration. Planck 2018 results. I. Overview and the cosmological legacy of Planck. A&A, 641:A1, September 2020, doi:10.1051/0004-6361/201833880, 1807.06205.

[4] Neta A. Bahcall. Large-scale structure in the universe indicated by galaxy clusters. ARA&A, 26:631–686, January 1988, doi:10.1146/annurev.aa.26.090188.003215.

[5] Shadab Alam, Metin Ata, Stephen Bailey, Florian Beutler, Dmitry Bizyaev, Jonathan A. Blazek, Adam S. Bolton, Joel R. Brownstein, Angela Burden, Chia-Hsun Chuang, Johan Comparat, Antonio J. Cuesta, Kyle S. Dawson, Daniel J. Eisenstein, Stephanie Escoffier, Héctor Gil-Marín, Jan Niklas Grieb, Nick Hand, Shirley Ho, Karen Kinemuchi, David Kirkby, Francisco Kitaura, Elena Malanushenko, Viktor Malanushenko, Claudia Maraston, Cameron K. McBride, Robert C. Nichol, Matthew D. Olmstead, Daniel Oravetz, Nikhil Padmanabhan, Nathalie Palanque-Delabrouille, Kaike Pan, Marcos Pellejero-Ibanez, Will J. Percival, Patrick Petitjean, Francisco Prada, Adrian M. Price-Whelan, Beth A. Reid, Sergio A. Rodríguez-Torres, Natalie A. Roe, Ashley J. Ross, Nicholas P. Ross, Graziano Rossi, Jose Alberto Rubiño-Martín, Shun Saito, Salvador Salazar-Albornoz, Lado Samushia, Ariel G. Sánchez, Siddharth Satpathy, David J. Schlegel, Donald P. Schneider, Claudia G. Scóccola, Hee-Jong Seo, Erin S. Sheldon, Audrey Simmons, Anže Slosar, Michael A. Strauss, Molly E. C. Swanson, Daniel Thomas, Jeremy L. Tinker, Rita Tojeiro, Mariana Vargas Magaña, Jose Alberto Vazquez, Licia Verde, David A. Wake, Yuting Wang, David H. Weinberg, Martin White, W. Michael Wood-Vasey, Christophe Yèche, Idit Zehavi, Zhongxu Zhai, and Gong-Bo Zhao. The clustering of galaxies in the completed SDSS-III Baryon Oscillation Spectroscopic Survey: cosmological analysis of the DR12 galaxy sample. MNRAS, 470(3):2617–2652, September 2017, doi:10.1093/mnras/stx721, 1607.03155.

[6] Dragan Huterer. Weak lensing, dark matter and dark energy. *General Relativity and Gravitation*, 42(9):2177–2195, September 2010, doi:10.1007/s10714-010-1051-z, 1001.1758.

[7] Richard Massey, Thomas Kitching, and Johan Richard. The dark matter of gravitational lensing. *Reports on Progress in Physics*, 73(8):086901, August 2010, doi:10.1088/0034-4885/73/8/086901, 1001.1739.

[8] Michael Rauch. The Lyman Alpha Forest in the Spectra of QSOs. ARA&A, 36:267–316, January 1998, doi:10.1146/annurev.astro.36.1.267, astro-ph/9806286.

[9] Matteo Viel, George D. Becker, James S. Bolton, and Martin G. Haehnelt. Warm dark matter as a solution to the small scale crisis: New constraints from high redshift Lyman-α forest data. Phys. Rev. D, 88(4):043502, August 2013, doi:10.1103/PhysRevD.88.043502, 1306.2314.

[10] Carlton M. Caves. Quantum-mechanical noise in an interferometer. *Phys. Rev. D*, 23:1693–1708, Apr 1981, doi:10.1103/PhysRevD.23.1693.

[11] J. Aasi et al., LIGO Scientific Collaboration. Enhanced sensitivity of the LIGO gravitational wave detector by using squeezed states of light. *Nature Photonics*, 7(8):613–619, August 2013, doi:10.1038/nphoton.2013.177, 1310.0383.

[12] Peter W. Graham, David E. Kaplan, Jeremy Mardon, Surjeet Rajendran, and William A. Terrano. Dark matter direct detection with accelerometers. Phys. Rev. D, 93(7):075029, April 2016, doi:10.1103/PhysRevD.93.075029, 1512.06165.

[13] Saptarshi Chaudhuri, Kent Irwin, Peter W. Graham, and Jeremy Mardon. Fundamental Limits of Electromagnetic Axion and Hidden-Photon Dark Matter Searches: Part I - The Quantum Limit. 2018, 1803.01627.

[14] Daniel Carney, Sohitri Ghosh, Gordan Krnjaic, and Jacob M. Taylor. Proposal for gravitational direct detection of dark matter. *Phys. Rev. D*, 102:072003, Oct 2020, doi:10.1103/PhysRevD.102.072003.

[15] Pierre Sikivie. Invisible axion search methods. *Reviews of Modern Physics*, 93(1):015004, January 2021, doi:10.1103/RevModPhys.93.015004, 2003.02206.

[16] Gianfranco Bertone, Dan Hooper, and Joseph Silk. Particle dark matter: evidence, candidates and constraints. Phys. Rep., 405(5–6):279–390, January 2005, doi:10.1016/j.physrep.2004.08.031, hep-ph/0404175.

[17] Matthew R. Buckley and Annika H. G. Peter. Gravitational probes of dark matter physics. Phys. Rep., 761:1–60, October 2018, doi:10.1016/j.physrep.2018.07.003, 1712.06615.

[18] M. A. C. Perryman, L. Lindegren, J. Kovalevsky, E. Hog, U. Bastian, P. L. Bernacca, M. Creze, F. Donati, M. Grenon, M. Grewing, F. van Leeuwen, H. van der Marel, F. Mignard, C. A. Murray, R. S. Le Poole, H. Schrijver, C. Turon, F. Arenou, M. Froeschle, and C. S. Petersen. The Hipparcos Catalogue. A&A, 500:501–504, July 1997.

[19] Devin Powell. Europe's star power. *Nature*, 502:22, 2013, doi:10.1038/502022a.

[20] Donald G. York, J. Adelman, Jr. Anderson, John E., Scott F. Anderson, James Annis, Neta A. Bahcall, J. A. Bakken, Robert Barkhouser, Steven Bastian, Eileen Berman, William N. Boroski, Steve Bracker, Charlie Briegel, John W. Briggs, J. Brinkmann, Robert Brunner, Scott Burles, Larry Carey, Michael A. Carr, Francisco J. Castander, Bing Chen, Patrick L. Colestock, A. J. Connolly, J. H. Crocker, István Csabai, Paul C. Czarapata, John Eric Davis, Mamoru Doi, Tom Dombeck, Daniel Eisenstein, Nancy Ellman, Brian R. Elms, Michael L. Evans, Xiaohui Fan, Glenn R. Federwitz, Larry Fiscelli, Scott Friedman, Joshua A. Frieman, Masataka Fukugita, Bruce Gillespie, James E. Gunn, Vijay K. Gurbani, Ernst de Haas, Merle Haldeman, Frederick H. Harris, J. Hayes, Timothy M. Heckman, G. S. Hennessy, Robert B. Hindsley, Scott Holm, Donald J. Holmgren, Chi-hao Huang, Charles Hull, Don Husby, Shin-Ichi Ichikawa, Takashi Ichikawa, Željko Ivezić, Stephen Kent, Rita S. J. Kim, E. Kinney, Mark Klaene, A. N. Kleinman, S. Kleinman, G. R. Knapp, John Korienek, Richard G. Kron, Peter Z. Kunszt, D. Q. Lamb, B. Lee, R. French Leger, Siriluk Limmongkol, Carl Lindenmeyer, Daniel C. Long, Craig Loomis, Jon Loveday, Rich Lucinio, Robert H. Lupton, Bryan MacKinnon, Edward J. Mannery, P. M. Mantsch, Bruce Margon, Peregrine McGehee, Timothy A. McKay, Avery Meiksin, Aronne Merelli, David G. Monet, Jeffrey A. Munn, Vijay K. Narayanan, Thomas Nash, Eric Neilsen, Rich Neswold, Heidi Jo Newberg, R. C. Nichol, Tom Nicinski, Mario Nonino, Norio Okada, Sadanori Okamura, Jeremiah P. Ostriker, Russell Owen, A. George Pauls, John Peoples, R. L. Peterson, Donald Petravick, Jeffrey R. Pier, Adrian Pope, Ruth Pordes, Angela Prosapio, Ron Rechenmacher, Thomas R. Quinn, Gordon T. Richards, Michael W. Richmond, Claudio H. Rivetta, Constance M. Rockosi, Kurt Ruthmansdorfer, Dale Sandford, David J. Schlegel, Donald P. Schneider, Maki Sekiguchi, Gary Sergey, Kazuhiro Shimasaku, Walter A. Siegmund, Stephen Smee, J. Allyn Smith, S. Snedden, R. Stone, Chris Stoughton, Michael A. Strauss, Christopher Stubbs, Mark SubbaRao, Alexander S. Szalay, Istvan Szapudi, Gyula P. Szokoly, Anirudda R. Thakar, Christy Tremonti, Douglas L. Tucker, Alan Uomoto, Dan Vanden Berk, Michael S. Vogeley, Patrick Waddell, Shu-i. Wang, Masaru Watanabe, David H. Weinberg, Brian Yanny, Naoki Yasuda, and SDSS Collaboration. The Sloan Digital Sky Survey: Technical Summary. AJ, 120(3):1579–1587, September 2000, doi:10.1086/301513, astro-ph/0006396.

[21] M. F. Skrutskie, R. M. Cutri, R. Stiening, M. D. Weinberg, S. Schneider, J. M. Carpenter, C. Beichman, R. Capps, T. Chester, J. Elias, J. Huchra, J. Liebert, C. Lonsdale, D. G. Monet,

S. Price, P. Seitzer, T. Jarrett, J. D. Kirkpatrick, J. E. Gizis, E. Howard, T. Evans, J. Fowler, L. Fullmer, R. Hurt, R. Light, E. L. Kopan, K. A. Marsh, H. L. McCallon, R. Tam, S. Van Dyk, and S. Wheelock. The Two Micron All Sky Survey (2MASS). AJ, 131(2):1163–1183, February 2006, doi:10.1086/498708.

[22] K. C. Chambers, E. A. Magnier, N. Metcalfe, H. A. Flewelling, M. E. Huber, C. Z. Waters, L. Denneau, P. W. Draper, D. Farrow, D. P. Finkbeiner, C. Holmberg, J. Koppenhoefer, P. A. Price, A. Rest, R. P. Saglia, E. F. Schlafly, S. J. Smartt, W. Sweeney, R. J. Wainscoat, W. S. Burgett, S. Chastel, T. Grav, J. N. Heasley, K. W. Hodapp, R. Jedicke, N. Kaiser, R. P. Kudritzki, G. A. Luppino, R. H. Lupton, D. G. Monet, J. S. Morgan, P. M. Onaka, B. Shiao, C. W. Stubbs, J. L. Tonry, R. White, E. Bañados, E. F. Bell, R. Bender, E. J. Bernard, M. Boegner, F. Boffi, M. T. Botticella, A. Calamida, S. Casertano, W. P. Chen, X. Chen, S. Cole, N. Deacon, C. Frenk, A. Fitzsimmons, S. Gezari, V. Gibbs, C. Goessl, T. Goggia, R. Gourgue, B. Goldman, P. Grant, E. K. Grebel, N. C. Hambly, G. Hasinger, A. F. Heavens, T. M. Heckman, R. Henderson, T. Henning, M. Holman, U. Hopp, W. H. Ip, S. Isani, M. Jackson, C. D. Keyes, A. M. Koekemoer, R. Kotak, D. Le, D. Liska, K. S. Long, J. R. Lucey, M. Liu, N. F. Martin, G. Masci, B. McLean, E. Mindel, P. Misra, E. Morganson, D. N. A. Murphy, A. Obaika, G. Narayan, M. A. Nieto-Santisteban, P. Norberg, J. A. Peacock, E. A. Pier, M. Postman, N. Primak, C. Rae, A. Rai, A. Riess, A. Riffeser, H. W. Rix, S. Röser, R. Russel, L. Rutz, E. Schilbach, A. S. B. Schultz, D. Scolnic, L. Strolger, A. Szalay, S. Seitz, E. Small, K. W. Smith, D. R. Soderblom, P. Taylor, R. Thomson, A. N. Taylor, A. R. Thakar, J. Thiel, D. Thilker, D. Unger, Y. Urata, J. Valenti, J. Wagner, T. Walder, F. Walter, S. P. Watters, S. Werner, W. M. Wood-Vasey, and R. Wyse. The Pan-STARRS1 Surveys. *arXiv e-prints*, page arXiv:1612.05560, December 2016, 1612.05560.

[23] T. M. C. Abbott, F. B. Abdalla, S. Allam, A. Amara, J. Annis, J. Asorey, S. Avila, O. Ballester, M. Banerji, W. Barkhouse, L. Baruah, M. Baumer, K. Bechtol, M. R. Becker, A. Benoit-Lévy, G. M. Bernstein, E. Bertin, J. Blazek, S. Bocquet, D. Brooks, D. Brout, E. Buckley-Geer, D. L. Burke, V. Busti, R. Campisano, L. Cardiel-Sas, A. Carnero Rosell, M. Carrasco Kind, J. Carretero, F. J. Castander, R. Cawthon, C. Chang, X. Chen, C. Conselice, G. Costa, M. Crocce, C. E. Cunha, C. B. D'Andrea, L. N. da Costa, R. Das, G. Daues, T. M. Davis, C. Davis, J. De Vicente, D. L. DePoy, J. DeRose, S. Desai, H. T. Diehl, J. P. Dietrich, S. Dodelson, P. Doel, A. Drlica-Wagner, T. F. Eifler, A. E. Elliott, A. E. Evrard, A. Farahi, A. Fausti Neto, E. Fernandez, D. A. Finley, B. Flaugher, R. J. Foley, P. Fosalba, D. N. Friedel, J. Frieman, J. García-Bellido, E. Gaztanaga, D. W. Gerdes, T. Giannantonio, M. S. S. Gill, K. Glazebrook, D. A. Goldstein, M. Gower, D. Gruen, R. A. Gruendl, J. Gschwend, R. R. Gupta, G. Gutierrez, S. Hamilton, W. G. Hartley, S. R. Hinton, J. M. Hislop, D. Hollowood, K. Honscheid, B. Hoyle, D. Huterer, B. Jain, D. J. James, T. Jeltema, M. W. G. Johnson, M. D. Johnson, T. Kacprzak, S. Kent, G. Khullar, M. Klein, A. Kovacs, A. M. G. Koziol, E. Krause, A. Kremin, R. Kron, K. Kuehn, S. Kuhlmann, N. Kuropatkin, O. Lahav, J. Lasker, T. S. Li, R. T. Li, A. R. Liddle, M. Lima, H. Lin, P. López-Reyes, N. MacCrann, M. A. G. Maia, J. D. Maloney, M. Manera, M. March, J. Marriner, J. L. Marshall, P. Martini, T. McClintock, T. McKay, R. G. McMahon, P. Melchior, F. Menanteau, C. J. Miller, R. Miquel, J. J. Mohr, E. Morganson, J. Mould, E. Neilsen, R. C. Nichol, F. Nogueira, B. Nord, P. Nugent, L. Nunes, R. L. C. Ogando, L. Old, A. B. Pace, A. Palmese, F. Paz-Chinchón, H. V. Peiris, W. J. Percival, D. Petravick, A. A. Plazas, J. Poh, C. Pond, A. Porredon, A. Pujol, A. Refregier, K. Reil, P. M. Ricker, R. P. Rollins, A. K. Romer, A. Roodman, P. Rooney, A. J. Ross, E. S. Rykoff, M. Sako, M. L. Sanchez, E. Sanchez, B. Santiago, A. Saro, V. Scarpine, D. Scolnic, S. Serrano, I. Sevilla-Noarbe, E. Sheldon, N. Shipp, M. L. Silveira, M. Smith, R. C. Smith, J. A. Smith, M. Soares-Santos, F. Sobreira, J. Song, A. Stebbins, E. Suchyta, M. Sullivan, M. E. C. Swanson, G. Tarle, J. Thaler, D. Thomas, R. C. Thomas, M. A. Troxel, D. L. Tucker, V. Vikram, A. K. Vivas, A. R. Walker, R. H. Wechsler, J. Weller, W. Wester, R. C. Wolf,

H. Wu, B. Yanny, A. Zenteno, Y. Zhang, J. Zuntz, DES Collaboration, S. Juneau, M. Fitzpatrick, R. Nikutta, D. Nidever, K. Olsen, A. Scott, and NOAO Data Lab. The Dark Energy Survey: Data Release 1. ApJS, 239(2):18, December 2018, doi:10.3847/1538-4365/aae9f0, 1801.03181.

[24] Gaia Collaboration, T. Prusti, J. H. J. de Bruijne, A. G. A. Brown, A. Vallenari, C. Babusiaux, C. A. L. Bailer-Jones, U. Bastian, M. Biermann, D. W. Evans, L. Eyer, F. Jansen, C. Jordi, S. A. Klioner, U. Lammers, L. Lindegren, X. Luri, F. Mignard, D. J. Milligan, C. Panem, V. Poinsignon, D. Pourbaix, S. Randich, G. Sarri, P. Sartoretti, H. I. Siddiqui, C. Soubiran, V. Valette, F. van Leeuwen, N. A. Walton, C. Aerts, F. Arenou, M. Cropper, R. Drimmel, E. Høg, D. Katz, M. G. Lattanzi, W. O'Mullane, E. K. Grebel, A. D. Holland, C. Huc, X. Passot, L. Bramante, C. Cacciari, J. Castañeda, L. Chaoul, N. Cheek, F. De Angeli, C. Fabricius, R. Guerra, J. Hernández, A. Jean-Antoine-Piccolo, E. Masana, R. Messineo, N. Mowlavi, K. Nienartowicz, D. Ordóñez-Blanco, P. Panuzzo, J. Portell, P. J. Richards, M. Riello, G. M. Seabroke, P. Tanga, F. Thévenin, J. Torra, S. G. Els, G. Gracia-Abril, G. Comoretto, M. Garcia-Reinaldos, T. Lock, E. Mercier, M. Altmann, R. Andrae, T. L. Astraatmadja, I. Bellas-Velidis, K. Benson, J. Berthier, R. Blomme, G. Busso, B. Carry, A. Cellino, G. Clementini, S. Cowell, O. Creevey, J. Cuypers, M. Davidson, J. De Ridder, A. de Torres, L. Delchambre, A. Dell'Oro, C. Ducourant, Y. Frémat, M. García-Torres, E. Gosset, J. L. Halbwachs, N. C. Hambly, D. L. Harrison, M. Hauser, D. Hestroffer, S. T. Hodgkin, H. E. Huckle, A. Hutton, G. Jasniewicz, S. Jordan, M. Kontizas, A. J. Korn, A. C. Lanzafame, M. Manteiga, A. Moitinho, K. Muinonen, J. Osinde, E. Pancino, T. Pauwels, J. M. Petit, A. Recio-Blanco, A. C. Robin, L. M. Sarro, C. Siopis, M. Smith, K. W. Smith, A. Sozzetti, W. Thuillot, W. van Reeven, Y. Viala, U. Abbas, A. Abreu Aramburu, S. Accart, J. J. Aguado, P. M. Allan, W. Allasia, G. Altavilla, M. A. Álvarez, J. Alves, R. I. Anderson, A. H. Andrei, E. Anglada Varela, E. Antiche, T. Antoja, S. Antón, B. Arcay, A. Atzei, L. Ayache, N. Bach, S. G. Baker, L. Balaguer-Núñez, C. Barache, C. Barata, A. Barbier, F. Barblan, M. Baroni, D. Barrado y Navascués, M. Barros, M. A. Barstow, U. Becciani, M. Bellazzini, G. Bellei, A. Bello García, V. Belokurov, P. Bendjoya, A. Berihuete, L. Bianchi, O. Bienaymé, F. Billebaud, N. Blagorodnova, S. Blanco-Cuaresma, T. Boch, A. Bombrun, R. Borrachero, S. Bouquillon, G. Bourda, H. Bouy, A. Bragaglia, M. A. Breddels, N. Brouillet, T. Brüsemeister, B. Bucciarelli, F. Budnik, P. Burgess, R. Burgon, A. Burlacu, D. Busonero, R. Buzzi, E. Caffau, J. Cambras, H. Campbell, R. Cancelliere, T. Cantat-Gaudin, T. Carlucci, J. M. Carrasco, M. Castellani, P. Charlot, J. Charnas, P. Charvet, F. Chassat, A. Chiavassa, M. Clotet, G. Cocozza, R. S. Collins, P. Collins, G. Costigan, F. Crifo, N. J. G. Cross, M. Crosta, C. Crowley, C. Dafonte, Y. Damerdji, A. Dapergolas, P. David, M. David, P. De Cat, F. de Felice, P. de Laverny, F. De Luise, R. De March, D. de Martino, R. de Souza, J. Debosscher, E. del Pozo, M. Delbo, A. Delgado, H. E. Delgado, F. di Marco, P. Di Matteo, S. Diakite, E. Distefano, C. Dolding, S. Dos Anjos, P. Drazinos, J. Durán, Y. Dzigan, E. Ecale, B. Edvardsson, H. Enke, M. Erdmann, D. Escolar, M. Espina, N. W. Evans, G. Eynard Bontemps, C. Fabre, M. Fabrizio, S. Faigler, A. J. Falcão, M. Farràs Casas, F. Faye, L. Federici, G. Fedorets, J. Fernández-Hernández, P. Fernique, A. Fienga, F. Figueras, F. Filippi, K. Findeisen, A. Fonti, M. Fouesneau, E. Fraile, M. Fraser, J. Fuchs, R. Furnell, M. Gai, S. Galleti, L. Galluccio, D. Garabato, F. García-Sedano, P. Garé, A. Garofalo, N. Garralda, P. Gavras, J. Gerssen, R. Geyer, G. Gilmore, S. Girona, G. Giuffrida, M. Gomes, A. González-Marcos, J. González-Núñez, J. J. González-Vidal, M. Granvik, A. Guerrier, P. Guillout, J. Guiraud, A. Gúrpide, R. Gutiérrez-Sánchez, L. P. Guy, R. Haigron, D. Hatzidimitriou, M. Haywood, U. Heiter, A. Helmi, D. Hobbs, W. Hofmann, B. Holl, G. Holland, J. A. S. Hunt, A. Hypki, V. Icardi, M. Irwin, G. Jevardat de Fombelle, P. Jofré, P. G. Jonker, A. Jorissen, F. Julbe, A. Karampelas, A. Kochoska, R. Kohley, K. Kolenberg, E. Kontizas, S. E. Koposov, G. Kordopatis, P. Koubsky, A. Kowalczyk, A. Krone-Martins, M. Kudryashova, I. Kull, R. K. Bachchan, F. Lacoste-Seris, A. F. Lanza, J. B. Lavigne, C. Le Poncin-Lafitte, Y. Lebre-

ton, T. Lebzelter, S. Leccia, N. Leclerc, I. Lecoeur-Taibi, V. Lemaitre, H. Lenhardt, F. Leroux, S. Liao, E. Licata, H. E. P. Lindstrøm, T. A. Lister, E. Livanou, A. Lobel, W. Löffler, M. López, A. Lopez-Lozano, D. Lorenz, T. Loureiro, I. MacDonald, T. Magalhães Fernandes, S. Managau, R. G. Mann, G. Mantelet, O. Marchal, J. M. Marchant, M. Marconi, J. Marie, S. Marinoni, P. M. Marrese, G. Marschalkó, D. J. Marshall, J. M. Martín-Fleitas, M. Martino, N. Mary, G. Matijevič, T. Mazeh, P. J. McMillan, S. Messina, A. Mestre, D. Michalik, N. R. Millar, B. M. H. Miranda, D. Molina, R. Molinaro, M. Molinaro, L. Molnár, M. Moniez, P. Montegriffo, D. Monteiro, R. Mor, A. Mora, R. Morbidelli, T. Morel, S. Morgenthaler, T. Morley, D. Morris, A. F. Mulone, T. Muraveva, I. Musella, J. Narbonne, G. Nelemans, L. Nicastro, L. Noval, C. Ordénovic, J. Ordieres-Meré, P. Osborne, C. Pagani, I. Pagano, F. Pailler, H. Palacin, L. Palaversa, P. Parsons, T. Paulsen, M. Pecoraro, R. Pedrosa, H. Pentikäinen, J. Pereira, B. Pichon, A. M. Piersimoni, F. X. Pineau, E. Plachy, G. Plum, E. Poujoulet, A. Prša, L. Pulone, S. Ragaini, S. Rago, N. Rambaux, M. Ramos-Lerate, P. Ranalli, G. Rauw, A. Read, S. Regibo, F. Renk, C. Reylé, R. A. Ribeiro, L. Rimoldini, V. Ripepi, A. Riva, G. Rixon, M. Roelens, M. Romero-Gómez, N. Rowell, F. Royer, A. Rudolph, L. Ruiz-Dern, G. Sadowski, T. Sagristà Sellés, J. Sahlmann, J. Salgado, E. Salguero, M. Sarasso, H. Savietto, A. Schnorhk, M. Schultheis, E. Sciacca, M. Segol, J. C. Segovia, D. Segransan, E. Serpell, I. C. Shih, R. Smareglia, R. L. Smart, C. Smith, E. Solano, F. Solitro, R. Sordo, S. Soria Nieto, J. Souchay, A. Spagna, F. Spoto, U. Stampa, I. A. Steele, H. Steidelmüller, C. A. Stephenson, H. Stoev, F. F. Suess, M. Süveges, J. Surdej, L. Szabados, E. Szegedi-Elek, D. Tapiador, F. Taris, G. Tauran, M. B. Taylor, R. Teixeira, D. Terrett, B. Tingley, S. C. Trager, C. Turon, A. Ulla, E. Utrilla, G. Valentini, A. van Elteren, E. Van Hemelryck, M. van Leeuwen, M. Varadi, A. Vecchiato, J. Veljanoski, T. Via, D. Vicente, S. Vogt, H. Voss, V. Votruba, S. Voutsinas, G. Walmsley, M. Weiler, K. Weingrill, D. Werner, T. Wevers, G. Whitehead, Ł. Wyrzykowski, A. Yoldas, M. Žerjal, S. Zucker, C. Zurbach, T. Zwitter, A. Alecu, M. Allen, C. Allende Prieto, A. Amorim, G. Anglada-Escudé, V. Arsenijevic, S. Azaz, P. Balm, M. Beck, H. H. Bernstein, L. Bigot, A. Bijaoui, C. Blasco, M. Bonfigli, G. Bono, S. Boudreault, A. Bressan, S. Brown, P. M. Brunet, P. Bunclark, R. Buonanno, A. G. Butkevich, C. Carret, C. Carrion, L. Chemin, F. Chéreau, L. Corcione, E. Darmigny, K. S. de Boer, P. de Teodoro, P. T. de Zeeuw, C. Delle Luche, C. D. Domingues, P. Dubath, F. Fodor, B. Frézouls, A. Fries, D. Fustes, D. Fyfe, E. Gallardo, J. Gallegos, D. Gardiol, M. Gebran, A. Gomboc, A. Gómez, E. Grux, A. Gueguen, A. Heyrovsky, J. Hoar, G. Iannicola, Y. Isasi Parache, A. M. Janotto, E. Joliet, A. Jonckheere, R. Keil, D. W. Kim, P. Klagyivik, J. Klar, J. Knude, O. Kochukhov, I. Kolka, J. Kos, A. Kutka, V. Lainey, D. LeBouquin, C. Liu, D. Loreggia, V. V. Makarov, M. G. Marseille, C. Martayan, O. Martinez-Rubi, B. Massart, F. Meynadier, S. Mignot, U. Munari, A. T. Nguyen, T. Nordlander, P. Ocvirk, K. S. O'Flaherty, A. Olias Sanz, P. Ortiz, J. Osorio, D. Oszkiewicz, A. Ouzounis, M. Palmer, P. Park, E. Pasquato, C. Peltzer, J. Peralta, F. Péturaud, T. Pieniluoma, E. Pigozzi, J. Poels, G. Prat, T. Prod'homme, F. Raison, J. M. Rebordao, D. Risquez, B. Rocca-Volmerange, S. Rosen, M. I. Ruiz-Fuertes, F. Russo, S. Sembay, I. Serraller Vizcaino, A. Short, A. Siebert, H. Silva, D. Sinachopoulos, E. Slezak, M. Soffel, D. Sosnowska, V. Straižys, M. ter Linden, D. Terrell, S. Theil, C. Tiede, L. Troisi, P. Tsalmantza, D. Tur, M. Vaccari, F. Vachier, P. Valles, W. Van Hamme, L. Veltz, J. Virtanen, J. M. Wallut, R. Wichmann, M. I. Wilkinson, H. Ziaeepour, and S. Zschocke. The Gaia mission. A&A, 595:A1, November 2016, doi:10.1051/0004-6361/201629272, 1609.04153.

[25] L. Lindegren, J. Hernández, A. Bombrun, S. Klioner, U. Bastian, M. Ramos-Lerate, A. de Torres, H. Steidelmüller, C. Stephenson, D. Hobbs, U. Lammers, M. Biermann, R. Geyer, T. Hilger, D. Michalik, U. Stampa, P. J. McMillan, J. Castañeda, M. Clotet, G. Comoretto, M. Davidson, C. Fabricius, G. Gracia, N. C. Hambly, A. Hutton, A. Mora, J. Portell, F. van Leeuwen, U. Abbas, A. Abreu, M. Altmann, A. Andrei, E. Anglada, L. Balaguer-Núñez, C. Barache,

U. Becciani, S. Bertone, L. Bianchi, S. Bouquillon, G. Bourda, T. Brüsemeister, B. Bucciarelli, D. Busonero, R. Buzzi, R. Cancelliere, T. Carlucci, P. Charlot, N. Cheek, M. Crosta, C. Crowley, J. de Bruijne, F. de Felice, R. Drimmel, P. Esquej, A. Fienga, E. Fraile, M. Gai, N. Garralda, J. J. González-Vidal, R. Guerra, M. Hauser, W. Hofmann, B. Holl, S. Jordan, M. G. Lattanzi, H. Lenhardt, S. Liao, E. Licata, T. Lister, W. Löffler, J. Marchant, J. M. Martin-Fleitas, R. Messineo, F. Mignard, R. Morbidelli, E. Poggio, A. Riva, N. Rowell, E. Salguero, M. Sarasso, E. Sciacca, H. Siddiqui, R. L. Smart, A. Spagna, I. Steele, F. Taris, J. Torra, A. van Elteren, W. van Reeven, and A. Vecchiato. Gaia Data Release 2. The astrometric solution. A&A, 616:A2, August 2018, doi:10.1051/0004-6361/201832727, 1804.09366.

[26] Gaia Collaboration, A. G. A. Brown, A. Vallenari, T. Prusti, J. H. J. de Bruijne, C. Babusiaux, M. Biermann, O. L. Creevey, D. W. Evans, L. Eyer, A. Hutton, F. Jansen, C. Jordi, S. A. Klioner, U. Lammers, L. Lindegren, X. Luri, F. Mignard, C. Panem, D. Pourbaix, S. Randich, P. Sartoretti, C. Soubiran, N. A. Walton, F. Arenou, C. A. L. Bailer-Jones, U. Bastian, M. Cropper, R. Drimmel, D. Katz, M. G. Lattanzi, F. van Leeuwen, J. Bakker, C. Cacciari, J. Castañeda, F. De Angeli, C. Ducourant, C. Fabricius, M. Fouesneau, Y. Frémat, R. Guerra, A. Guerrier, J. Guiraud, A. Jean-Antoine Piccolo, E. Masana, R. Messineo, N. Mowlavi, C. Nicolas, K. Nienartowicz, F. Pailler, P. Panuzzo, F. Riclet, W. Roux, G. M. Seabroke, R. Sordo, P. Tanga, F. Thévenin, G. Gracia-Abril, J. Portell, D. Teyssier, M. Altmann, R. Andrae, I. Bellas-Velidis, K. Benson, J. Berthier, R. Blomme, E. Brugaletta, P. W. Burgess, G. Busso, B. Carry, A. Cellino, N. Cheek, G. Clementini, Y. Damerdji, M. Davidson, L. Delchambre, A. Dell'Oro, J. Fernández-Hernández, L. Galluccio, P. García-Lario, M. Garcia-Reinaldos, J. González-Núñez, E. Gosset, R. Haigron, J. L. Halbwachs, N. C. Hambly, D. L. Harrison, D. Hatzidimitriou, U. Heiter, J. Hernández, D. Hestroffer, S. T. Hodgkin, B. Holl, K. Janσen, G. Jevardat de Fombelle, S. Jordan, A. Krone-Martins, A. C. Lanzafame, W. Löffler, A. Lorca, M. Manteiga, O. Marchal, P. M. Marrese, A. Moitinho, A. Mora, K. Muinonen, P. Osborne, E. Pancino, T. Pauwels, J. M. Petit, A. Recio-Blanco, P. J. Richards, M. Riello, L. Rimoldini, A. C. Robin, T. Roegiers, J. Rybizki, L. M. Sarro, C. Siopis, M. Smith, A. Sozzetti, A. Ulla, E. Utrilla, M. van Leeuwen, W. van Reeven, U. Abbas, A. Abreu Aramburu, S. Accart, C. Aerts, J. J. Aguado, M. Ajaj, G. Altavilla, M. A. Álvarez, J. Álvarez Cid-Fuentes, J. Alves, R. I. Anderson, E. Anglada Varela, T. Antoja, M. Audard, D. Baines, S. G. Baker, L. Balaguer-Núñez, E. Balbinot, Z. Balog, C. Barache, D. Barbato, M. Barros, M. A. Barstow, S. Bartolomé, J. L. Bassilana, N. Bauchet, A. Baudesson-Stella, U. Becciani, M. Bellazzini, M. Bernet, S. Bertone, L. Bianchi, S. Blanco-Cuaresma, T. Boch, A. Bombrun, D. Bossini, S. Bouquillon, A. Bragaglia, L. Bramante, E. Breedt, A. Bressan, N. Brouillet, B. Bucciarelli, A. Burlacu, D. Busonero, A. G. Butkevich, R. Buzzi, E. Caffau, R. Cancelliere, H. Cánovas, T. Cantat-Gaudin, R. Carballo, T. Carlucci, M. I. Carnerero, J. M. Carrasco, L. Casamiquela, M. Castellani, A. Castro-Ginard, P. Castro Sampol, L. Chaoul, P. Charlot, L. Chemin, A. Chiavassa, M. R. L. Cioni, G. Comoretto, W. J. Cooper, T. Cornez, S. Cowell, F. Crifo, M. Crosta, C. Crowley, C. Dafonte, A. Dapergolas, M. David, P. David, P. de Laverny, F. De Luise, R. De March, J. De Ridder, R. de Souza, P. de Teodoro, A. de Torres, E. F. del Peloso, E. del Pozo, M. Delbo, A. Delgado, H. E. Delgado, J. B. Delisle, P. Di Matteo, S. Diakite, C. Diener, E. Distefano, C. Dolding, D. Eappachen, B. Edvardsson, H. Enke, P. Esquej, C. Fabre, M. Fabrizio, S. Faigler, G. Fedorets, P. Fernique, A. Fienga, F. Figueras, C. Fouron, F. Fragkoudi, E. Fraile, F. Franke, M. Gai, D. Garabato, A. Garcia-Gutierrez, M. García-Torres, A. Garofalo, P. Gavras, E. Gerlach, R. Geyer, P. Giacobbe, G. Gilmore, S. Girona, G. Giuffrida, R. Gomel, A. Gomez, I. Gonzalez-Santamaria, J. J. González-Vidal, M. Granvik, R. Gutiérrez-Sánchez, L. P. Guy, M. Hauser, M. Haywood, A. Helmi, S. L. Hidalgo, T. Hilger, N. Hładczuk, D. Hobbs, G. Holland, H. E. Huckle, G. Jasniewicz, P. G. Jonker, J. Juaristi Campillo, F. Julbe, L. Karbevska, P. Kervella, S. Khanna, A. Kochoska, M. Kontizas, G. Kordopatis, A. J. Korn,

Z. Kostrzewa-Rutkowska, K. Kruszyńska, S. Lambert, A. F. Lanza, Y. Lasne, J. F. Le Campion, Y. Le Fustec, Y. Lebreton, T. Lebzelter, S. Leccia, N. Leclerc, I. Lecoeur-Taibi, S. Liao, E. Licata, E. P. Lindstrøm, T. A. Lister, E. Livanou, A. Lobel, P. Madrero Pardo, S. Managau, R. G. Mann, J. M. Marchant, M. Marconi, M. M. S. Marcos Santos, S. Marinoni, F. Marocco, D. J. Marshall, L. Martin Polo, J. M. Martín-Fleitas, A. Masip, D. Massari, A. Mastrobuono-Battisti, T. Mazeh, P. J. McMillan, S. Messina, D. Michalik, N. R. Millar, A. Mints, D. Molina, R. Molinaro, L. Molnár, P. Montegriffo, R. Mor, R. Morbidelli, T. Morel, D. Morris, A. F. Mulone, D. Munoz, T. Muraveva, C. P. Murphy, I. Musella, L. Noval, C. Ordénovic, G. Orrù, J. Osinde, C. Pagani, I. Pagano, L. Palaversa, P. A. Palicio, A. Panahi, M. Pawlak, X. Peñalosa Esteller, A. Penttilä, A. M. Piersimoni, F. X. Pineau, E. Plachy, G. Plum, E. Poggio, E. Poretti, E. Poujoulet, A. Prša, L. Pulone, E. Racero, S. Ragaini, M. Rainer, C. M. Raiteri, N. Rambaux, P. Ramos, M. Ramos-Lerate, P. Re Fiorentin, S. Regibo, C. Reylé, V. Ripepi, A. Riva, G. Rixon, N. Robichon, C. Robin, M. Roelens, L. Rohrbasser, M. Romero-Gómez, N. Rowell, F. Royer, K. A. Rybicki, G. Sadowski, A. Sagristà Sellés, J. Sahlmann, J. Salgado, E. Salguero, N. Samaras, V. Sanchez Gimenez, N. Sanna, R. Santoveña, M. Sarasso, M. Schultheis, E. Sciacca, M. Segol, J. C. Segovia, D. Ségransan, D. Semeux, S. Shahaf, H. I. Siddiqui, A. Siebert, L. Siltala, E. Slezak, R. L. Smart, E. Solano, F. Solitro, D. Souami, J. Souchay, A. Spagna, F. Spoto, I. A. Steele, H. Steidelmüller, C. A. Stephenson, M. Süveges, L. Szabados, E. Szegedi-Elek, F. Taris, G. Tauran, M. B. Taylor, R. Teixeira, W. Thuillot, N. Tonello, F. Torra, J. Torra, C. Turon, N. Unger, M. Vaillant, E. van Dillen, O. Vanel, A. Vecchiato, Y. Viala, D. Vicente, S. Voutsinas, M. Weiler, T. Wevers, Ł. Wyrzykowski, A. Yoldas, P. Yvard, H. Zhao, J. Zorec, S. Zucker, C. Zurbach, and T. Zwitter. Gaia Early Data Release 3. Summary of the contents and survey properties. A&A, 649:A1, May 2021, doi:10.1051/0004-6361/202039657, 2012.01533.

[27] Gaia Collaboration, A. G. A. Brown, A. Vallenari, T. Prusti, J. H. J. de Bruijne, C. Babusiaux, C. A. L. Bailer-Jones, M. Biermann, D. W. Evans, L. Eyer, F. Jansen, C. Jordi, S. A. Klioner, U. Lammers, L. Lindegren, X. Luri, F. Mignard, C. Panem, D. Pourbaix, S. Randich, P. Sartoretti, H. I. Siddiqui, C. Soubiran, F. van Leeuwen, N. A. Walton, F. Arenou, U. Bastian, M. Cropper, R. Drimmel, D. Katz, M. G. Lattanzi, J. Bakker, C. Cacciari, J. Castañeda, L. Chaoul, N. Cheek, F. De Angeli, C. Fabricius, R. Guerra, B. Holl, E. Masana, R. Messineo, N. Mowlavi, K. Nienartowicz, P. Panuzzo, J. Portell, M. Riello, G. M. Seabroke, P. Tanga, F. Thévenin, G. Gracia-Abril, G. Comoretto, M. Garcia-Reinaldos, D. Teyssier, M. Altmann, R. Andrae, M. Audard, I. Bellas-Velidis, K. Benson, J. Berthier, R. Blomme, P. Burgess, G. Busso, B. Carry, A. Cellino, G. Clementini, M. Clotet, O. Creevey, M. Davidson, J. De Ridder, L. Delchambre, A. Dell'Oro, C. Ducourant, J. Fernández-Hernández, M. Fouesneau, Y. Frémat, L. Galluccio, M. García-Torres, J. González-Núñez, J. J. González-Vidal, E. Gosset, L. P. Guy, J. L. Halbwachs, N. C. Hambly, D. L. Harrison, J. Hernández, D. Hestroffer, S. T. Hodgkin, A. Hutton, G. Jasniewicz, A. Jean-Antoine-Piccolo, S. Jordan, A. J. Korn, A. Krone-Martins, A. C. Lanzafame, T. Lebzelter, W. Löffler, M. Manteiga, P. M. Marrese, J. M. Martín-Fleitas, A. Moitinho, A. Mora, K. Muinonen, J. Osinde, E. Pancino, T. Pauwels, J. M. Petit, A. Recio-Blanco, P. J. Richards, L. Rimoldini, A. C. Robin, L. M. Sarro, C. Siopis, M. Smith, A. Sozzetti, M. Süveges, J. Torra, W. van Reeven, U. Abbas, A. Abreu Aramburu, S. Accart, C. Aerts, G. Altavilla, M. A. Álvarez, R. Alvarez, J. Alves, R. I. Anderson, A. H. Andrei, E. Anglada Varela, E. Antiche, T. Antoja, B. Arcay, T. L. Astraatmadja, N. Bach, S. G. Baker, L. Balaguer-Núñez, P. Balm, C. Barache, C. Barata, D. Barbato, F. Barblan, P. S. Barklem, D. Barrado, M. Barros, M. A. Barstow, S. Bartholomé Muñoz, J. L. Bassilana, U. Becciani, M. Bellazzini, A. Berihuete, S. Bertone, L. Bianchi, O. Bienaymé, S. Blanco-Cuaresma, T. Boch, C. Boeche, A. Bombrun, R. Borrachero, D. Bossini, S. Bouquillon, G. Bourda, A. Bragaglia, L. Bramante, M. A. Breddels, A. Bressan, N. Brouillet, T. Brüsemeister, E. Brugaletta, B. Bucciarelli, A. Burlacu, D. Busonero, A. G. Butke-

vich, R. Buzzi, E. Caffau, R. Cancelliere, G. Cannizzaro, T. Cantat-Gaudin, R. Carballo, T. Carlucci, J. M. Carrasco, L. Casamiquela, M. Castellani, A. Castro-Ginard, P. Charlot, L. Chemin, A. Chiavassa, G. Cocozza, G. Costigan, S. Cowell, F. Crifo, M. Crosta, C. Crowley, J. Cuypers, C. Dafonte, Y. Damerdji, A. Dapergolas, P. David, M. David, P. de Laverny, F. De Luise, R. De March, D. de Martino, R. de Souza, A. de Torres, J. Debosscher, E. del Pozo, M. Delbo, A. Delgado, H. E. Delgado, P. Di Matteo, S. Diakite, C. Diener, E. Distefano, C. Dolding, P. Drazinos, J. Durán, B. Edvardsson, H. Enke, K. Eriksson, P. Esquej, G. Eynard Bontemps, C. Fabre, M. Fabrizio, S. Faigler, A. J. Falcão, M. Farràs Casas, L. Federici, G. Fedorets, P. Fernique, F. Figueras, F. Filippi, K. Findeisen, A. Fonti, E. Fraile, M. Fraser, B. Frézouls, M. Gai, S. Galleti, D. Garabato, F. García-Sedano, A. Garofalo, N. Garralda, A. Gavel, P. Gavras, J. Gerssen, R. Geyer, P. Giacobbe, G. Gilmore, S. Girona, G. Giuffrida, F. Glass, M. Gomes, M. Granvik, A. Gueguen, A. Guerrier, J. Guiraud, R. Gutiérrez-Sánchez, R. Haigron, D. Hatzidimitriou, M. Hauser, M. Haywood, U. Heiter, A. Helmi, J. Heu, T. Hilger, D. Hobbs, W. Hofmann, G. Holland, H. E. Huckle, A. Hypki, V. Icardi, K. Janσen, G. Jevardat de Fombelle, P. G. Jonker, Á. L. Juhász, F. Julbe, A. Karampelas, A. Kewley, J. Klar, A. Kochoska, R. Kohley, K. Kolenberg, M. Kontizas, E. Kontizas, S. E. Koposov, G. Kordopatis, Z. Kostrzewa-Rutkowska, P. Koubsky, S. Lambert, A. F. Lanza, Y. Lasne, J. B. Lavigne, Y. Le Fustec, C. Le Poncin-Lafitte, Y. Lebreton, S. Leccia, N. Leclerc, I. Lecoeur-Taibi, H. Lenhardt, F. Leroux, S. Liao, E. Licata, H. E. P. Lindstrøm, T. A. Lister, E. Livanou, A. Lobel, M. López, S. Managau, R. G. Mann, G. Mantelet, O. Marchal, J. M. Marchant, M. Marconi, S. Marinoni, G. Marschalkó, D. J. Marshall, M. Martino, G. Marton, N. Mary, D. Massari, G. Matijevič, T. Mazeh, P. J. McMillan, S. Messina, D. Michalik, N. R. Millar, D. Molina, R. Molinaro, L. Molnár, P. Montegriffo, R. Mor, R. Morbidelli, T. Morel, D. Morris, A. F. Mulone, T. Muraveva, I. Musella, G. Nelemans, L. Nicastro, L. Noval, W. O'Mullane, C. Ordénovic, D. Ordóñez-Blanco, P. Osborne, C. Pagani, I. Pagano, F. Pailler, H. Palacin, L. Palaversa, A. Panahi, M. Pawlak, A. M. Piersimoni, F. X. Pineau, E. Plachy, G. Plum, E. Poggio, E. Poujoulet, A. Prša, L. Pulone, E. Racero, S. Ragaini, N. Rambaux, M. Ramos-Lerate, S. Regibo, C. Reylé, F. Riclet, V. Ripepi, A. Riva, A. Rivard, G. Rixon, T. Roegiers, M. Roelens, M. Romero-Gómez, N. Rowell, F. Royer, L. Ruiz-Dern, G. Sadowski, T. Sagristà Sellés, J. Sahlmann, J. Salgado, E. Salguero, N. Sanna, T. Santana-Ros, M. Sarasso, H. Savietto, M. Schultheis, E. Sciacca, M. Segol, J. C. Segovia, D. Ségransan, I. C. Shih, L. Siltala, A. F. Silva, R. L. Smart, K. W. Smith, E. Solano, F. Solitro, R. Sordo, S. Soria Nieto, J. Souchay, A. Spagna, F. Spoto, U. Stampa, I. A. Steele, H. Steidelmüller, C. A. Stephenson, H. Stoev, F. F. Suess, J. Surdej, L. Szabados, E. Szegedi-Elek, D. Tapiador, F. Taris, G. Tauran, M. B. Taylor, R. Teixeira, D. Terrett, P. Teyssandier, W. Thuillot, A. Titarenko, F. Torra Clotet, C. Turon, A. Ulla, E. Utrilla, S. Uzzi, M. Vaillant, G. Valentini, V. Valette, A. van Elteren, E. Van Hemelryck, M. van Leeuwen, M. Vaschetto, A. Vecchiato, J. Veljanoski, Y. Viala, D. Vicente, S. Vogt, C. von Essen, H. Voss, V. Votruba, S. Voutsinas, G. Walmsley, M. Weiler, O. Wertz, T. Wevers, Ł. Wyrzykowski, A. Yoldas, M. Žerjal, H. Ziaeepour, J. Zorec, S. Zschocke, S. Zucker, C. Zurbach, and T. Zwitter. Gaia Data Release 2. Summary of the contents and survey properties. A&A, 616:A1, August 2018, doi:10.1051/0004-6361/201833051, 1804.09365.

[28] F. Arenou, X. Luri, C. Babusiaux, C. Fabricius, A. Helmi, T. Muraveva, A. C. Robin, F. Spoto, A. Vallenari, T. Antoja, et al. Gaia data release 2-catalogue validation. *Astronomy & Astrophysics*, 616:A17, 2018, doi:10.1051/0004-6361/201833234.

[29] Austin Hinkel, Susan Gardner, and Brian Yanny. Probing axial symmetry breaking in the galaxy with gaia data release 2. *The Astrophysical Journal*, 893(2):105, 2020, doi:10.3847/1538-4357/ab8235.

[30] Catherine Zucker, Joshua S. Speagle, Edward F. Schlafly, Gregory M. Green, Douglas P. Finkbeiner, Alyssa Goodman, and João Alves. A compendium of distances to molecular clouds in the Star Formation Handbook. A&A, 633:A51, January 2020, doi:10.1051/0004-6361/201936145, 2001.00591.

[31] Andrzej K. Drukier, Katherine Freese, and David N. Spergel. Detecting cold dark-matter candidates. Phys. Rev. D, 33(12):3495–3508, June 1986, doi:10.1103/PhysRevD.33.3495.

[32] David H. Weinberg, James S. Bullock, Fabio Governato, Rachel Kuzio de Naray, and Annika H. G. Peter. Cold dark matter: Controversies on small scales. *Proceedings of the National Academy of Science*, 112(40):12249–12255, October 2015, doi:10.1073/pnas.1308716112, 1306.0913.

[33] James S. Bullock and Michael Boylan-Kolchin. Small-Scale Challenges to the ΛCDM Paradigm. ARA&A, 55(1):343–387, August 2017, doi:10.1146/annurev-astro-091916-055313, 1707.04256.

[34] Joss Bland-Hawthorn and Ortwin Gerhard. The Galaxy in Context: Structural, Kinematic, and Integrated Properties. ARA&A, 54:529–596, Sep 2016, doi:10.1146/annurev-astro-081915-023441, 1602.07702.

[35] Mehran Kardar. *Statistical Physics of Particles*. Cambridge University Press, 1 edition, 2007.

[36] G. F. Bertsch, H. Kruse, and S. Das Gupta. Boltzmann equation for heavy ion collisions. Phys. Rev. C, 29(2):673–675, February 1984, doi:10.1103/PhysRevC.29.673.

[37] H. Kruse, B. V. Jacak, J. J. Molitoris, G. D. Westfall, and H. Stöcker. Vlasov-uehling-uhlenbeck theory of medium energy heavy ion reactions: Role of mean field dynamics and two body collisions. *Phys. Rev. C*, 31:1770–1774, May 1985, doi:10.1103/PhysRevC.31.1770.

[38] James Binney and Scott Tremaine. *Galactic Dynamics*. Princeton University Press, 2008.

[39] J. H. Jeans. On the theory of star-streaming and the structure of the universe. *Monthly Notices of the Royal Astronomical Society*, 76:70–84, Dec 1915, doi:10.1093/mnras/76.2.70.

[40] Emmy Noether. Invariant Variation Problems. *Nachr. v. d. Ges. d. Wiss. Zu Göttingen*, pages 235–237, Jan 1918.

[41] Herbert Goldstein. *Classical Mechanics*. Addison-Wesley, 2 edition, 1980.

[42] V. I. Arnold. *Mathematical Methods of Classical Mechanics*. Cambridge University Press, 2 edition, 1989.

[43] Peter J Olver. *Applications of Lie groups to differential equations*. Springer-Verlag, 2 edition, 1993.

[44] Susan Gardner, Austin Hinkel, and Brian Yanny. Applying noether's theorem to matter in the milky way: Evidence for external perturbations and non-steady-state effects from gaia data release 2. *The Astrophysical Journal*, 890(2):110, feb 2020, doi:10.3847/1538-4357/ab66c8.

[45] Lee Lindblom. On the Symmetries of Equilibrium Stellar Models. *Philosophical Transactions of the Royal Society of London Series A*, 340(1658):353–364, September 1992, doi:10.1098/rsta.1992.0072.

[46] J. An, N. W. Evans, and J. L. Sanders. Reflection symmetries of Isolated Self-consistent Stellar Systems. MNRAS, 467(2):1281–1286, May 2017, doi:10.1093/mnras/stx195, 1610.01701.

[47] A. E. Schulz, W. Dehnen, G. Jungman, and S. Tremaine. Gravitational collapse in one dimension. MNRAS, 431:49–62, May 2013, doi:10.1093/mnras/stt073, 1206.0299.

[48] Annie C. Robin, C. Reylé, S. Derriere, and S. Picaud. A synthetic view on structure and evolution of the milky way. *Astronomy & Astrophysics*, 409(2):523–540, 2003, doi:10.1051/0004-6361:20031117.

[49] A. C. Robin, D. J. Marshall, M. Schultheis, and C. Reylé. Stellar populations in the Milky Way bulge region: towards solving the Galactic bulge and bar shapes using 2MASS data. A&A, 538:A106, February 2012, doi:10.1051/0004-6361/201116512, 1111.5744.

[50] James Binney. Actions for axisymmetric potentials. *Monthly Notices of the Royal Astronomical Society*, 426(2):1324–1327, 2012, doi:10.1111/j.1365-2966.2012.21757.x.

[51] J Binney, Benedict Burnett, Georges Kordopatis, Matthias Steinmetz, G Gilmore, Olivier Bienayme, Joss Bland-Hawthorn, Benoit Famaey, Eva K Grebel, Amina Helmi, et al. Galactic kinematics and dynamics from radial velocity experiment stars. *Monthly Notices of the Royal Astronomical Society*, 439(2):1231–1244, 2014, doi:10.1093/mnras/stt2367.

[52] James Binney. Modelling our galaxy. *arXiv preprint arXiv:1909.02455*, 2019, doi:10.1017/S1743921319008214.

[53] Mark W. Goodman and Edward Witten. Detectability of Certain Dark Matter Candidates. *Phys.Rev.*, D31:3059, 1985, doi:10.1103/PhysRevD.31.3059.

[54] R.J. Gaitskell. Direct detection of dark matter. *Ann.Rev.Nucl.Part.Sci.*, 54:315–359, 2004, doi:10.1146/annurev.nucl.54.070103.181244.

[55] Dan Hooper and Edward A. Baltz. Strategies for Determining the Nature of Dark Matter. *Annual Review of Nuclear and Particle Science*, 58(1):293–314, November 2008, doi:10.1146/annurev.nucl.58.110707.171217, 0802.0702.

[56] Anne M. Green. Astrophysical Uncertainties on Direct Detection Experiments. *Modern Physics Letters A*, 27(3):1230004–1–1230004–20, January 2012, doi:10.1142/S0217732312300042, 1112.0524.

[57] Anne M. Green. Astrophysical uncertainties on the local dark matter distribution and direct detection experiments. *Journal of Physics G Nuclear Physics*, 44(8):084001, August 2017, doi:10.1088/1361-6471/aa7819, 1703.10102.

[58] Annika H. G. Peter. Dark matter in the Solar System. I. The distribution function of WIMPs at the Earth from solar capture. Phys. Rev. D, 79(10):103531, May 2009, doi:10.1103/PhysRevD.79.103531, 0902.1344.

[59] Annika H. G. Peter. Dark matter in the Solar System. III. The distribution function of WIMPs at the Earth from gravitational capture. Phys. Rev. D, 79(10):103533, May 2009, doi:10.1103/PhysRevD.79.103533, 0902.1348.

[60] Jonathan L. Feng. Dark Matter Candidates from Particle Physics and Methods of Detection. ARA&A, 48:495–545, September 2010, doi:10.1146/annurev-astro-082708-101659, 1003.0904.

[61] Rouven Essig, Jeremy Mardon, and Tomer Volansky. Direct Detection of Sub-GeV Dark Matter. *Phys. Rev. D*, 85:076007, 2012, doi:10.1103/PhysRevD.85.076007, 1108.5383.

[62] Rouven Essig, Marivi Fernandez-Serra, Jeremy Mardon, Adrian Soto, Tomer Volansky, and Tien-Tien Yu. Direct Detection of sub-GeV Dark Matter with Semiconductor Targets. *JHEP*, 05:046, 2016, doi:10.1007/JHEP05(2016)046, 1509.01598.

[63] Yonit Hochberg, Yue Zhao, and Kathryn M. Zurek. Superconducting Detectors for Superlight Dark Matter. *Phys. Rev. Lett.*, 116(1):011301, January 2016, doi:10.1103/PhysRevLett.116.011301, 1504.07237.

[64] Yonit Hochberg, Matt Pyle, Yue Zhao, and Kathryn M. Zurek. Detecting superlight dark matter with Fermi-degenerate materials. *Journal of High Energy Physics*, 2016(8):57, August 2016, doi:10.1007/JHEP08(2016)057, 1512.04533.

[65] Yonit Hochberg, Yonatan Kahn, Mariangela Lisanti, Christopher G. Tully, and Kathryn M. Zurek. Directional detection of dark matter with two-dimensional targets. *Physics Letters B*, 772:239–246, September 2017, doi:10.1016/j.physletb.2017.06.051, 1606.08849.

[66] Yonit Hochberg, Yonatan Kahn, Mariangela Lisanti, Kathryn M. Zurek, Adolfo G. Grushin, Roni Ilan, Sinéad M. Griffin, Zhen-Fei Liu, Sophie F. Weber, and Jeffrey B. Neaton. Detection of sub-MeV dark matter with three-dimensional Dirac materials. *Phys. Rev. D*, 97(1):015004, January 2018, doi:10.1103/PhysRevD.97.015004, 1708.08929.

[67] Yonit Hochberg, Ilya Charaev, Sae-Woo Nam, Varun Verma, Marco Colangelo, and Karl K. Berggren. Detecting Sub-GeV Dark Matter with Superconducting Nanowires. *Phys. Rev. Lett.*, 123(15):151802, October 2019, doi:10.1103/PhysRevLett.123.151802, 1903.05101.

[68] Ahmet Coskuner, Andrea Mitridate, Andres Olivares, and Kathryn M. Zurek. Directional Dark Matter Detection in Anisotropic Dirac Materials. *arXiv e-prints*, page arXiv:1909.09170, September 2019, 1909.09170.

[69] Noah Kurinsky, To Chin Yu, Yonit Hochberg, and Blas Cabrera. Diamond detectors for direct detection of sub-GeV dark matter. *Phys. Rev. D*, 99(12):123005, June 2019, doi:10.1103/PhysRevD.99.123005, 1901.07569.

[70] Carlos Blanco, J. I. Collar, Yonatan Kahn, and Benjamin Lillard. Dark matter-electron scattering from aromatic organic targets. *Phys. Rev. D*, 101(5):056001, March 2020, doi:10.1103/PhysRevD.101.056001, 1912.02822.

[71] Carlos Blanco, Yonatan Kahn, Benjamin Lillard, and Samuel D. McDermott. Dark Matter Daily Modulation With Anisotropic Organic Crystals. *arXiv e-prints*, page arXiv:2103.08601, March 2021, 2103.08601.

[72] Javier Tiffenberg, Miguel Sofo-Haro, Alex Drlica-Wagner, Rouven Essig, Yann Guardincerri, Steve Holland, Tomer Volansky, and Tien-Tien Yu, SENSEI. Single-electron and single-photon sensitivity with a silicon Skipper CCD. *Phys. Rev. Lett.*, 119(13):131802, 2017, doi:10.1103/PhysRevLett.119.131802, 1706.00028.

[73] Liron Barak et al., SENSEI. SENSEI: Direct-Detection Results on sub-GeV Dark Matter from a New Skipper-CCD. *Phys. Rev. Lett.*, 125(17):171802, 2020, doi:10.1103/PhysRevLett.125.171802, 2004.11378.

[74] Aria Radick, Anna-Maria Taki, and Tien-Tien Yu. Dependence of dark matter - electron scattering on the galactic dark matter velocity distribution. *J. Cosmology Astropart. Phys.*, 2021(2):004, February 2021, doi:10.1088/1475-7516/2021/02/004, 2011.02493.

[75] Riccardo Catena, Timon Emken, Nicola A. Spaldin, and Walter Tarantino. Atomic responses to general dark matter-electron interactions. *Phys. Rev. Res.*, 2(3):033195, 2020, doi:10.1103/PhysRevResearch.2.033195, 1912.08204.

[76] Susan Gardner and George M. Fuller. Dark matter studies entrain nuclear physics. *Progress in Particle and Nuclear Physics*, 71:167–184, July 2013, doi:10.1016/j.ppnp.2013.03.001, 1303.4758.

[77] Vera Gluscevic, Moira I. Gresham, Samuel D. McDermott, Annika H. G. Peter, and Kathryn M. Zurek. Identifying the theory of dark matter with direct detection. *J. Cosmology Astropart. Phys.*, 2015(12):057, December 2015, doi:10.1088/1475-7516/2015/12/057, 1506.04454.

[78] Samuel K. Lee, Mariangela Lisanti, Annika H. G. Peter, and Benjamin R. Safdi. Effect of Gravitational Focusing on Annual Modulation in Dark-Matter Direct-Detection Experiments. *Phys. Rev. Lett.*, 112(1):011301, January 2014, doi:10.1103/PhysRevLett.112.011301, 1308.1953.

[79] F. Mayet, A. M. Green, J. B. R. Battat, J. Billard, N. Bozorgnia, G. B. Gelmini, P. Gondolo, B. J. Kavanagh, S. K. Lee, D. Loomba, J. Monroe, B. Morgan, C. A. J. O'Hare, A. H. G. Peter, N. S. Phan, and S. E. Vahsen. A review of the discovery reach of directional Dark Matter detection. *Phys. Rep.*, 627:1–49, April 2016, doi:10.1016/j.physrep.2016.02.007, 1602.03781.

[80] Samuel K. Lee and Annika H. G. Peter. Probing the local velocity distribution of WIMP dark matter with directional detectors. *J. Cosmology Astropart. Phys.*, 2012(4):029, April 2012, doi:10.1088/1475-7516/2012/04/029, 1202.5035.

[81] David Tucker-Smith and Neal Weiner. Inelastic dark matter. *Phys. Rev. D*, 64:043502, 2001, doi:10.1103/PhysRevD.64.043502, hep-ph/0101138.

[82] JiJi Fan, Andrey Katz, and Jessie Shelton. Direct and indirect detection of dissipative dark matter. *JCAP*, 06:059, 2014, doi:10.1088/1475-7516/2014/06/059, 1312.1336.

[83] Maxim Yu. Khlopov. Composite dark matter from 4th generation. *Pisma Zh. Eksp. Teor. Fiz.*, 83:3–6, 2006, doi:10.1134/S0021364006010012, astro-ph/0511796.

[84] Susan Gardner. Possibility of Observing Dark Matter via the Gyromagnetic Faraday Effect. *Phys. Rev. Lett.*, 100(4):041303, February 2008, doi:10.1103/PhysRevLett.100.041303, astro-ph/0611684.

[85] Daniele S. M. Alves, Siavosh R. Behbahani, Philip Schuster, and Jay G. Wacker. Composite Inelastic Dark Matter. *Phys. Lett. B*, 692:323–326, 2010, doi:10.1016/j.physletb.2010.08.006, 0903.3945.

[86] Graham D. Kribs, Tuhin S. Roy, John Terning, and Kathryn M. Zurek. Quirky Composite Dark Matter. *Phys. Rev. D*, 81:095001, 2010, doi:10.1103/PhysRevD.81.095001, 0909.2034.

[87] A. Liam Fitzpatrick, Wick Haxton, Emanuel Katz, Nicholas Lubbers, and Yiming Xu. The Effective Field Theory of Dark Matter Direct Detection. *JCAP*, 02:004, 2013, doi:10.1088/1475-7516/2013/02/004, 1203.3542.

[88] A. Liam Fitzpatrick, Wick Haxton, Emanuel Katz, Nicholas Lubbers, and Yiming Xu. Model Independent Direct Detection Analyses. 11 2012, 1211.2818.

[89] JiJi Fan, Matthew Reece, and Lian-Tao Wang. Non-relativistic effective theory of dark matter direct detection. *JCAP*, 11:042, 2010, doi:10.1088/1475-7516/2010/11/042, 1008.1591.

[90] Nikhil Anand, A. Liam Fitzpatrick, and W. C. Haxton. Weakly interacting massive particle-nucleus elastic scattering response. *Phys. Rev. C*, 89(6):065501, 2014, doi:10.1103/PhysRevC.89.065501, 1308.6288.

[91] Patrick J. Fox, Jia Liu, and Neal Weiner. Integrating Out Astrophysical Uncertainties. *Phys. Rev. D*, 83:103514, 2011, doi:10.1103/PhysRevD.83.103514, 1011.1915.

[92] Annika H. G. Peter. Getting the astrophysics and particle physics of dark matter out of next-generation direct detection experiments. Phys. Rev. D, 81(8):087301, April 2010, doi:10.1103/PhysRevD.81.087301, 0910.4765.

[93] D. Lynden-Bell. Statistical mechanics of violent relaxation in stellar systems. MNRAS, 136:101, January 1967, doi:10.1093/mnras/136.1.101.

[94] Mariangela Lisanti and David N. Spergel. Dark Matter Debris Flows in the Milky Way. *Phys. Dark Univ.*, 1:155–161, 2012, doi:10.1016/j.dark.2012.10.007, 1105.4166.

[95] Michael Kuhlen, Mariangela Lisanti, and David N. Spergel. Direct Detection of Dark Matter Debris Flows. *Phys. Rev. D*, 86:063505, 2012, doi:10.1103/PhysRevD.86.063505, 1202.0007.

[96] James Binney and Tilmann Piffl. The distribution function of the galaxy's dark halo. *Monthly Notices of the Royal Astronomical Society*, 454(4):3653–3663, 2015, doi:10.1093/mnras/stv2225.

[97] Przemek Mróz, Andrzej Udalski, Dorota M Skowron, Jan Skowron, Igor Soszyński, Paweł Pietrukowicz, Michał K Szymański, Radosław Poleski, Szymon Kozłowski, and Krzysztof Ulaczyk. Rotation curve of the milky way from classical cepheids. *The Astrophysical Journal Letters*, 870(1):L10, 2019, doi:10.3847/2041-8213/aaf73f, 1810.02131.

[98] Rob P. Olling and Michael R. Merrifield. Two measures of the shape of the dark halo of the Milky Way. MNRAS, 311(2):361–369, January 2000, doi:10.1046/j.1365-8711.2000.03053.x, astro-ph/9907353.

[99] E. S. Levine, Leo Blitz, and Carl Heiles. The Vertical Structure of the Outer Milky Way H I Disk. ApJ, 643(2):881–896, June 2006, doi:10.1086/503091, astro-ph/0601697.

[100] P. M. W. Kalberla, L. Dedes, J. Kerp, and U. Haud. Dark matter in the Milky Way. II. The HI gas distribution as a tracer of the gravitational potential. A&A, 469(2):511–527, July 2007, doi:10.1051/0004-6361:20066362, 0704.3925.

[101] C. Alard. Flaring and warping of the milky way disk: not only in the gas. *arXiv preprint astro-ph/0007013*, 2000.

[102] Deborah Ferguson, Susan Gardner, and Brian Yanny. Milky Way Tomography with K and M Dwarf Stars: The Vertical Structure of the Galactic Disk. ApJ, 843(2):141, July 2017, doi:10.3847/1538-4357/aa77fd, 1706.01900.

[103] Xiaodian Chen, Shu Wang, Licai Deng, Richard de Grijs, Chao Liu, and Hao Tian. An intuitive 3D map of the Galactic warp's precession traced by classical Cepheids. *Nature Astronomy*, 3:320–325, February 2019, doi:10.1038/s41550-018-0686-7, 1902.00998.

[104] Dorota M. Skowron, Jan Skowron, Przemek Mróz, Andrzej Udalski, Paweł Pietrukowicz, Igor Soszyński, Michał K. Szymański, Radosław Poleski, Szymon Kozłowski, Krzysztof Ulaczyk, Krzysztof Rybicki, and Patryk Iwanek. A three-dimensional map of the Milky Way using classical Cepheid variable stars. *Science*, 365(6452):478–482, August 2019, doi:10.1126/science.aau3181, 1806.10653.

[105] Robert W Nelson and Scott Tremaine. The damping and excitation of galactic warps by dynamical friction. *Monthly Notices of the Royal Astronomical Society*, 275(4):897–920, 1995, doi:10.1093/mnras/275.4.897.

[106] Juntai Shen and JA Sellwood. Galactic warps induced by cosmic infall. *Monthly Notices of the Royal Astronomical Society*, 370(1):2–14, 2006, doi:10.1111/j.1365-2966.2006.10477.x.

[107] Martin D. Weinberg and Leo Blitz. A Magellanic Origin for the Warp of the Galaxy. ApJ, 641(1):L33–L36, April 2006, doi:10.1086/503607, astro-ph/0601694.

[108] J. H. J. Hagen, A. Helmi, P. T. de Zeeuw, and L. Posti. The tilt of the velocity ellipsoid in the Milky Way with Gaia DR2. A&A, 629:A70, September 2019, doi:10.1051/0004-6361/201935264, 1902.05268.

[109] Lorenzo Posti and Amina Helmi. Mass and shape of the Milky Way's dark matter halo with globular clusters from Gaia and Hubble. A&A, 621:A56, January 2019, doi:10.1051/0004-6361/201833355, 1805.01408.

[110] Arunima Banerjee and Chanda J. Jog. Progressively More Prolate Dark Matter Halo in the Outer Galaxy as Traced by Flaring H I Gas. ApJ, 732(1):L8, May 2011, doi:10.1088/2041-8205/732/1/L8, 1103.5821.

[111] M. Ideta, S. Hozumi, T. Tsuchiya, and M. Takizawa. Time evolution of galactic warps in prolate haloes. MNRAS, 311(4):733–740, February 2000, doi:10.1046/j.1365-8711.2000.03092.x, astro-ph/9910030.

[112] Matthew H. Chequers, Lawrence M. Widrow, and Keir Darling. Bending waves in the milky way's disc from halo substructure. *Monthly Notices of the Royal Astronomical Society*, 480(3):4244–4258, 2018, doi:10.1093/mnras/sty2114.

[113] Frank C. van den Bosch, Go Ogiya, Oliver Hahn, and Andreas Burkert. Disruption of dark matter substructure: fact or fiction? MNRAS, 474(3):3043–3066, March 2018, doi:10.1093/mnras/stx2956, 1711.05276.

[114] Alan H. Guth. The Inflationary Universe: A Possible Solution to the Horizon and Flatness Problems. *Phys. Rev. D*, 23:347–356, 1981, doi:10.1103/PhysRevD.23.347.

[115] Alan H. Guth and S. Y. Pi. Fluctuations in the New Inflationary Universe. *Phys. Rev. Lett.*, 49:1110–1113, 1982, doi:10.1103/PhysRevLett.49.1110.

[116] Andreas Albrecht and Paul J. Steinhardt. Cosmology for Grand Unified Theories with Radiatively Induced Symmetry Breaking. *Phys. Rev. Lett.*, 48:1220–1223, 1982, doi:10.1103/PhysRevLett.48.1220.

[117] James M. Bardeen, Paul J. Steinhardt, and Michael S. Turner. Spontaneous Creation of Almost Scale - Free Density Perturbations in an Inflationary Universe. *Phys. Rev. D*, 28:679, 1983, doi:10.1103/PhysRevD.28.679.

[118] P. J. E. Peebles. Large-scale background temperature and mass fluctuations due to scale-invariant primeval perturbations. ApJ, 263:L1–L5, December 1982, doi:10.1086/183911.

[119] E. R. Harrison. Fluctuations at the Threshold of Classical Cosmology. Phys. Rev. D, 1(10):2726–2730, May 1970, doi:10.1103/PhysRevD.1.2726.

[120] Yaa B. Zeldovich. A hypothesis, unifying the structure and the entropy of the Universe. MNRAS, 160:1P, January 1972, doi:10.1093/mnras/160.1.1P.

[121] William H. Press and Paul Schechter. Formation of Galaxies and Clusters of Galaxies by Self-Similar Gravitational Condensation. ApJ, 187:425–438, February 1974, doi:10.1086/152650.

[122] S. D. M. White and M. J. Rees. Core condensation in heavy halos: a two-stage theory for galaxy formation and clustering. MNRAS, 183:341–358, May 1978, doi:10.1093/mnras/183.3.341.

[123] G. R. Blumenthal, S. M. Faber, J. R. Primack, and M. J. Rees. Formation of galaxies and large-scale structure with cold dark matter. Nature, 311:517–525, October 1984, doi:10.1038/311517a0.

[124] J. P. Ostriker, P. J. E. Peebles, and A. Yahil. The Size and Mass of Galaxies, and the Mass of the Universe. ApJ, 193:L1, October 1974, doi:10.1086/181617.

[125] Jaan Einasto, Ants Kaasik, and Enn Saar. Dynamic evidence on massive coronas of galaxies. Nature, 250(5464):309–310, July 1974, doi:10.1038/250309a0.

[126] Scott Tremaine. Comments on Ostriker, Peebles, & Yahil (1974) "The Size and Mass of Galaxies, and the Mass of the Universe". ApJ, 525C:1223, November 1999.

[127] M. Davis, G. Efstathiou, C. S. Frenk, and S. D. M. White. The evolution of large-scale structure in a universe dominated by cold dark matter. ApJ, 292:371–394, May 1985, doi:10.1086/163168.

[128] Solène Chabanier, Marius Millea, and Nathalie Palanque-Delabrouille. Matter power spectrum: from Ly α forest to CMB scales. MNRAS, 489(2):2247–2253, October 2019, doi:10.1093/mnras/stz2310, 1905.08103.

[129] P. J. E. Peebles. *The large-scale structure of the universe.* Princeton University Press, 1980.

[130] Bhuvnesh Jain and Edmund Bertschinger. Second-Order Power Spectrum and Nonlinear Evolution at High Redshift. ApJ, 431:495, August 1994, doi:10.1086/174502, astro-ph/9311070.

[131] Jordan Carlson, Martin White, and Nikhil Padmanabhan. Critical look at cosmological perturbation theory techniques. Phys. Rev. D, 80(4):043531, August 2009, doi:10.1103/PhysRevD.80.043531, 0905.0479.

[132] John Joseph M. Carrasco, Mark P. Hertzberg, and Leonardo Senatore. The effective field theory of cosmological large scale structures. *Journal of High Energy Physics*, 2012:82, September 2012, doi:10.1007/JHEP09(2012)082, 1206.2926.

[133] Matthew Lewandowski and Leonardo Senatore. IR-safe and UV-safe integrands in the EFTofLSS with exact time dependence. *JCAP*, 08:037, 2017, doi:10.1088/1475-7516/2017/08/037, 1701.07012.

[134] Matthew Lewandowski and Leonardo Senatore. An analytic implementation of the IR-resummation for the BAO peak. *JCAP*, 03:018, 2020, doi:10.1088/1475-7516/2020/03/018, 1810.11855.

[135] Frank C. van den Bosch and Go Ogiya. Dark matter substructure in numerical simulations: a tale of discreteness noise, runaway instabilities, and artificial disruption. MNRAS, 475(3):4066–4087, April 2018, doi:10.1093/mnras/sty084, 1801.05427.

[136] Sheridan B. Green and Frank C. van den Bosch. The tidal evolution of dark matter substructure - I. subhalo density profiles. MNRAS, 490(2):2091–2101, December 2019, doi:10.1093/mnras/stz2767, 1908.08537.

[137] Sheridan B. Green, Frank C. van den Bosch, and Fangzhou Jiang. The tidal evolution of dark matter substructure - II. The impact of artificial disruption on subhalo mass functions and radial profiles. MNRAS, March 2021, doi:10.1093/mnras/stab696, 2103.01227.

[138] Julio F. Navarro, Carlos S. Frenk, and Simon D. M. White. The assembly of galaxies in a hierarchically clustering universe. MNRAS, 275(1):56–66, July 1995, doi:10.1093/mnras/275.1.56, astro-ph/9408067.

[139] Julio F. Navarro, Carlos S. Frenk, and Simon D. M. White. The Structure of Cold Dark Matter Halos. ApJ, 462:563, May 1996, doi:10.1086/177173, astro-ph/9508025.

[140] Julio F. Navarro, Carlos S. Frenk, and Simon D. M. White. A Universal Density Profile from Hierarchical Clustering. ApJ, 490(2):493–508, December 1997, doi:10.1086/304888, astro-ph/9611107.

[141] J. F. Navarro, E. Hayashi, C. Power, A. R. Jenkins, C. S. Frenk, S. D. M. White, V. Springel, J. Stadel, and T. R. Quinn. The inner structure of ΛCDM haloes - III. Universality and asymptotic slopes. MNRAS, 349(3):1039–1051, April 2004, doi:10.1111/j.1365-2966.2004.07586.x, astro-ph/0311231.

[142] Julio F. Navarro, Aaron Ludlow, Volker Springel, Jie Wang, Mark Vogelsberger, Simon D. M. White, Adrian Jenkins, Carlos S. Frenk, and Amina Helmi. The diversity and similarity of simulated cold dark matter haloes. MNRAS, 402(1):21–34, February 2010, doi:10.1111/j.1365-2966.2009.15878.x, 0810.1522.

[143] Jie Wang, Sownak Bose, Carlos S. Frenk, Liang Gao, Adrian Jenkins, Volker Springel, and Simon D. M. White. Universal structure of dark matter haloes over a mass range of 20 orders of magnitude. *Nature*, 585(7823):39–42, 2020, doi:10.1038/s41586-020-2642-9, 1911.09720.

[144] Stelios Kazantzidis, Lucio Mayer, Chiara Mastropietro, Jürg Diemand, Joachim Stadel, and Ben Moore. Density Profiles of Cold Dark Matter Substructure: Implications for the Missing-Satellites Problem. ApJ, 608(2):663–679, June 2004, doi:10.1086/420840, astro-ph/0312194.

[145] Sean Tulin and Hai-Bo Yu. Dark Matter Self-interactions and Small Scale Structure. *Phys. Rept.*, 730:1–57, 2018, doi:10.1016/j.physrep.2017.11.004, 1705.02358.

[146] A. Huss, B. Jain, and M. Steinmetz. How Universal Are the Density Profiles of Dark Halos? ApJ, 517(1):64–69, May 1999, doi:10.1086/307161, astro-ph/9803117.

[147] B. Moore, T. Quinn, F. Governato, J. Stadel, and G. Lake. Cold collapse and the core catastrophe. MNRAS, 310(4):1147–1152, December 1999, doi:10.1046/j.1365-8711.1999.03039.x, astro-ph/9903164.

[148] Neal Dalal, Yoram Lithwick, and Michael Kuhlen. The origin of dark matter halo profiles. *arXiv preprint arXiv:1010.2539*, 2010.

[149] Stacy Y. Kim, Annika H. G. Peter, and Jonathan R. Hargis. Missing Satellites Problem: Completeness Corrections to the Number of Satellite Galaxies in the Milky Way are Consistent with Cold Dark Matter Predictions. Phys. Rev. Lett., 121(21):211302, November 2018, doi:10.1103/PhysRevLett.121.211302, 1711.06267.

[150] P. A. Zyla et al. 2020 Review of Particle Physics. *Prog. Theor. Exp. Phys.*, 2020:083C01, 2020, doi:10.1093/ptep/ptaa104.

[151] F. Zwicky. On the Formation of Clusters of Nebulae and the Cosmological Time Scale. *Proceedings of the National Academy of Science*, 25(12):604–609, December 1939, doi:10.1073/pnas.25.12.604.

[152] H. Mo, F. van der Bosch, and S. White. *Galaxy Formation and Evolution*. Cambridge University Press, 2010.

[153] Kip S. Thorne and Roger D. Blandford. *Modern Classical Physics*. Princeton University Press, 2017.

[154] Eliott Rosenberg and JiJi Fan. Cooling in a Dissipative Dark Sector. *Phys. Rev. D*, 96(12):123001, 2017, doi:10.1103/PhysRevD.96.123001, 1705.10341.

[155] JiJi Fan, Andrey Katz, Lisa Randall, and Matthew Reece. Double-Disk Dark Matter. *Phys. Dark Univ.*, 2:139–156, 2013, doi:10.1016/j.dark.2013.07.001, 1303.1521.

[156] JiJi Fan, Andrey Katz, Lisa Randall, and Matthew Reece. Dark-Disk Universe. *Phys. Rev. Lett.*, 110(21):211302, 2013, doi:10.1103/PhysRevLett.110.211302, 1303.3271.

[157] Michael G. Hauser and Eli Dwek. The Cosmic Infrared Background: Measurements and Implications. ARA&A, 39:249–307, January 2001, doi:10.1146/annurev.astro.39.1.249, astro-ph/0105539.

[158] G. Gilmore and N. Reid. New light on faint stars - III. Galactic structure towards the South Pole and the Galactic thick disc. MNRAS, 202:1025–1047, March 1983, doi:10.1093/mnras/202.4.1025.

[159] Joss Bland-Hawthorn and Ortwin Gerhard. The galaxy in context: structural, kinematic, and integrated properties. *Annual Review of Astronomy and Astrophysics*, 54:529–596, 2016, doi:10.1146/annurev-astro-081915-023441.

[160] Michael R. Hayden, Jo Bovy, Jon A. Holtzman, David L. Nidever, Jonathan C. Bird, David H. Weinberg, Brett H. Andrews, Steven R. Majewski, Carlos Allende Prieto, Friedrich Anders, Timothy C. Beers, Dmitry Bizyaev, Cristina Chiappini, Katia Cunha, Peter Frinchaboy, D. A. García-Herńandez, Ana E. García Pérez, Léo Girardi, Paul Harding, Fred R. Hearty, Jennifer A. Johnson, Szabolcs Mészáros, Ivan Minchev, Robert O'Connell, Kaike Pan, Annie C. Robin, Ricardo P. Schiavon, Donald P. Schneider, Mathias Schultheis, Matthew Shetrone, Michael Skrutskie, Matthias Steinmetz, Verne Smith, John C. Wilson, Olga Zamora, and Gail Zasowski. Chemical Cartography with APOGEE: Metallicity Distribution Functions and the Chemical Structure of the Milky Way Disk. ApJ, 808(2):132, August 2015, doi:10.1088/0004-637X/808/2/132, 1503.02110.

[161] Joss Bland-Hawthorn, Sanjib Sharma, Thor Tepper-Garcia, James Binney, Ken C. Freeman, Michael R. Hayden, Janez Kos, Gayandhi M. De Silva, Simon Ellis, Geraint F. Lewis, Martin Asplund, Sven Buder, Andrew R. Casey, Valentina D'Orazi, Ly Duong, Shourya Khanna, Jane Lin, Karin Lind, Sarah L. Martell, Melissa K. Ness, Jeffrey D. Simpson, Daniel B. Zucker, Tomaž Zwitter, Prajwal R. Kafle, Alice C. Quillen, Yuan-Sen Ting, and Rosemary F. G. Wyse. The GALAH survey and Gaia DR2: dissecting the stellar disc's phase space by age, action, chemistry, and location. MNRAS, 486(1):1167–1191, June 2019, doi:10.1093/mnras/stz217, 1809.02658.

[162] WenTing Wang, JiaXin Han, Marius Cautun, ZhaoZhou Li, and Miho N. Ishigaki. The mass of our Milky Way. *Science China Physics, Mechanics, and Astronomy*, 63(10):109801, May 2020, doi:10.1007/s11433-019-1541-6, 1912.02599.

[163] Gurtina Besla. The Orbits and Total Mass of the Magellanic Clouds. *arXiv e-prints*, page arXiv:1511.03346, November 2015, 1511.03346.

[164] X. X. Xue, H. W. Rix, G. Zhao, P. Re Fiorentin, T. Naab, M. Steinmetz, F. C. van den Bosch, T. C. Beers, Y. S. Lee, E. F. Bell, C. Rockosi, B. Yanny, H. Newberg, R. Wilhelm, X. Kang, M. C. Smith, and D. P. Schneider. The Milky Way's Circular Velocity Curve to 60 kpc and an Estimate of the Dark Matter Halo Mass from the Kinematics of ~2400 SDSS Blue Horizontal-Branch Stars. ApJ, 684(2):1143–1158, September 2008, doi:10.1086/589500, 0801.1232.

[165] K. M. Stringer, A. Drlica-Wagner, L. Macri, C. E. Martínez-Vázquez, A. K. Vivas, P. Ferguson, A. B. Pace, A. R. Walker, E. Neilsen, K. Tavangar, W. Wester, T. M. C. Abbott, M. Aguena, S. Allam, D. Bacon, K. Bechtol, E. Bertin, D. Brooks, D. L. Burke, A. Carnero Rosell, M. Carrasco Kind, J. Carretero, M. Costanzi, M. Crocce, L. N. da Costa, M. E. S. Pereira, J. De Vicente, S. Desai, H. T. Diehl, P. Doel, I. Ferrero, J. García-Bellido, E. Gaztanaga, D. W. Gerdes, D. Gruen, R. A. Gruendl, J. Gschwend, G. Gutierrez, S. R. Hinton, D. L. Hollowood, K. Honscheid, B. Hoyle, D. J. James, K. Kuehn, N. Kuropatkin, T. S. Li, M. A. G. Maia, J. L. Marshall, F. Menanteau, R. Miquel, R. Morgan, R. L. C. Ogando, A. Palmese, F. Paz-Chinchón, A. A. Plazas, A. Roodman, E. Sanchez, M. Schubnell, S. Serrano, I. Sevilla-Noarbe, M. Smith, M. Soares-Santos, E. Suchyta, G. Tarle, D. Thomas, C. To, T. N. Varga, R. D. Wilkinson, Y. Zhang, and the DES Collaboration. Identifying RR Lyrae Variable Stars in Six Years of the Dark Energy Survey. *arXiv e-prints*, page arXiv:2011.13930, November 2020, doi:10.3847/1538-4357/abe873, 2011.13930.

[166] Matthew G. Walker and Jorge Peñarrubia. A Method for Measuring (Slopes of) the Mass Profiles of Dwarf Spheroidal Galaxies. ApJ, 742(1):20, November 2011, doi:10.1088/0004-637X/742/1/20, 1108.2404.

[167] J. I. Read and G. Gilmore. Mass loss from dwarf spheroidal galaxies: the origins of shallow dark matter cores and exponential surface brightness profiles. MNRAS, 356(1):107–124, January 2005, doi:10.1111/j.1365-2966.2004.08424.x, astro-ph/0409565.

[168] Alyson M. Brooks, Michael Kuhlen, Adi Zolotov, and Dan Hooper. A Baryonic Solution to the Missing Satellites Problem. ApJ, 765(1):22, March 2013, doi:10.1088/0004-637X/765/1/22, 1209.5394.

[169] J. N. Bahcall and R. A. Wolf. Star distribution around a massive black hole in a globular cluster. ApJ, 209:214–232, October 1976, doi:10.1086/154711.

[170] Roeland P. van der Marel, Joris Gerssen, Puragra Guhathakurta, Ruth C. Peterson, and Karl Gebhardt. Hubble Space Telescope Evidence for an Intermediate-Mass Black Hole in the Globular Cluster M15. I. STIS Spectroscopy and WFPC2 Photometry. AJ, 124(6):3255–3269, December 2002, doi:10.1086/344583, astro-ph/0209314.

[171] Jeremy Tinker, Andrey V. Kravtsov, Anatoly Klypin, Kevork Abazajian, Michael Warren, Gustavo Yepes, Stefan Gottlöber, and Daniel E. Holz. Toward a Halo Mass Function for Precision Cosmology: The Limits of Universality. ApJ, 688(2):709–728, December 2008, doi:10.1086/591439, 0803.2706.

[172] Greg L. Bryan and Michael L. Norman. Statistical Properties of X-Ray Clusters: Analytic and Numerical Comparisons. ApJ, 495(1):80–99, March 1998, doi:10.1086/305262, astro-ph/9710107.

[173] Surhud More, Benedikt Diemer, and Andrey V. Kravtsov. The Splashback Radius as a Physical Halo Boundary and the Growth of Halo Mass. ApJ, 810(1):36, September 2015, doi:10.1088/0004-637X/810/1/36, 1504.05591.

[174] Gurtina Besla, Nitya Kallivayalil, Lars Hernquist, Brant Robertson, T. J. Cox, Roeland P. van der Marel, and Charles Alcock. Are the Magellanic Clouds on Their First Passage about the Milky Way? ApJ, 668(2):949–967, October 2007, doi:10.1086/521385, astro-ph/0703196.

[175] Nitya Kallivayalil, Roeland P. van der Marel, Charles Alcock, Tim Axelrod, Kem H. Cook, A. J. Drake, and M. Geha. The Proper Motion of the Large Magellanic Cloud Using HST. ApJ, 638(2):772–785, February 2006, doi:10.1086/498972, astro-ph/0508457.

[176] M. Ségall, R. A. Ibata, M. J. Irwin, N. F. Martin, and S. Chapman. Draco, a flawless dwarf galaxy*. MNRAS, 375(3):831–842, March 2007, doi:10.1111/j.1365-2966.2006.11356.x, astro-ph/0612263.

[177] N. Shipp et al., DES. Stellar Streams Discovered in the Dark Energy Survey. *Astrophys. J.*, 862(2):114, 2018, doi:10.3847/1538-4357/aacdab, 1801.03097.

[178] Roeland P. van der Marel and Puragra Guhathakurta. M31 Transverse Velocity and Local Group Mass from Satellite Kinematics. ApJ, 678(1):187–199, May 2008, doi:10.1086/533430, 0709.3747.

[179] Erik J. Tollerud, Rachael L. Beaton, Marla C. Geha, James S. Bullock, Puragra Guhathakurta, Jason S. Kalirai, Steve R. Majewski, Evan N. Kirby, Karoline M. Gilbert, Basilio Yniguez, Richard J. Patterson, James C. Ostheimer, Jeff Cooke, Claire E. Dorman, Abrar Choudhury, and Michael C. Cooper. The SPLASH Survey: Spectroscopy of 15 M31 Dwarf Spheroidal Satellite Galaxies. ApJ, 752(1):45, June 2012, doi:10.1088/0004-637X/752/1/45, 1112.1067.

[180] J. P. Ostriker and P. J. E. Peebles. A Numerical Study of the Stability of Flattened Galaxies: or, can Cold Galaxies Survive? ApJ, 186:467–480, December 1973, doi:10.1086/152513.

[181] Gerard Gilmore, Rosemary F. G. Wyse, and Konrad Kuijken. Kinematics, chemistry, and structure of the Galaxy. ARA&A, 27:555–627, January 1989, doi:10.1146/annurev.aa.27.090189.003011.

[182] Amina Helmi, Carine Babusiaux, Helmer H. Koppelman, Davide Massari, Jovan Veljanoski, and Anthony G. A. Brown. The merger that led to the formation of the Milky Way's inner stellar halo and thick disk. Nature, 563(7729):85–88, October 2018, doi:10.1038/s41586-018-0625-x, 1806.06038.

[183] V Belokurov, Denis Erkal, NW Evans, SE Koposov, and AJ Deason. Co-formation of the disc and the stellar halo. *Monthly Notices of the Royal Astronomical Society*, 478(1):611–619, 2018, doi:10.1093/mnras/sty982.

[184] Fiorenzo Vincenzo, Emanuele Spitoni, Francesco Calura, Francesca Matteucci, Victor Silva Aguirre, Andrea Miglio, and Gabriele Cescutti. The Fall of a Giant. Chemical evolution of Enceladus, alias the Gaia Sausage. MNRAS, 487(1):L47–L52, July 2019, doi:10.1093/mnrasl/slz070, 1903.03465.

[185] Robert J. J. Grand, Daisuke Kawata, Vasily Belokurov, Alis J. Deason, Azadeh Fattahi, Francesca Fragkoudi, Facundo A. Gómez, Federico Marinacci, and Rüdiger Pakmor. The dual origin of the Galactic thick disc and halo from the gas-rich Gaia-Enceladus Sausage merger. MNRAS, 497(2):1603–1618, September 2020, doi:10.1093/mnras/staa2057, 2001.06009.

[186] T. Bensby, A. Alves-Brito, M. S. Oey, D. Yong, and J. Meléndez. A First Constraint on the Thick Disk Scale Length: Differential Radial Abundances in K Giants at Galactocentric Radii 4, 8, and 12 kpc. ApJ, 735(2):L46, July 2011, doi:10.1088/2041-8205/735/2/L46, 1106.1914.

[187] Thomas Donlon, Heidi Jo Newberg, Robyn Sanderson, and Lawrence M. Widrow. The milky way's shell structure reveals the time of a radial collision. *The Astrophysical Journal*, 902(2):119, oct 2020, doi:10.3847/1538-4357/abb5f6, 2006.08764.

[188] Eloisa Poggio, Chervin F. P. Laporte, Kathryn V. Johnston, Elena D'Onghia, Ronald Drimmel, and Douglas Grion Filho. Measuring the vertical response of the Galactic disc to an infalling satellite. *arXiv e-prints*, page arXiv:2011.11642, November 2020, 2011.11642.

[189] Douglas Grion Filho, Kathryn V. Johnston, Eloisa Poggio, Chervin F. P. Laporte, Ronald Drimmel, and Elena D'Onghia. A Holistic Review of a Galactic Interaction. *arXiv e-prints*, page arXiv:2012.07778, December 2020, 2012.07778.

[190] Joss Bland-Hawthorn and Thor Tepper-García. Galactic seismology: the evolving "phase spiral" after the Sagittarius dwarf impact. MNRAS, March 2021, doi:10.1093/mnras/stab704, 2009.02434.

[191] Chris W. Purcell, James S. Bullock, Erik J. Tollerud, Miguel Rocha, and Sukanya Chakrabarti. The Sagittarius impact as an architect of spirality and outer rings in the Milky Way. Nature, 477(7364):301–303, September 2011, doi:10.1038/nature10417, 1109.2918.

[192] D. Erkal, V. Belokurov, C. F. P. Laporte, S. E. Koposov, T. S. Li, C. J. Grillmair, N. Kallivayalil, A. M. Price-Whelan, N. W. Evans, K. Hawkins, D. Hendel, C. Mateu, J. F. Navarro, A. del Pino, C. T. Slater, S. T. Sohn, and Orphan Aspen Treasury Collaboration. The total mass of the Large Magellanic Cloud from its perturbation on the Orphan stream. MNRAS, 487(2):2685–2700, August 2019, doi:10.1093/mnras/stz1371, 1812.08192.

[193] Charlie Conroy, Rohan P. Naidu, Nicolás Garavito-Camargo, Gurtina Besla, Dennis Zaritsky, Ana Bonaca, and Benjamin D. Johnson. All-sky dynamical response of the Galactic halo to the Large Magellanic Cloud. Nature, 592(7855):534–536, January 2021, doi:10.1038/s41586-021-03385-7, 2104.09515.

[194] Eugene Vasiliev, Vasily Belokurov, and Denis Erkal. Tango for three: Sagittarius, LMC, and the Milky Way. MNRAS, 501(2):2279–2304, February 2021, doi:10.1093/mnras/staa3673, 2009.10726.

[195] F. J. Kerr. A magellanic effect on the galaxy. *The Astronomical Journal*, 62:93–93, 1957, doi:10.1086/107466.

[196] Yan Xu, Heidi Jo Newberg, Jeffrey L. Carlin, Chao Liu, Licai Deng, Jing Li, Ralph Schönrich, and Brian Yanny. Rings and Radial Waves in the Disk of the Milky Way. ApJ, 801(2):105, March 2015, doi:10.1088/0004-637X/801/2/105, 1503.00257.

[197] T. Antoja, A. Helmi, M. Romero-Gómez, D. Katz, C. Babusiaux, R. Drimmel, D. W. Evans, F. Figueras, E. Poggio, C. Reylé, A. C. Robin, G. Seabroke, and C. Soubiran. A dynamically young and perturbed Milky Way disk. Nature, 561(7723):360–362, September 2018, doi:10.1038/s41586-018-0510-7, 1804.10196.

[198] Shourya Khanna, Sanjib Sharma, Thor Tepper-Garcia, Joss Bland-Hawthorn, Michael Hayden, Martin Asplund, Sven Buder, Boquan Chen, Gayandhi M. De Silva, Ken C. Freeman, Janez Kos, Geraint F. Lewis, Jane Lin, Sarah L. Martell, Jeffrey D. Simpson, Thomas Nordlander, Dennis Stello, Yuan-Sen Ting, Daniel B. Zucker, and Tomaž Zwitter. The GALAH survey and Gaia DR2: Linking ridges, arches, and vertical waves in the kinematics of the Milky Way. MNRAS, 489(4):4962–4979, November 2019, doi:10.1093/mnras/stz2462, 1902.10113.

[199] Xiang-Xiang Xue, Hans-Walter Rix, Zhibo Ma, Heather Morrison, Jo Bovy, Branimir Sesar, and William Janesh. THE RADIAL PROFILE AND FLATTENING OF THE MILKY WAY's STELLAR HALO TO 80 kpc FROM THE SEGUE k-GIANT SURVEY. *The Astrophysical Journal*, 809(2):144, aug 2015, doi:10.1088/0004-637x/809/2/144.

[200] Amina Helmi. Is the dark halo of our Galaxy spherical? MNRAS, 351(2):643–648, June 2004, doi:10.1111/j.1365-2966.2004.07812.x, astro-ph/0309579.

[201] Andrew R. Zentner, Andrey V. Kravtsov, Oleg Y. Gnedin, and Anatoly A. Klypin. The Anisotropic Distribution of Galactic Satellites. ApJ, 629(1):219–232, August 2005, doi:10.1086/431355, astro-ph/0502496.

[202] David R. Law and Steven R. Majewski. The Sagittarius Dwarf Galaxy: A Model for Evolution in a Triaxial Milky Way Halo. ApJ, 714(1):229–254, May 2010, doi:10.1088/0004-637X/714/1/229, 1003.1132.

[203] H. Baumgardt, P. Côté, M. Hilker, M. Rejkuba, S. Mieske, S. G. Djorgovski, and Peter Stetson. The velocity dispersion and mass-to-light ratio of the remote halo globular cluster NGC2419. MNRAS, 396(4):2051–2060, July 2009, doi:10.1111/j.1365-2966.2009.14932.x, 0904.3329.

[204] Scott Tremaine. Dark Matter in the Solar System. In D. Lynden-Bell and G. Gilmore, editors, *Neutron Stars and Their Birth Events*, volume 306 of *NATO Advanced Study Institute (ASI) Series C*, page 37, January 1990, `https://link.springer.com/chapter/10.1007/978-94-009-0565-8_3`.

[205] S. M. Faber and J. S. Gallagher. Masses and mass-to-light ratios of galaxies. ARA&A, 17:135–187, January 1979, doi:10.1146/annurev.aa.17.090179.001031.

[206] Anna-Christina Eilers, David W. Hogg, Hans-Walter Rix, and Melissa K. Ness. The circular velocity curve of the milky way from 5 to 25 kpc. *The Astrophysical Journal*, 871(1):120, 2019, doi:10.3847/1538-4357/aaf648, 1810.09466.

[207] Jo Bovy. A purely acceleration-based measurement of the fundamental Galactic parameters. *arXiv e-prints*, page arXiv:2012.02169, December 2020, 2012.02169.

[208] Maria Selina Nitschai, Anna-Christina Eilers, Nadine Neumayer, Michele Cappellari, and Hans-Walter Rix. Dynamical Model of the Milky Way Using APOGEE and Gaia Data. ApJ, 916(2):112, August 2021, doi:10.3847/1538-4357/ac04b5, 2106.05286.

[209] Gravity Collaboration: Abuter et al. Detection of the gravitational redshift in the orbit of the star s2 near the galactic centre massive black hole. *Astronomy & Astrophysics*, 615:L15, 2018, doi:10.1051/0004-6361/201833718.

[210] R. Gravity Collaboration: Abuter, A. Amorim, M. Bauböck, J. P. Berger, H. Bonnet, W. Brandner, Y. Clénet, V. Coudé du Foresto, P. T. de Zeeuw, J. Dexter, et al. A geometric distance measurement to the galactic center black hole with 0.3% uncertainty. *Astronomy & Astrophysics*, 625:L10, 2019, doi:10.1051/0004-6361/201935656.

[211] Gravity Collaboration, R. Abuter, A. Amorim, M. Bauböck, J. P. Berger, H. Bonnet, W. Brandner, Y. Clénet, R. Davies, P. T. de Zeeuw, J. Dexter, Y. Dallilar, A. Drescher, A. Eckart, F. Eisenhauer, N. M. Förster Schreiber, P. Garcia, F. Gao, E. Gendron, R. Genzel, S. Gillessen, M. Habibi, X. Haubois, G. Heiσel, T. Henning, S. Hippler, M. Horrobin, A. Jiménez-Rosales, L. Jochum, L. Jocou, A. Kaufer, P. Kervella, S. Lacour, V. Lapeyrère, J. B. Le Bouquin, P. Léna, D. Lutz,

M. Nowak, T. Ott, T. Paumard, K. Perraut, G. Perrin, O. Pfuhl, S. Rabien, G. Rodríguez-Coira, J. Shangguan, T. Shimizu, S. Scheithauer, J. Stadler, O. Straub, C. Straubmeier, E. Sturm, L. J. Tacconi, F. Vincent, S. von Fellenberg, I. Waisberg, F. Widmann, E. Wieprecht, E. Wiezorrek, J. Woillez, S. Yazici, A. Young, and G. Zins. Improved GRAVITY astrometric accuracy from modeling optical aberrations. A&A, 647:A59, March 2021, doi:10.1051/0004-6361/202040208, 2101.12098.

[212] M. J. Reid, K. M. Menten, A. Brunthaler, X. W. Zheng, T. M. Dame, Y. Xu, Y. Wu, B. Zhang, A. Sanna, M. Sato, et al. Trigonometric parallaxes of high mass star forming regions: the structure and kinematics of the milky way. *The Astrophysical Journal*, 783(2):130, 2014, doi:10.1088/0004-637X/783/2/130.

[213] Austin Hinkel, Susan Gardner, and Brian Yanny. Axial Asymmetry Studies in Gaia Data Release 2 Yield the Pattern Speed of the Galactic Bar. ApJ, 899(1):L14, August 2020, doi:10.3847/2041-8213/aba905, 2007.12699.

[214] Y. Huang, X. W. Liu, H. B. Yuan, M. S. Xiang, H. W. Zhang, B. Q. Chen, J. J. Ren, C. Wang, Y. Zhang, Y. H. Hou, Y. F. Wang, and Z. H. Cao. The Milky Way's rotation curve out to 100 kpc and its constraint on the Galactic mass distribution. MNRAS, 463(3):2623–2639, December 2016, doi:10.1093/mnras/stw2096, 1604.01216.

[215] Eric David Kramer and Lisa Randall. Updated Kinematic Constraints on a Dark Disk. ApJ, 824(2):116, June 2016, doi:10.3847/0004-637X/824/2/116, 1604.01407.

[216] Noam I. Libeskind, Yehuda Hoffman, R. Brent Tully, Helene M. Courtois, Daniel Pomarède, Stefan Gottlöber, and Matthias Steinmetz. Planes of satellite galaxies and the cosmic web. MNRAS, 452(1):1052–1059, September 2015, doi:10.1093/mnras/stv1302, 1503.05915.

[217] Noam I. Libeskind, Elmo Tempel, Yehuda Hoffman, R. Brent Tully, and Hélène Courtois. Filaments from the galaxy distribution and from the velocity field in the local universe. MNRAS, 453(1):L108–L112, October 2015, doi:10.1093/mnrasl/slv099, 1505.07454.

[218] Oliver Müller, Marcel S. Pawlowski, Federico Lelli, Katja Fahrion, Marina Rejkuba, Michael Hilker, Jamie Kanehisa, Noam Libeskind, and Helmut Jerjen. The coherent motion of Cen A dwarf satellite galaxies remains a challenge for ΛCDM cosmology. A&A, 645:L5, January 2021, doi:10.1051/0004-6361/202039973, 2012.08138.

[219] Priyamvada Natarajan, Urmila Chadayammuri, Mathilde Jauzac, Johan Richard, Jean-Paul Kneib, Harald Ebeling, Fangzhou Jiang, Frank van den Bosch, Marceau Limousin, Eric Jullo, Hakim Atek, Annalisa Pillepich, Cristina Popa, Federico Marinacci, Lars Hernquist, Massimo Meneghetti, and Mark Vogelsberger. Mapping substructure in the HST Frontier Fields cluster lenses and in cosmological simulations. MNRAS, 468(2):1962–1980, June 2017, doi:10.1093/mnras/stw3385, 1702.04348.

[220] Roeland P van der Marel. The Large Magellanic Cloud: structure and kinematics. In Mario Livio and Thomas M. Brown, editors, *The Local Group as an Astrophysical Laboratory*, 2011.

[221] Nitya Kallivayalil, Roeland P. van der Marel, Gurtina Besla, Jay Anderson, and Charles Alcock. Third-epoch Magellanic Cloud Proper Motions. I. Hubble Space Telescope/WFC3 Data and Orbit Implications. ApJ, 764(2):161, Feb 2013, doi:10.1088/0004-637X/764/2/161, 1301.0832.

[222] Ekta Patel, Gurtina Besla, and Sangmo Tony Sohn. Orbits of massive satellite galaxies–i. a close look at the large magellanic cloud and a new orbital history for m33. *Monthly Notices of the Royal Astronomical Society*, 464(4):3825–3849, 2016, doi:10.1093/mnras/stw2616.

[223] Chervin FP Laporte, Kathryn V Johnston, Facundo A Gómez, Nicolas Garavito-Camargo, and Gurtina Besla. The influence of sagittarius and the large magellanic cloud on the stellar disc of the milky way galaxy. *Monthly Notices of the Royal Astronomical Society*, 481(1):286–306, 2018, doi:10.1093/mnras/sty1574.

[224] Michael S. Petersen and Jorge Peñarrubia. Detection of the Milky Way reflex motion due to the Large Magellanic Cloud infall. *Nature Astronomy*, November 2020, doi:10.1038/s41550-020-01254-3, 2011.10581.

[225] Denis Erkal, Alis J. Deason, Vasily Belokurov, Xiang-Xiang Xue, Sergey E. Koposov, Sarah A. Bird, Chao Liu, Iulia T. Simion, Chengqun Yang, Lan Zhang, and Gang Zhao. Detection of the LMC-induced sloshing of the Galactic halo. *arXiv e-prints*, page arXiv:2010.13789, October 2020, 2010.13789.

[226] Eugene Vasiliev, Vasily Belokurov, and Denis Erkal. Tango for three: Sagittarius, LMC, and the Milky Way. MNRAS, 501(2):2279–2304, February 2021, doi:10.1093/mnras/staa3673, 2009.10726.

[227] Denis Erkal, Vasily A. Belokurov, and Daniel L. Parkin. Equilibrium models of the Milky Way mass are biased high by the LMC. MNRAS, 498(4):5574–5580, November 2020, doi:10.1093/mnras/staa2840, 2001.11030.

[228] Nitya Kallivayalil, Laura V. Sales, Paul Zivick, Tobias K. Fritz, Andrés Del Pino, Sangmo Tony Sohn, Gurtina Besla, Roeland P. van der Marel, Julio F. Navarro, and Elena Sacchi. The Missing Satellites of the Magellanic Clouds? Gaia Proper Motions of the Recently Discovered Ultra-faint Galaxies. ApJ, 867(1):19, November 2018, doi:10.3847/1538-4357/aadfee, 1805.01448.

[229] Ekta Patel, Nitya Kallivayalil, Nicolas Garavito-Camargo, Gurtina Besla, Daniel R. Weisz, Roeland P. van der Marel, Michael Boylan-Kolchin, Marcel S. Pawlowski, and Facundo A. Gómez. The Orbital Histories of Magellanic Satellites Using Gaia DR2 Proper Motions. ApJ, 893(2):121, April 2020, doi:10.3847/1538-4357/ab7b75, 2001.01746.

[230] Denis Erkal and Vasily A. Belokurov. Limit on the LMC mass from a census of its satellites. MNRAS, 495(3):2554–2563, July 2020, doi:10.1093/mnras/staa1238, 1907.09484.

[231] Gurtina Besla, Annika Peter, and Nicolas Garavito-Camargo. The highest-speed local dark matter particles come from the large magellanic cloud. *arXiv preprint arXiv:1909.04140*, 2019, doi:10.1088/1475-7516/2019/11/013.

[232] Immanuel Kant. *Universal Natural History and Theory of the Heavens (1755)*. Richer Resources Publications, 2009.

[233] G. J. Whitrow. Kant and the Extragalactic Nebulae. QJRAS, 8:48, March 1967.

[234] E. P. Hubble. A general study of diffuse galactic nebulae. ApJ, 56:162–199, October 1922, doi:10.1086/142698.

[235] Sownak Bose, Alis J. Deason, Vasily Belokurov, and Carlos S. Frenk. The little things matter: relating the abundance of ultrafaint satellites to the hosts' assembly history. MNRAS, 495(1):743–757, June 2020, doi:10.1093/mnras/staa1199, 1909.04039.

[236] A. Drlica-Wagner et al., DES Collaboration. Eight Ultra-faint Galaxy Candidates Discovered in Year Two of the Dark Energy Survey. ApJ, 813(2):109, November 2015, doi:10.1088/0004-637X/813/2/109, 1508.03622.

[237] K. Bechtol et al., DES Collaboration. Eight New Milky Way Companions Discovered in First-year Dark Energy Survey Data. ApJ, 807(1):50, July 2015, doi:10.1088/0004-637X/807/1/50, 1503.02584.

[238] Sergey E. Koposov, Vasily Belokurov, Gabriel Torrealba, and N. Wyn Evans. Beasts of the Southern Wild: Discovery of Nine Ultra Faint Satellites in the Vicinity of the Magellanic Clouds. ApJ, 805(2):130, June 2015, doi:10.1088/0004-637X/805/2/130, 1503.02079.

[239] Joshua D. Simon. The Faintest Dwarf Galaxies. ARA&A, 57:375–415, August 2019, doi:10.1146/annurev-astro-091918-104453, 1901.05465.

[240] Erik J. Tollerud, James S. Bullock, Louis E. Strigari, and Beth Willman. Hundreds of Milky Way Satellites? Luminosity Bias in the Satellite Luminosity Function. ApJ, 688(1):277–289, November 2008, doi:10.1086/592102, 0806.4381.

[241] Jonathan R. Hargis, Beth Willman, and Annika H. G. Peter. Too Many, Too Few, or Just Right? The Predicted Number and Distribution of Milky Way Dwarf Galaxies. ApJ, 795(1):L13, November 2014, doi:10.1088/2041-8205/795/1/L13, 1407.4470.

[242] P. Jethwa, D. Erkal, and V. Belokurov. The upper bound on the lowest mass halo. MNRAS, 473(2):2060–2083, January 2018, doi:10.1093/mnras/stx2330, 1612.07834.

[243] Oliver Newton, Marius Cautun, Adrian Jenkins, Carlos S. Frenk, and John C. Helly. The total satellite population of the Milky Way. MNRAS, 479(3):2853–2870, September 2018, doi:10.1093/mnras/sty1085, 1708.04247.

[244] Alex Drlica-Wagner et al., LSST Dark Matter Group. Probing the Fundamental Nature of Dark Matter with the Large Synoptic Survey Telescope. 2 2019, 1902.01055.

[245] Joseph Silk. Cosmic Black-Body Radiation and Galaxy Formation. ApJ, 151:459, February 1968, doi:10.1086/149449.

[246] P. J. E. Peebles and J. T. Yu. Primeval Adiabatic Perturbation in an Expanding Universe. ApJ, 162:815, December 1970, doi:10.1086/150713.

[247] III Gott, J. R. and M. J. Rees. A theory of galaxy formation and clustering. A&A, 45:365–376, December 1975.

[248] J. R. Bond, G. Efstathiou, and J. Silk. Massive Neutrinos and the Large-Scale Structure of the Universe. Phys. Rev. Lett., 45(24):1980–1984, December 1980, doi:10.1103/PhysRevLett.45.1980.

[249] J. R. Bond and A. S. Szalay. The collisionless damping of density fluctuations in an expanding universe. ApJ, 274:443–468, November 1983, doi:10.1086/161460.

[250] J. R. Bond and G. Efstathiou. Cosmic background radiation anisotropies in universes dominated by nonbaryonic dark matter. ApJ, 285:L45–L48, October 1984, doi:10.1086/184362.

[251] J. R. Bond and G. Efstathiou. The statistics of cosmic background radiation fluctuations. MN-RAS, 226:655–687, June 1987, doi:10.1093/mnras/226.3.655.

[252] Heidi Jo Newberg and Jeffrey L. Carlin. *Tidal Streams in the Local Group and Beyond*, volume 420. Springer, 2016, doi:10.1007/978-3-319-19336-6.

[253] Michael Odenkirchen, Eva K. Grebel, Constance M. Rockosi, Walter Dehnen, Rodrigo Ibata, Hans-Walter Rix, Andrea Stolte, Christian Wolf, Jr. Anderson, John E., Neta A. Bahcall, Jon Brinkmann, István Csabai, G. Hennessy, Robert B. Hindsley, Željko Ivezić, Robert H. Lupton, Jeffrey A. Munn, Jeffrey R. Pier, Chris Stoughton, and Donald G. York. Detection of Massive Tidal Tails around the Globular Cluster Palomar 5 with Sloan Digital Sky Survey Commissioning Data. ApJ, 548(2):L165–L169, February 2001, doi:10.1086/319095, astro-ph/0012311.

[254] Kathryn V. Johnston, Lars Hernquist, and Michael Bolte. Fossil Signatures of Ancient Accretion Events in the Halo. ApJ, 465:278, July 1996, doi:10.1086/177418, astro-ph/9602060.

[255] Kathryn V. Johnston. A Prescription for Building the Milky Way's Halo from Disrupted Satellites. ApJ, 495(1):297–308, March 1998, doi:10.1086/305273, astro-ph/9710007.

[256] John Dubinski, J. Christopher Mihos, and Lars Hernquist. Constraining Dark Halo Potentials with Tidal Tails. ApJ, 526(2):607–622, December 1999, doi:10.1086/308024, astro-ph/9902217.

[257] James S. Bullock and Kathryn V. Johnston. Tracing galaxy formation with stellar halos. 1. Methods. *Astrophys. J.*, 635:931–949, 2005, doi:10.1086/497422, astro-ph/0506467.

[258] Eric F. Bell, Daniel B. Zucker, Vasily Belokurov, Sanjib Sharma, Kathryn V. Johnston, James S. Bullock, David W. Hogg, Knud Jahnke, Jelte T. A. De Jong, Timothy C. Beers, et al. The accretion origin of the milky way's stellar halo. *The Astrophysical Journal*, 680(1):295, 2008, doi:10.1086/588032.

[259] Kathryn V. Johnston, HongSheng Zhao, David N. Spergel, and Lars Hernquist. Tidal Streams as Probes of the Galactic Potential. ApJ, 512(2):L109–L112, February 1999, doi:10.1086/311876, astro-ph/9807243.

[260] Kathryn V. Johnston, David R. Law, and Steven R. Majewski. A Two Micron All Sky Survey View of the Sagittarius Dwarf Galaxy. III. Constraints on the Flattening of the Galactic Halo. ApJ, 619(2):800–806, February 2005, doi:10.1086/426777, astro-ph/0407565.

[261] Sergey E. Koposov, Hans-Walter Rix, and David W. Hogg. Constraining the Milky Way Potential with a Six-Dimensional Phase-Space Map of the GD-1 Stellar Stream. ApJ, 712(1):260–273, March 2010, doi:10.1088/0004-637X/712/1/260, 0907.1085.

[262] Jason L. Sanders and James Binney. Stream-orbit misalignment - I. The dangers of orbit-fitting. MNRAS, 433(3):1813–1825, August 2013, doi:10.1093/mnras/stt806, 1305.1935.

[263] Jason L. Sanders and James Binney. Stream-orbit misalignment - II. A new algorithm to constrain the Galactic potential. MNRAS, 433(3):1826–1836, August 2013, doi:10.1093/mnras/stt816, 1305.1937.

[264] Jo Bovy. Dynamical Modeling of Tidal Streams. ApJ, 795(1):95, November 2014, doi:10.1088/0004-637X/795/1/95, 1401.2985.

[265] Robyn E. Sanderson, Amina Helmi, and David W. Hogg. Action-space Clustering of Tidal Streams to Infer the Galactic Potential. ApJ, 801(2):98, March 2015, doi:10.1088/0004-637X/801/2/98, 1404.6534.

[266] Ana Bonaca, Marla Geha, Andreas H. W. Küpper, Jürg Diemand, Kathryn V. Johnston, and David W. Hogg. Milky Way Mass and Potential Recovery Using Tidal Streams in a Realistic Halo. ApJ, 795(1):94, November 2014, doi:10.1088/0004-637X/795/1/94, 1406.6063.

[267] S. L. J. Gibbons, V. Belokurov, and N. W. Evans. 'Skinny Milky Way please', says Sagittarius. MNRAS, 445(4):3788–3802, December 2014, doi:10.1093/mnras/stu1986, 1406.2243.

[268] Adrian M. Price-Whelan, David W. Hogg, Kathryn V. Johnston, and David Hendel. Inferring the Gravitational Potential of the Milky Way with a Few Precisely Measured Stars. ApJ, 794(1):4, October 2014, doi:10.1088/0004-637X/794/1/4, 1405.6721.

[269] A. Bowden, V. Belokurov, and N. W. Evans. Dipping our toes in the water: first models of GD-1 as a stream. MNRAS, 449(2):1391–1400, May 2015, doi:10.1093/mnras/stv285, 1502.00484.

[270] Andreas H. W. Küpper, Eduardo Balbinot, Ana Bonaca, Kathryn V. Johnston, David W. Hogg, Pavel Kroupa, and Basilio X. Santiago. Globular Cluster Streams as Galactic High-Precision Scales—the Poster Child Palomar 5. ApJ, 803(2):80, April 2015, doi:10.1088/0004-637X/803/2/80, 1502.02658.

[271] Jo Bovy, Anita Bahmanyar, Tobias K. Fritz, and Nitya Kallivayalil. The Shape of the Inner Milky Way Halo from Observations of the Pal 5 and GD–1 Stellar Streams. ApJ, 833(1):31, December 2016, doi:10.3847/1538-4357/833/1/31, 1609.01298.

[272] Harshil Kamdar, Charlie Conroy, and Yuan-Sen Ting. Stellar Streams in the Galactic Disk: Predicted Lifetimes and Their Utility in Measuring the Galactic Potential. *arXiv e-prints*, page arXiv:2106.02050, June 2021, 2106.02050.

[273] Alexander Knebe, Stuart P. D. Gill, Daisuke Kawata, and Brad K. Gibson. Mapping substructures in dark matter haloes. MNRAS, 357(1):L35–L39, February 2005, doi:10.1111/j.1745-3933.2005.08666.x, astro-ph/0407418.

[274] Adrian M. Price-Whelan, Kathryn V. Johnston, Monica Valluri, Sarah Pearson, Andreas H. W. Küpper, and David W. Hogg. Chaotic dispersal of tidal debris. MNRAS, 455(1):1079–1098, January 2016, doi:10.1093/mnras/stv2383, 1507.08662.

[275] Carl J. Grillmair and Jeffrey L. Carlin. *Stellar Streams and Clouds in the Galactic Halo*, volume 420, chapter 6, page 87. Springer, 2016, doi:10.1007/978-3-319-19336-6_4.

[276] Stefan Meingast, João Alves, and Verena Fürnkranz. Extended stellar systems in the solar neighborhood . II. Discovery of a nearby 120° stellar stream in Gaia DR2. A&A, 622:L13, February 2019, doi:10.1051/0004-6361/201834950, 1901.06387.

[277] Rodrigo A. Ibata, Michele Bellazzini, Khyati Malhan, Nicolas Martin, and Paolo Bianchini. Identification of the long stellar stream of the prototypical massive globular cluster ω Centauri. *Nature Astronomy*, 3:667–672, April 2019, doi:10.1038/s41550-019-0751-x, 1902.09544.

[278] Lina Necib, Bryan Ostdiek, Mariangela Lisanti, Timothy Cohen, Marat Freytsis, Shea Garrison-Kimmel, Philip F. Hopkins, Andrew Wetzel, and Robyn Sanderson. Evidence for a vast prograde stellar stream in the solar vicinity. *Nature Astronomy*, 4:1078–1083, July 2020, doi:10.1038/s41550-020-1131-2, 1907.07190.

[279] T. S. Li et al., S^5. The southern stellar stream spectroscopic survey (S^5): Overview, target selection, data reduction, validation, and early science. *Mon. Not. Roy. Astron. Soc.*, 490(3):3508–3531, 2019, doi:10.1093/mnras/stz2731, 1907.09481.

[280] David Martinez-Delgado, Andrew P. Cooper, Javier Roman, Annalisa Pillepich, Denis Erkal, Sarah Pearson, John Moustakas, Chervin F. P. Laporte, Seppo Laine, Mohammad Akhlaghi, Dustin Lang, Dmitry Makarov, Alejandro S. Borlaff, Giuseppe Donatiello, William J. Pearson, Juan Miro-Carretero, Jean-Charles Cuillandre, Helena Dominguez, Santi Roca-Fabrega, Carlos S. Frenk, Judy Schmidt, Maria A. Gomez-Flechoso, Rafael Guzman, Noam I. Libeskind, Arjun Dey, Benjamin A. Weaver, David Schlegel, Adam D. Myers, and Frank G. Valdes. Hidden Depths in the Local Universe: the Stellar Stream Legacy Survey. *arXiv e-prints*, page arXiv:2104.06071, April 2021, 2104.06071.

[281] Kathryn V Johnston, David N Spergel, and Christian Haydn. How lumpy is the milky way's dark matter halo? *The Astrophysical Journal*, 570(2):656, 2002, doi:10.1086/339791.

[282] R. A. Ibata, G. F. Lewis, M. J. Irwin, and T. Quinn. Uncovering cold dark matter halo substructure with tidal streams. MNRAS, 332(4):915–920, June 2002, doi:10.1046/j.1365-8711.2002.05358.x, astro-ph/0110690.

[283] Joo Heon Yoon, Kathryn V. Johnston, and David W. Hogg. Clumpy Streams from Clumpy Halos: Detecting Missing Satellites with Cold Stellar Structures. ApJ, 731(1):58, April 2011, doi:10.1088/0004-637X/731/1/58, 1012.2884.

[284] R. G. Carlberg. Dark Matter Sub-halo Counts via Star Stream Crossings. ApJ, 748(1):20, March 2012, doi:10.1088/0004-637X/748/1/20, 1109.6022.

[285] Denis Erkal and Vasily Belokurov. Properties of dark subhaloes from gaps in tidal streams. MNRAS, 454(4):3542–3558, December 2015, doi:10.1093/mnras/stv2122, 1507.05625.

[286] Denis Erkal, Vasily Belokurov, Jo Bovy, and Jason L. Sanders. The number and size of subhalo-induced gaps in stellar streams. MNRAS, 463(1):102–119, November 2016, doi:10.1093/mnras/stw1957, 1606.04946.

[287] S. Vegetti, D. J. Lagattuta, J. P. McKean, M. W. Auger, C. D. Fassnacht, and L. V. E. Koopmans. Gravitational detection of a low-mass dark satellite galaxy at cosmological distance. Nature, 481(7381):341–343, January 2012, doi:10.1038/nature10669, 1201.3643.

[288] Shude Mao and Peter Schneider. Evidence for substructure in lens galaxies? MNRAS, 295(3):587–594, April 1998, doi:10.1046/j.1365-8711.1998.01319.x, astro-ph/9707187.

[289] Yashar Hezaveh, Neal Dalal, Gilbert Holder, Theodore Kisner, Michael Kuhlen, and Laurence Perreault Levasseur. Measuring the power spectrum of dark matter substructure using strong gravitational lensing. J. Cosmology Astropart. Phys., 2016(11):048, November 2016, doi:10.1088/1475-7516/2016/11/048, 1403.2720.

[290] S. Vegetti, L. V. E. Koopmans, A. Bolton, T. Treu, and R. Gavazzi. Detection of a dark substructure through gravitational imaging. MNRAS, 408(4):1969–1981, November 2010, doi:10.1111/j.1365-2966.2010.16865.x, 0910.0760.

[291] Massimo Meneghetti, Guido Davoli, Pietro Bergamini, Piero Rosati, Priyamvada Natarajan, Carlo Giocoli, Gabriel B. Caminha, R. Benton Metcalf, Elena Rasia, Stefano Borgani, Francesco Calura, Claudio Grillo, Amata Mercurio, and Eros Vanzella. An excess of small-scale gravitational lenses observed in galaxy clusters. *Science*, 369(6509):1347–1351, September 2020, doi:10.1126/science.aax5164, 2009.04471.

[292] Nick Kaiser, Gordon Squires, and Tom Broadhurst. A Method for Weak Lensing Observations. ApJ, 449:460, August 1995, doi:10.1086/176071, astro-ph/9411005.

[293] G. Meylan, Jetzer P., and P. North, editors. *Gravitational Lensing: Strong, Weak and Micro*, January 2006, astro-ph/0407232.

[294] B. Paczynski. Gravitational Microlensing by the Galactic Halo. ApJ, 304:1, May 1986, doi:10.1086/164140.

[295] Andrey Katz, Joachim Kopp, Sergey Sibiryakov, and Wei Xue. Femtolensing by dark matter revisited. J. Cosmology Astropart. Phys., 2018(12):005, December 2018, doi:10.1088/1475-7516/2018/12/005, 1807.11495.

[296] Peter Schneider, Jürgen Ehlers, and Emilio E. Falco. *Gravitational Lenses.* Springer, 1992, doi:10.1007/978-3-662-03758-4.

[297] Alexandre Refregier and Abraham Loeb. Gravitational Lensing by Clusters of Galaxies. ApJ, 478(2):476–491, March 1997, doi:10.1086/303830, astro-ph/9610248.

[298] Matthias Bartelmann. TOPICAL REVIEW Gravitational lensing. *Classical and Quantum Gravity*, 27(23):233001, December 2010, doi:10.1088/0264-9381/27/23/233001, 1010.3829.

[299] Jean-Paul Kneib and Priyamvada Natarajan. Cluster lenses. A&A Rev., 19:47, November 2011, doi:10.1007/s00159-011-0047-3, 1202.0185.

[300] C. C. Cheung et al. Fermi Large Area Telescope Detection of Gravitational Lens Delayed γ-Ray Flares from Blazar B0218+357. ApJ, 782(2):L14, February 2014, doi:10.1088/2041-8205/782/2/L14, 1401.0548.

[301] Gaia Collaboration, A. G. A. Brown, A. Vallenari, T. Prusti, J. H. J. de Bruijne, F. Mignard, R. Drimmel, C. Babusiaux, C. A. L. Bailer-Jones, U. Bastian, M. Biermann, D. W. Evans, L. Eyer, F. Jansen, C. Jordi, D. Katz, S. A. Klioner, U. Lammers, L. Lindegren, X. Luri, W. O'Mullane, C. Panem, D. Pourbaix, S. Randich, P. Sartoretti, H. I. Siddiqui, C. Soubiran, V. Valette, F. van Leeuwen, N. A. Walton, C. Aerts, F. Arenou, M. Cropper, E. Høg, M. G. Lattanzi, E. K. Grebel, A. D. Holland, C. Huc, X. Passot, M. Perryman, L. Bramante, C. Cacciari, J. Castañeda, L. Chaoul, N. Cheek, F. De Angeli, C. Fabricius, R. Guerra, J. Hernández, A. Jean-Antoine-Piccolo, E. Masana, R. Messineo, N. Mowlavi, K. Nienartowicz, D. Ordóñez-Blanco, P. Panuzzo, J. Portell, P. J. Richards, M. Riello, G. M. Seabroke, P. Tanga, F. Thévenin, J. Torra, S. G. Els, G. Gracia-Abril, G. Comoretto, M. Garcia-Reinaldos, T. Lock, E. Mercier, M. Altmann, R. Andrae, T. L. Astraatmadja, I. Bellas-Velidis, K. Benson, J. Berthier, R. Blomme, G. Busso, B. Carry, A. Cellino, G. Clementini, S. Cowell, O. Creevey, J. Cuypers, M. Davidson, J. De Ridder, A. de Torres, L. Delchambre, A. Dell'Oro, C. Ducourant, Y. Frémat, M. García-Torres, E. Gosset, J. L. Halbwachs, N. C. Hambly, D. L. Harrison, M. Hauser, D. Hestroffer, S. T. Hodgkin, H. E. Huckle, A. Hutton, G. Jasniewicz, S. Jordan, M. Kontizas, A. J. Korn, A. C. Lanzafame, M. Manteiga, A. Moitinho, K. Muinonen, J. Osinde, E. Pancino, T. Pauwels, J. M. Petit, A. Recio-Blanco, A. C. Robin, L. M. Sarro, C. Siopis, M. Smith, K. W. Smith, A. Sozzetti, W. Thuillot, W. van Reeven, Y. Viala, U. Abbas, A. Abreu Aramburu, S. Accart, J. J. Aguado, P. M. Allan, W. Allasia, G. Altavilla, M. A. Álvarez, J. Alves, R. I. Anderson, A. H. Andrei, E. Anglada Varela, E. Antiche, T. Antoja, S. Antón, B. Arcay, N. Bach, S. G. Baker, L. Balaguer-Núñez, C. Barache, C. Barata, A. Barbier, F. Barblan, D. Barrado y Navascués, M. Barros, M. A. Barstow, U. Becciani, M. Bellazzini, A. Bello García, V. Belokurov, P. Bendjoya, A. Berihuete, L. Bianchi, O. Bienaymé, F. Billebaud, N. Blagorodnova,

S. Blanco-Cuaresma, T. Boch, A. Bombrun, R. Borrachero, S. Bouquillon, G. Bourda, H. Bouy, A. Bragaglia, M. A. Breddels, N. Brouillet, T. Brüsemeister, B. Bucciarelli, P. Burgess, R. Burgon, A. Burlacu, D. Busonero, R. Buzzi, E. Caffau, J. Cambras, H. Campbell, R. Cancelliere, T. Cantat-Gaudin, T. Carlucci, J. M. Carrasco, M. Castellani, P. Charlot, J. Charnas, A. Chiavassa, M. Clotet, G. Cocozza, R. S. Collins, G. Costigan, F. Crifo, N. J. G. Cross, M. Crosta, C. Crowley, C. Dafonte, Y. Damerdji, A. Dapergolas, P. David, M. David, P. De Cat, F. de Felice, P. de Laverny, F. De Luise, R. De March, D. de Martino, R. de Souza, J. Debosscher, E. del Pozo, M. Delbo, A. Delgado, H. E. Delgado, P. Di Matteo, S. Diakite, E. Distefano, C. Dolding, S. Dos Anjos, P. Drazinos, J. Duran, Y. Dzigan, B. Edvardsson, H. Enke, N. W. Evans, G. Eynard Bontemps, C. Fabre, M. Fabrizio, S. Faigler, A. J. Falcão, M. Farràs Casas, L. Federici, G. Fedorets, J. Fernández-Hernández, P. Fernique, A. Fienga, F. Figueras, F. Filippi, K. Findeisen, A. Fonti, M. Fouesneau, E. Fraile, M. Fraser, J. Fuchs, M. Gai, S. Galleti, L. Galluccio, D. Garabato, F. García-Sedano, A. Garofalo, N. Garralda, P. Gavras, J. Gerssen, R. Geyer, G. Gilmore, S. Girona, G. Giuffrida, M. Gomes, A. González-Marcos, J. González-Núñez, J. J. González-Vidal, M. Granvik, A. Guerrier, P. Guillout, J. Guiraud, A. Gúrpide, R. Gutiérrez-Sánchez, L. P. Guy, R. Haigron, D. Hatzidimitriou, M. Haywood, U. Heiter, A. Helmi, D. Hobbs, W. Hofmann, B. Holl, G. Holland, J. A. S. Hunt, A. Hypki, V. Icardi, M. Irwin, G. Jevardat de Fombelle, P. Jofré, P. G. Jonker, A. Jorissen, F. Julbe, A. Karampelas, A. Kochoska, R. Kohley, K. Kolenberg, E. Kontizas, S. E. Koposov, G. Kordopatis, P. Koubsky, A. Krone-Martins, M. Kudryashova, I. Kull, R. K. Bachchan, F. Lacoste-Seris, A. F. Lanza, J. B. Lavigne, C. Le Poncin-Lafitte, Y. Lebreton, T. Lebzelter, S. Leccia, N. Leclerc, I. Lecoeur-Taibi, V. Lemaitre, H. Lenhardt, F. Leroux, S. Liao, E. Licata, H. E. P. Lindstrøm, T. A. Lister, E. Livanou, A. Lobel, W. Löffler, M. López, D. Lorenz, I. MacDonald, T. Magalhães Fernandes, S. Managau, R. G. Mann, G. Mantelet, O. Marchal, J. M. Marchant, M. Marconi, S. Marinoni, P. M. Marrese, G. Marschalkó, D. J. Marshall, J. M. Martín-Fleitas, M. Martino, N. Mary, G. Matijevič, T. Mazeh, P. J. McMillan, S. Messina, D. Michalik, N. R. Millar, B. M. H. Miranda, D. Molina, R. Molinaro, M. Molinaro, L. Molnár, M. Moniez, P. Montegriffo, R. Mor, A. Mora, R. Morbidelli, T. Morel, S. Morgenthaler, D. Morris, A. F. Mulone, T. Muraveva, I. Musella, J. Narbonne, G. Nelemans, L. Nicastro, L. Noval, C. Ordénovic, J. Ordieres-Meré, P. Osborne, C. Pagani, I. Pagano, F. Pailler, H. Palacin, L. Palaversa, P. Parsons, M. Pecoraro, R. Pedrosa, H. Pentikäinen, B. Pichon, A. M. Piersimoni, F. X. Pineau, E. Plachy, G. Plum, E. Poujoulet, A. Prša, L. Pulone, S. Ragaini, S. Rago, N. Rambaux, M. Ramos-Lerate, P. Ranalli, G. Rauw, A. Read, S. Regibo, C. Reylé, R. A. Ribeiro, L. Rimoldini, V. Ripepi, A. Riva, G. Rixon, M. Roelens, M. Romero-Gómez, N. Rowell, F. Royer, L. Ruiz-Dern, G. Sadowski, T. Sagristà Sellés, J. Sahlmann, J. Salgado, E. Salguero, M. Sarasso, H. Savietto, M. Schultheis, E. Sciacca, M. Segol, J. C. Segovia, D. Segransan, I. C. Shih, R. Smareglia, R. L. Smart, E. Solano, F. Solitro, R. Sordo, S. Soria Nieto, J. Souchay, A. Spagna, F. Spoto, U. Stampa, I. A. Steele, H. Steidelmüller, C. A. Stephenson, H. Stoev, F. F. Suess, M. Süveges, J. Surdej, L. Szabados, E. Szegedi-Elek, D. Tapiador, F. Taris, G. Tauran, M. B. Taylor, R. Teixeira, D. Terrett, B. Tingley, S. C. Trager, C. Turon, A. Ulla, E. Utrilla, G. Valentini, A. van Elteren, E. Van Hemelryck, M. van Leeuwen, M. Varadi, A. Vecchiato, J. Veljanoski, T. Via, D. Vicente, S. Vogt, H. Voss, V. Votruba, S. Voutsinas, G. Walmsley, M. Weiler, K. Weingrill, T. Wevers, Ł. Wyrzykowski, A. Yoldas, M. Žerjal, S. Zucker, C. Zurbach, T. Zwitter, A. Alecu, M. Allen, C. Allende Prieto, A. Amorim, G. Anglada-Escudé, V. Arsenijevic, S. Azaz, P. Balm, M. Beck, H. H. Bernstein, L. Bigot, A. Bijaoui, C. Blasco, M. Bonfigli, G. Bono, S. Boudreault, A. Bressan, S. Brown, P. M. Brunet, P. Bunclark, R. Buonanno, A. G. Butkevich, C. Carret, C. Carrion, L. Chemin, F. Chéreau, L. Corcione, E. Darmigny, K. S. de Boer, P. de Teodoro, P. T. de Zeeuw, C. Delle Luche, C. D. Domingues, P. Dubath, F. Fodor, B. Frézouls, A. Fries, D. Fustes, D. Fyfe, E. Gallardo, J. Gallegos, D. Gardiol, M. Gebran, A. Gomboc, A. Gómez, E. Grux, A. Gueguen, A. Heyrovsky, J. Hoar, G. Iannicola, Y. Isasi

Parache, A. M. Janotto, E. Joliet, A. Jonckheere, R. Keil, D. W. Kim, P. Klagyivik, J. Klar, J. Knude, O. Kochukhov, I. Kolka, J. Kos, A. Kutka, V. Lainey, D. LeBouquin, C. Liu, D. Loreggia, V. V. Makarov, M. G. Marseille, C. Martayan, O. Martinez-Rubi, B. Massart, F. Meynadier, S. Mignot, U. Munari, A. T. Nguyen, T. Nordlander, P. Ocvirk, K. S. O'Flaherty, A. Olias Sanz, P. Ortiz, J. Osorio, D. Oszkiewicz, A. Ouzounis, M. Palmer, P. Park, E. Pasquato, C. Peltzer, J. Peralta, F. Péturaud, T. Pieniluoma, E. Pigozzi, J. Poels, G. Prat, T. Prod'homme, F. Raison, J. M. Rebordao, D. Risquez, B. Rocca-Volmerange, S. Rosen, M. I. Ruiz-Fuertes, F. Russo, S. Sembay, I. Serraller Vizcaino, A. Short, A. Siebert, H. Silva, D. Sinachopoulos, E. Slezak, M. Soffel, D. Sosnowska, V. Straižys, M. ter Linden, D. Terrell, S. Theil, C. Tiede, L. Troisi, P. Tsalmantza, D. Tur, M. Vaccari, F. Vachier, P. Valles, W. Van Hamme, L. Veltz, J. Virtanen, J. M. Wallut, R. Wichmann, M. I. Wilkinson, H. Ziaeepour, and S. Zschocke. Gaia Data Release 1. Summary of the astrometric, photometric, and survey properties. A&A, 595:A2, November 2016, doi:10.1051/0004-6361/201629512, 1609.04172.

[302] Jo Bovy, Iain Murray, and David W. Hogg. Dynamical Inference from a Kinematic Snapshot: The Force Law in the Solar System. ApJ, 711(2):1157–1167, March 2010, doi:10.1088/0004-637X/711/2/1157, 0903.5308.

[303] Gregory M. Green and Yuan-Sen Ting. Deep Potential: Recovering the gravitational potential from a snapshot of phase space. In *34th Conference on Neural Information Processing Systems*, 11 2020, 2011.04673.

[304] Ken Van Tilburg, Anna-Maria Taki, and Neal Weiner. Halometry from astrometry. *Journal of Cosmology and Astroparticle Physics*, 2018(07):041, 2018, doi:10.1088/1475-7516/2018/07/041.

[305] Cristina Mondino, Anna-Maria Taki, Ken Van Tilburg, and Neal Weiner. First Results on Dark Matter Substructure from Astrometric Weak Lensing. *Phys. Rev. Lett.*, 125(11):111101, 2020, doi:10.1103/PhysRevLett.125.111101, 2002.01938.

[306] Kyriakos Vattis, Michael W. Toomey, and Savvas M. Koushiappas. Deep learning the astrometric signature of dark matter substructure. 8 2020, 2008.11577.

[307] Siddharth Mishra-Sharma, Ken Van Tilburg, and Neal Weiner. The power of halometry. *arXiv preprint arXiv:2003.02264*, 2020, doi:10.1103/PhysRevD.102.023026.

[308] Claudia Quercellini, Luca Amendola, and Amedeo Balbi. Mapping the galactic gravitational potential with peculiar acceleration. *Mon. Not. Roy. Astron. Soc.*, 391:1308–1314, 2008, doi:10.1111/j.1365-2966.2008.13968.x, 0807.3237.

[309] Aakash Ravi, Nicholas Langellier, David F. Phillips, Malte Buschmann, Benjamin R. Safdi, and Ronald L. Walsworth. Probing Dark Matter Using Precision Measurements of Stellar Accelerations. *Phys. Rev. Lett.*, 123(9):091101, 2019, doi:10.1103/PhysRevLett.123.091101, 1812.07578.

[310] Hamish Silverwood and Richard Easther. Stellar accelerations and the galactic gravitational field. PASA, 36:e038, October 2019, doi:10.1017/pasa.2019.25, 1812.07581.

[311] Sukanya Chakrabarti, Jason Wright, Philip Chang, Alice Quillen, Peter Craig, Joey Territo, Elena D'Onghia, Kathryn V. Johnston, Robert J. De Rosa, Daniel Huber, Katherine L. Rhode, and Eric Nielsen. Toward a Direct Measure of the Galactic Acceleration. ApJ, 902(1):L28, October 2020, doi:10.3847/2041-8213/abb9b5, 2007.15097.

[312] David F. Phillips, Aakash Ravi, Reza Ebadi, and Ronald L. Walsworth. Milky Way Accelerometry via Millisecond Pulsar Timing. 8 2020, doi:10.1103/PhysRevLett.126.141103, 2008.13052.

[313] Sukanya Chakrabarti, Philip Chang, Michael T. Lam, Sarah J. Vigeland, and Alice C. Quillen. A Measurement of the Galactic Plane Mass Density from Binary Pulsar Accelerations. ApJ, 907(2):L26, February 2021, doi:10.3847/2041-8213/abd635, 2010.04018.

[314] Malte Buschmann, Benjamin R. Safdi, and Katelin Schutz. The Galactic potential and dark matter density from angular stellar accelerations. 3 2021, 2103.05000.

[315] Naoki Seto and Asantha Cooray. Searching for primordial black hole dark matter with pulsar timing arrays. *Astrophys. J. Lett.*, 659:L33–L36, 2007, doi:10.1086/516570, astro-ph/0702586.

[316] Shant Baghram, Niayesh Afshordi, and Kathryn M. Zurek. Prospects for Detecting Dark Matter Halo Substructure with Pulsar Timing. *Phys. Rev. D*, 84:043511, 2011, doi:10.1103/PhysRevD.84.043511, 1101.5487.

[317] Jeff A. Dror, Harikrishnan Ramani, Tanner Trickle, and Kathryn M. Zurek. Pulsar Timing Probes of Primordial Black Holes and Subhalos. *Phys. Rev. D*, 100(2):023003, 2019, doi:10.1103/PhysRevD.100.023003, 1901.04490.

[318] Harikrishnan Ramani, Tanner Trickle, and Kathryn M. Zurek. Observability of Dark Matter Substructure with Pulsar Timing Correlations. *JCAP*, 12:033, 2020, doi:10.1088/1475-7516/2020/12/033, 2005.03030.

[319] Vincent S. H. Lee, Stephen R. Taylor, Tanner Trickle, and Kathryn M. Zurek. Bayesian Forecasts for Dark Matter Substructure Searches with Mock Pulsar Timing Data. *arXiv e-prints*, page arXiv:2104.05717, April 2021, 2104.05717.

[320] Scott Dodelson and Lawrence M. Widrow. Sterile-neutrinos as dark matter. *Phys. Rev. Lett.*, 72:17–20, 1994, doi:10.1103/PhysRevLett.72.17, hep-ph/9303287.

[321] Matteo Viel, Julien Lesgourgues, Martin G. Haehnelt, Sabino Matarrese, and Antonio Riotto. Constraining warm dark matter candidates including sterile neutrinos and light gravitinos with WMAP and the Lyman-α forest. Phys. Rev. D, 71(6):063534, March 2005, doi:10.1103/PhysRevD.71.063534, astro-ph/0501562.

[322] Aurel Schneider, Robert E. Smith, Andrea V. Macciò, and Ben Moore. Non-linear evolution of cosmological structures in warm dark matter models. MNRAS, 424(1):684–698, July 2012, doi:10.1111/j.1365-2966.2012.21252.x, 1112.0330.

[323] R. Murgia, A. Merle, M. Viel, M. Totzauer, and A. Schneider. "Non-cold" dark matter at small scales: a general approach. J. Cosmology Astropart. Phys., 2017(11):046, November 2017, doi:10.1088/1475-7516/2017/11/046, 1704.07838.

[324] Daniel Boyanovsky and Jun Wu. Small scale aspects of warm dark matter : power spectra and acoustic oscillations. *Phys. Rev. D*, 83:043524, 2011, doi:10.1103/PhysRevD.83.043524, 1008.0992.

[325] E. O. Nadler, A. Drlica-Wagner, K. Bechtol, S. Mau, R. H. Wechsler, V. Gluscevic, K. Boddy, A. B. Pace, T. S. Li, M. McNanna, A. H. Riley, J. García-Bellido, Y. Y. Mao, G. Green, D. L. Burke, A. Peter, B. Jain, T. M. C. Abbott, M. Aguena, S. Allam, J. Annis, S. Avila, D. Brooks, M. Carrasco Kind, J. Carretero, M. Costanzi, L. N. da Costa, J. De Vicente, S. Desai, H. T. Diehl, P. Doel, S. Everett, A. E. Evrard, B. Flaugher, J. Frieman, D. W. Gerdes, D. Gruen, R. A. Gruendl, J. Gschwend, G. Gutierrez, S. R. Hinton, K. Honscheid, D. Huterer, D. J. James, E. Krause, K. Kuehn, N. Kuropatkin, O. Lahav, M. A. G. Maia, J. L. Marshall, F. Menanteau, R. Miquel, A. Palmese, F. Paz-Chinchón, A. A. Plazas, A. K. Romer, E. Sanchez, V. Scarpine,

S. Serrano, I. Sevilla-Noarbe, M. Smith, M. Soares-Santos, E. Suchyta, M. E. C. Swanson, G. Tarle, D. L. Tucker, A. R. Walker, W. Wester, and DES Collaboration. Constraints on Dark Matter Properties from Observations of Milky Way Satellite Galaxies. Phys. Rev. Lett., 126(9):091101, March 2021, doi:10.1103/PhysRevLett.126.091101, 2008.00022.

[326] V. Springel, J. Wang, M. Vogelsberger, A. Ludlow, A. Jenkins, A. Helmi, J. F. Navarro, C. S. Frenk, and S. D. M. White. The Aquarius Project: the subhaloes of galactic haloes. MNRAS, 391(4):1685–1711, December 2008, doi:10.1111/j.1365-2966.2008.14066.x, 0809.0898.

[327] Till Sawala, Pauli Pihajoki, Peter H. Johansson, Carlos S. Frenk, Julio F. Navarro, Kyle A. Oman, and Simon D. M. White. Shaken and stirred: the Milky Way's dark substructures. MNRAS, 467(4):4383–4400, June 2017, doi:10.1093/mnras/stx360, 1609.01718.

[328] Sownak Bose, Wojciech A. Hellwing, Carlos S. Frenk, Adrian Jenkins, Mark R. Lovell, John C. Helly, Baojiu Li, Violeta Gonzalez-Perez, and Liang Gao. Substructure and galaxy formation in the Copernicus Complexio warm dark matter simulations. MNRAS, 464(4):4520–4533, February 2017, doi:10.1093/mnras/stw2686, 1604.07409.

[329] Matthias Hoeft, Gustavo Yepes, Stefan Gottlöber, and Volker Springel. Dwarf galaxies in voids: suppressing star formation with photoheating. MNRAS, 371(1):401–414, September 2006, doi:10.1111/j.1365-2966.2006.10678.x, astro-ph/0501304.

[330] Takashi Okamoto, Liang Gao, and Tom Theuns. Mass loss of galaxies due to an ultraviolet background. MNRAS, 390(3):920–928, November 2008, doi:10.1111/j.1365-2966.2008.13830.x, 0806.0378.

[331] Till Sawala, Carlos S. Frenk, Azadeh Fattahi, Julio F. Navarro, Richard G. Bower, Robert A. Crain, Claudio Dalla Vecchia, Michelle Furlong, Adrian Jenkins, Ian G. McCarthy, Yan Qu, Matthieu Schaller, Joop Schaye, and Tom Theuns. Bent by baryons: the low-mass galaxy-halo relation. MNRAS, 448(3):2941–2947, April 2015, doi:10.1093/mnras/stu2753, 1404.3724.

[332] Ferah Munshi, Alyson M. Brooks, Charlotte Christensen, Elaad Applebaum, Kelly Holley-Bockelmann, Thomas R. Quinn, and James Wadsley. Dancing in the Dark: Uncertainty in Ultrafaint Dwarf Galaxy Predictions from Cosmological Simulations. ApJ, 874(1):40, March 2019, doi:10.3847/1538-4357/ab0085, 1810.12417.

[333] Ferah Munshi, Alyson Brooks, Elaad Applebaum, Charlotte Christensen, Jordan P. Sligh, and T. Quinn. Quantifying scatter in galaxy formation at the lowest masses. arXiv e-prints, page arXiv:2101.05822, January 2021, 2101.05822.

[334] Erik Zackrisson and Teresa Riehm. Gravitational Lensing as a Probe of Cold Dark Matter Sub-halos. Advances in Astronomy, 2010:478910, January 2010, doi:10.1155/2010/478910, 0905.4075.

[335] N. Dalal and C. S. Kochanek. Direct Detection of Cold Dark Matter Substructure. ApJ, 572(1):25–33, June 2002, doi:10.1086/340303, astro-ph/0111456.

[336] A. Udalski, M. Szymanski, J. Kaluzny, M. Kubiak, and Mario Mateo. The Optical Gravitational Lensing Experiment. Acta Astron., 42:253–284, October 1992.

[337] A. Udalski, M. K. Szymański, and G. Szymański. OGLE-IV: Fourth Phase of the Optical Gravitational Lensing Experiment. Acta Astron., 65(1):1–38, March 2015, 1504.05966.

[338] C. Alcock et al. MACHO Project Limits on Black Hole Dark Matter in the 1-30 M_{solar} Range. ApJ, 550(2):L169–L172, April 2001, doi:10.1086/319636, astro-ph/0011506.

[339] P. Tisserand et al., EROS-2. Limits on the Macho content of the Galactic Halo from the EROS-2 Survey of the Magellanic Clouds. A&A, 469(2):387–404, July 2007, doi:10.1051/0004-6361:20066017, astro-ph/0607207.

[340] Hiroko Niikura, Masahiro Takada, Naoki Yasuda, Robert H. Lupton, Takahiro Sumi, Surhud More, Toshiki Kurita, Sunao Sugiyama, Anupreeta More, Masamune Oguri, and Masashi Chiba. Microlensing constraints on primordial black holes with Subaru/HSC Andromeda observations. *Nature Astronomy*, 3:524–534, April 2019, doi:10.1038/s41550-019-0723-1, 1701.02151.

[341] Nolan Smyth, Stefano Profumo, Samuel English, Tesla Jeltema, Kevin McKinnon, and Puragra Guhathakurta. Updated Constraints on Asteroid-Mass Primordial Black Holes as Dark Matter. *Phys. Rev. D*, 101(6):063005, 2020, doi:10.1103/PhysRevD.101.063005, 1910.01285.

[342] Djuna Croon, David McKeen, and Nirmal Raj. Gravitational microlensing by dark matter in extended structures. *Phys. Rev. D*, 101(8):083013, 2020, doi:10.1103/PhysRevD.101.083013, 2002.08962.

[343] Djuna Croon, David McKeen, Nirmal Raj, and Zihui Wang. Subaru-HSC through a different lens: Microlensing by extended dark matter structures. *Phys. Rev. D*, 102(8):083021, 2020, doi:10.1103/PhysRevD.102.083021, 2007.12697.

[344] Ethan O. Nadler, Simon Birrer, Daniel Gilman, Risa H. Wechsler, Xiaolong Du, Andrew Benson, Anna M. Nierenberg, and Tommaso Treu. Dark Matter Constraints from a Unified Analysis of Strong Gravitational Lenses and Milky Way Satellite Galaxies. *arXiv e-prints*, page arXiv:2101.07810, January 2021, 2101.07810.

[345] Vincent S. H. Lee, Andrea Mitridate, Tanner Trickle, and Kathryn M. Zurek. Probing Small-Scale Power Spectra with Pulsar Timing Arrays. 12 2020, 2012.09857.

[346] Denis Erkal, Sergey E. Koposov, and Vasily Belokurov. A sharper view of Pal 5's tails: discovery of stream perturbations with a novel non-parametric technique. MNRAS, 470(1):60–84, September 2017, doi:10.1093/mnras/stx1208, 1609.01282.

[347] Jun-Hwan Choi, Martin D. Weinberg, and Neal Katz. The dynamics of tidal tails from massive satellites. MNRAS, 381(3):987–1000, November 2007, doi:10.1111/j.1365-2966.2007.12313.x, astro-ph/0702353.

[348] Sarah Pearson, Adrian M. Price-Whelan, and Kathryn V. Johnston. Gaps and length asymmetry in the stellar stream Palomar 5 as effects of Galactic bar rotation. *Nature Astronomy*, 1:633–639, August 2017, doi:10.1038/s41550-017-0220-3, 1703.04627.

[349] Nilanjan Banik and Jo Bovy. Effects of baryonic and dark matter substructure on the Pal 5 stream. MNRAS, 484(2):2009–2020, April 2019, doi:10.1093/mnras/stz142, 1809.09640.

[350] Mark Gieles, Denis Erkal, Fabio Antonini, Eduardo Balbinot, and Jorge Peñarrubia. A supra massive population of stellar-mass black holes in the globular cluster Palomar 5. *arXiv e-prints*, page arXiv:2102.11348, February 2021, 2102.11348.

[351] Nicola C. Amorisco, Facundo A. Gómez, Simona Vegetti, and Simon D. M. White. Gaps in globular cluster streams: giant molecular clouds can cause them too. MNRAS, 463(1):L17–L21, November 2016, doi:10.1093/mnrasl/slw148, 1606.02715.

[352] Ana Bonaca, David W. Hogg, Adrian M. Price-Whelan, and Charlie Conroy. The Spur and the Gap in GD-1: Dynamical Evidence for a Dark Substructure in the Milky Way Halo. ApJ, 880(1):38, July 2019, doi:10.3847/1538-4357/ab2873, 1811.03631.

[353] Nilanjan Banik, Gianfranco Bertone, Jo Bovy, and Nassim Bozorgnia. Probing the nature of dark matter particles with stellar streams. J. Cosmology Astropart. Phys., 2018(7):061, July 2018, doi:10.1088/1475-7516/2018/07/061, 1804.04384.

[354] Nilanjan Banik, Jo Bovy, Gianfranco Bertone, Denis Erkal, and T. J. L. de Boer. Novel constraints on the particle nature of dark matter from stellar streams. *arXiv e-prints*, page arXiv:1911.02663, November 2019, 1911.02663.

[355] Nilanjan Banik, Jo Bovy, Gianfranco Bertone, Denis Erkal, and T. J. L. de Boer. Evidence of a population of dark subhaloes from Gaia and Pan-STARRS observations of the GD-1 stream. MNRAS, 502(2):2364–2380, April 2021, doi:10.1093/mnras/stab210, 1911.02662.

[356] Khyati Malhan, Monica Valluri, and Katherine Freese. Probing the nature of dark matter with accreted globular cluster streams. MNRAS, 501(1):179–200, January 2021, doi:10.1093/mnras/staa3597, 2005.12919.

[357] Eric D. Carlson, Marie E. Machacek, and Lawrence J. Hall. Self-interacting Dark Matter. ApJ, 398:43, October 1992, doi:10.1086/171833.

[358] Marie E. Machacek. Growth of Adiabatic Perturbations in Self-interacting Dark Matter. ApJ, 431:41, August 1994, doi:10.1086/174465.

[359] Manuel A. Buen-Abad, Razieh Emami, and Martin Schmaltz. Cannibal dark matter and large scale structure. Phys. Rev. D, 98(8):083517, October 2018, doi:10.1103/PhysRevD.98.083517, 1803.08062.

[360] Stefan Heimersheim, Nils Schöneberg, Deanna C. Hooper, and Julien Lesgourgues. Cannibalism hinders growth: Cannibal Dark Matter and the S_8 tension. J. Cosmology Astropart. Phys., 2020(12):016, December 2020, doi:10.1088/1475-7516/2020/12/016, 2008.08486.

[361] Xiang-Dong Shi and George M. Fuller. A New dark matter candidate: Nonthermal sterile neutrinos. *Phys. Rev. Lett.*, 82:2832–2835, 1999, doi:10.1103/PhysRevLett.82.2832, astro-ph/9810076.

[362] Lawrence J. Hall, Karsten Jedamzik, John March-Russell, and Stephen M. West. Freeze-In Production of FIMP Dark Matter. *JHEP*, 03:080, 2010, doi:10.1007/JHEP03(2010)080, 0911.1120.

[363] Gordan Krnjaic. Freezing In, Heating Up, and Freezing Out: Predictive Nonthermal Dark Matter and Low-Mass Direct Detection. *JHEP*, 10:136, 2018, doi:10.1007/JHEP10(2018)136, 1711.11038.

[364] Jared A. Evans, Cristian Gaidau, and Jessie Shelton. Leak-in Dark Matter. *JHEP*, 01:032, 2020, doi:10.1007/JHEP01(2020)032, 1909.04671.

[365] Cora Dvorkin, Tongyan Lin, and Katelin Schutz. Making dark matter out of light: Freeze-in from plasma effects. Phys. Rev. D, 99(11):115009, June 2019, doi:10.1103/PhysRevD.99.115009, 1902.08623.

[366] Cora Dvorkin, Tongyan Lin, and Katelin Schutz. The cosmology of sub-MeV dark matter freeze-in. *arXiv e-prints*, page arXiv:2011.08186, November 2020, 2011.08186.

[367] Tongyan Lin. Dark matter models and direct detection. *PoS*, 333:009, 2019, doi:10.22323/1.333.0009, 1904.07915.

[368] B. J. Carr and S. W. Hawking. Black holes in the early Universe. MNRAS, 168:399–416, August 1974, doi:10.1093/mnras/168.2.399.

[369] Mark B. Wise and Yue Zhang. Stable Bound States of Asymmetric Dark Matter. *Phys. Rev. D*, 90(5):055030, 2014, doi:10.1103/PhysRevD.90.055030, 1407.4121. [Erratum: Phys.Rev.D 91, 039907 (2015)].

[370] Mark B. Wise and Yue Zhang. Yukawa Bound States of a Large Number of Fermions. *JHEP*, 02:023, 2015, doi:10.1007/JHEP02(2015)023, 1411.1772. [Erratum: JHEP 10, 165 (2015)].

[371] Edward Hardy, Robert Lasenby, John March-Russell, and Stephen M. West. Big Bang Synthesis of Nuclear Dark Matter. *JHEP*, 06:011, 2015, doi:10.1007/JHEP06(2015)011, 1411.3739.

[372] Edward Hardy, Robert Lasenby, John March-Russell, and Stephen M. West. Signatures of Large Composite Dark Matter States. *JHEP*, 07:133, 2015, doi:10.1007/JHEP07(2015)133, 1504.05419.

[373] Moira I. Gresham, Hou Keong Lou, and Kathryn M. Zurek. Early Universe synthesis of asymmetric dark matter nuggets. *Phys. Rev. D*, 97(3):036003, 2018, doi:10.1103/PhysRevD.97.036003, 1707.02316.

[374] Moira I. Gresham, Hou Keong Lou, and Kathryn M. Zurek. Nuclear Structure of Bound States of Asymmetric Dark Matter. *Phys. Rev. D*, 96(9):096012, 2017, doi:10.1103/PhysRevD.96.096012, 1707.02313.

[375] Moira I. Gresham, Hou Keong Lou, and Kathryn M. Zurek. Astrophysical Signatures of Asymmetric Dark Matter Bound States. *Phys. Rev. D*, 98(9):096001, 2018, doi:10.1103/PhysRevD.98.096001, 1805.04512.

[376] Shmuel Nussinov and Yongchao Zhang. Dark Matter Clusters and Time Correlations in Direct Detection Experiments. *JHEP*, 03:133, 2020, doi:10.1007/JHEP03(2020)133, 1807.00846.

[377] Dorota M. Grabowska, Tom Melia, and Surjeet Rajendran. Detecting Dark Blobs. *Phys. Rev. D*, 98(11):115020, 2018, doi:10.1103/PhysRevD.98.115020, 1807.03788.

[378] Paulo Montero-Camacho, Xiao Fang, Gabriel Vasquez, Makana Silva, and Christopher M. Hirata. Revisiting constraints on asteroid-mass primordial black holes as dark matter candidates. *JCAP*, 08:031, 2019, doi:10.1088/1475-7516/2019/08/031, 1906.05950.

[379] Lam Hui. Wave Dark Matter. *arXiv e-prints*, page arXiv:2101.11735, January 2021, 2101.11735.

[380] Wayne Hu, Rennan Barkana, and Andrei Gruzinov. Cold and fuzzy dark matter. *Phys. Rev. Lett.*, 85:1158–1161, 2000, doi:10.1103/PhysRevLett.85.1158, astro-ph/0003365.

[381] Lam Hui, Jeremiah P. Ostriker, Scott Tremaine, and Edward Witten. Ultralight scalars as cosmological dark matter. *Phys. Rev. D*, 95(4):043541, 2017, doi:10.1103/PhysRevD.95.043541, 1610.08297.

[382] Katelin Schutz. Subhalo mass function and ultralight bosonic dark matter. Phys. Rev. D, 101(12):123026, June 2020, doi:10.1103/PhysRevD.101.123026, 2001.05503.

[383] María Benito, Juan Carlos Criado, Gert Hütsi, Martti Raidal, and Hardi Veermäe. Implications of Milky Way substructures for the nature of dark matter. Phys. Rev. D, 101(10):103023, May 2020, doi:10.1103/PhysRevD.101.103023, 2001.11013.

[384] Diego Blas, Diana López Nacir, and Sergey Sibiryakov. Secular effects of ultralight dark matter on binary pulsars. Phys. Rev. D, 101(6):063016, March 2020, doi:10.1103/PhysRevD.101.063016, 1910.08544.

[385] Johannes Diehl and Jochen Weller. Constraining Ultra-light Axions with Galaxy Cluster Number Counts. arXiv e-prints, page arXiv:2103.08674, March 2021, 2103.08674.

[386] D. V. Semikoz and I. I. Tkachev. Kinetics of Bose condensation. Phys. Rev. Lett., 74:3093–3097, 1995, doi:10.1103/PhysRevLett.74.3093, hep-ph/9409202.

[387] Alan H. Guth, Mark P. Hertzberg, and C. Prescod-Weinstein. Do Dark Matter Axions Form a Condensate with Long-Range Correlation? Phys. Rev. D, 92(10):103513, 2015, doi:10.1103/PhysRevD.92.103513, 1412.5930.

[388] D. G. Levkov, A. G. Panin, and I. I. Tkachev. Gravitational Bose-Einstein condensation in the kinetic regime. Phys. Rev. Lett., 121(15):151301, 2018, doi:10.1103/PhysRevLett.121.151301, 1804.05857.

[389] Mark P. Hertzberg, Enrico D. Schiappacasse, and Tsutomu T. Yanagida. Axion Star Nucleation in Dark Minihalos around Primordial Black Holes. Phys. Rev. D, 102(2):023013, 2020, doi:10.1103/PhysRevD.102.023013, 2001.07476.

[390] Kay Kirkpatrick, Anthony E. Mirasola, and Chanda Prescod-Weinstein. Relaxation times for Bose-Einstein condensation in axion miniclusters. Phys. Rev. D, 102(10):103012, 2020, doi:10.1103/PhysRevD.102.103012, 2007.07438.

[391] Mark P. Hertzberg, Fabrizio Rompineve, and Jessie Yang. Decay of Boson Stars with Application to Glueballs and Other Real Scalars. Phys. Rev. D, 103(2):023536, 2021, doi:10.1103/PhysRevD.103.023536, 2010.07927.

[392] J. N. Bahcall, P. Hut, and S. Tremaine. Maximum mass of objects that constitute unseen disk material. ApJ, 290:15–20, March 1985, doi:10.1086/162953.

[393] Jaiyul Yoo, Julio Chanamé, and Andrew Gould. The End of the MACHO Era: Limits on Halo Dark Matter from Stellar Halo Wide Binaries. ApJ, 601(1):311–318, January 2004, doi:10.1086/380562, astro-ph/0307437.

[394] Timothy D. Brandt. Constraints on MACHO Dark Matter from Compact Stellar Systems in Ultra-faint Dwarf Galaxies. ApJ, 824(2):L31, June 2016, doi:10.3847/2041-8205/824/2/L31, 1605.03665.

[395] Qirong Zhu, Eugene Vasiliev, Yuexing Li, and Yipeng Jing. Primordial black holes as dark matter: constraints from compact ultra-faint dwarfs. MNRAS, 476(1):2–11, May 2018, doi:10.1093/mnras/sty079, 1710.05032.

[396] Jakob Stegmann, Pedro R. Capelo, Elisa Bortolas, and Lucio Mayer. Improved constraints from ultra-faint dwarf galaxies on primordial black holes as dark matter. MNRAS, 492(4):5247–5260, March 2020, doi:10.1093/mnras/staa170, 1910.04793.

[397] Miguel A. Monroy-Rodríguez and Christine Allen. The End of the MACHO Era, Revisited: New Limits on MACHO Masses from Halo Wide Binaries. ApJ, 790(2):159, August 2014, doi:10.1088/0004-637X/790/2/159, 1406.5169.

[398] Anne M. Green and Bradley J. Kavanagh. Primordial Black Holes as a dark matter candidate. J. Phys. G, 48(4):4, 2021, doi:10.1088/1361-6471/abc534, 2007.10722.

[399] David J. E. Marsh and Jens C. Niemeyer. Strong Constraints on Fuzzy Dark Matter from Ultrafaint Dwarf Galaxy Eridanus II. Phys. Rev. Lett., 123(5):051103, August 2019, doi:10.1103/PhysRevLett.123.051103, 1810.08543.

[400] Ethan O. Nadler, Vera Gluscevic, Kimberly K. Boddy, and Risa H. Wechsler. Constraints on Dark Matter Microphysics from the Milky Way Satellite Population. Astrophys. J. Lett., 878(2):32, 2019, doi:10.3847/2041-8213/ab1eb2, 1904.10000. [Erratum: Astrophys.J.Lett. 897, L46 (2020), Erratum: Astrophys.J. 897, L46 (2020)].

[401] Karime Maamari, Vera Gluscevic, Kimberly K. Boddy, Ethan O. Nadler, and Risa H. Wechsler. Bounds on velocity-dependent dark matter-proton scattering from Milky Way satellite abundance. Astrophys. J. Lett., 907(2):L46, 2021, doi:10.3847/2041-8213/abd807, 2010.02936.

[402] Gordan Krnjaic and Samuel D. McDermott. Implications of BBN bounds for cosmic ray upscattered dark matter. Phys. Rev. D, 101(12):123022, June 2020, doi:10.1103/PhysRevD.101.123022, 1908.00007.

[403] David N. Spergel and Paul J. Steinhardt. Observational evidence for selfinteracting cold dark matter. Phys. Rev. Lett., 84:3760–3763, 2000, doi:10.1103/PhysRevLett.84.3760, astro-ph/9909386.

[404] Ran Huo, Manoj Kaplinghat, Zhen Pan, and Hai-Bo Yu. Signatures of Self-Interacting Dark Matter in the Matter Power Spectrum and the CMB. Phys. Lett. B, 783:76–81, 2018, doi:10.1016/j.physletb.2018.06.024, 1709.09717.

[405] Omid Sameie, Andrew J. Benson, Laura V. Sales, Hai-Bo Yu, Leonidas A. Moustakas, and Peter Creasey. The Effect of Dark Matter–Dark Radiation Interactions on Halo Abundance: A Press–Schechter Approach. Astrophys. J., 874(1):101, 2019, doi:10.3847/1538-4357/ab0824, 1810.11040.

[406] Francis-Yan Cyr-Racine and Kris Sigurdson. Cosmology of atomic dark matter. Phys. Rev. D, 87(10):103515, 2013, doi:10.1103/PhysRevD.87.103515, 1209.5752.

[407] Francis-Yan Cyr-Racine, Roland de Putter, Alvise Raccanelli, and Kris Sigurdson. Constraints on Large-Scale Dark Acoustic Oscillations from Cosmology. Phys. Rev. D, 89(6):063517, 2014, doi:10.1103/PhysRevD.89.063517, 1310.3278.

[408] Daniel Egana-Ugrinovic, Rouven Essig, Daniel Gift, and Marilena LoVerde. The Cosmological Evolution of Self-interacting Dark Matter. 2 2021, 2102.06215.

[409] Shmuel Balberg and Stuart L. Shapiro. Gravothermal Collapse of Self-Interacting Dark Matter Halos and the Origin of Massive Black Holes. Phys. Rev. Lett., 88(10):101301, March 2002, doi:10.1103/PhysRevLett.88.101301, astro-ph/0111176.

[410] Shmuel Balberg, Stuart L. Shapiro, and Shogo Inagaki. Self-Interacting Dark Matter Halos and the Gravothermal Catastrophe. ApJ, 568(2):475–487, April 2002, doi:10.1086/339038, astro-ph/0110561.

[411] Abraham Loeb and Neal Weiner. Cores in Dwarf Galaxies from Dark Matter with a Yukawa Potential. Phys. Rev. Lett., 106(17):171302, April 2011, doi:10.1103/PhysRevLett.106.171302, 1011.6374.

[412] Rouven Essig, Samuel D. McDermott, Hai-Bo Yu, and Yi-Ming Zhong. Constraining Dissipative Dark Matter Self-Interactions. Phys. Rev. Lett., 123(12):121102, September 2019, doi:10.1103/PhysRevLett.123.121102, 1809.01144.

[413] Hiroya Nishikawa, Kimberly K. Boddy, and Manoj Kaplinghat. Accelerated core collapse in tidally stripped self-interacting dark matter halos. Phys. Rev. D, 101(6):063009, March 2020, doi:10.1103/PhysRevD.101.063009, 1901.00499.

[414] Camila A. Correa. Constraining velocity-dependent self-interacting dark matter with the Milky Way's dwarf spheroidal galaxies. MNRAS, 503(1):920–937, May 2021, doi:10.1093/mnras/stab506, 2007.02958.

[415] Daneng Yang and Hai-Bo Yu. Self-Interacting Dark Matter and the Excess of Small-Scale Gravitational Lenses. 2 2021, 2102.02375.

[416] Jesús Zavala, Mark R. Lovell, Mark Vogelsberger, and Jan D. Burger. Diverse dark matter density at sub-kiloparsec scales in Milky Way satellites: Implications for the nature of dark matter. Phys. Rev. D, 100(6):063007, September 2019, doi:10.1103/PhysRevD.100.063007, 1904.09998.

[417] David Curtin and Jack Setford. Signatures of Mirror Stars. JHEP, 03:041, 2020, doi:10.1007/JHEP03(2020)041, 1909.04072.

[418] David Curtin and Jack Setford. How To Discover Mirror Stars. Phys. Lett. B, 804:135391, 2020, doi:10.1016/j.physletb.2020.135391, 1909.04071.

[419] Maurício Hippert, Jack Setford, Hung Tan, David Curtin, Jacquelyn Noronha-Hostler, and Nicolas Yunes. Mirror Neutron Stars. 3 2021, 2103.01965.

[420] Katelin Schutz, Tongyan Lin, Benjamin R. Safdi, and Chih-Liang Wu. Constraining a Thin Dark Matter Disk with Gaia. Phys. Rev. Lett., 121(8):081101, 2018, doi:10.1103/PhysRevLett.121.081101, 1711.03103.

[421] Jatan Buch, Shing Chau (John) Leung, and JiJi Fan. Using Gaia DR2 to Constrain Local Dark Matter Density and Thin Dark Disk. JCAP, 04:026, 2019, doi:10.1088/1475-7516/2019/04/026, 1808.05603.

[422] Pablo F. de Salas and Axel Widmark. Dark matter local density determination: recent observations and future prospects. 12 2020, 2012.11477.

[423] J. A. Sellwood and J. J. Binney. Radial mixing in galactic discs. MNRAS, 336(3):785–796, November 2002, doi:10.1046/j.1365-8711.2002.05806.x, astro-ph/0203510.

[424] Heidi Jo Newberg, Brian Yanny, Connie Rockosi, Eva K. Grebel, Hans-Walter Rix, Jon Brinkmann, Istvan Csabai, Greg Hennessy, Robert B. Hindsley, Rodrigo Ibata, Zeljko Ivezić, Don Lamb, E. Thomas Nash, Michael Odenkirchen, Heather A. Rave, D. P. Schneider, J. Allyn Smith, Andrea Stolte, and Donald G. York. The Ghost of Sagittarius and Lumps in the Halo of the Milky Way. ApJ, 569(1):245–274, April 2002, doi:10.1086/338983, astro-ph/0111095.

[425] Eric Morganson, Blair Conn, Hans-Walter Rix, Eric F. Bell, William S. Burgett, Kenneth Chambers, Andrew Dolphin, Peter W. Draper, Heather Flewelling, Klaus Hodapp, Nick Kaiser, Eugene A. Magnier, Nicolas F. Martin, David Martinez-Delgado, Nigel Metcalfe, Edward F. Schlafly, Colin T. Slater, Richard J. Wainscoat, and Christopher Z. Waters. Mapping the Monoceros Ring in 3D with Pan-STARRS1. ApJ, 825(2):140, July 2016, doi:10.3847/0004-637X/825/2/140, 1604.07501.

[426] Adrian M Price-Whelan, Kathryn V Johnston, Allyson A Sheffield, Chervin FP Laporte, and Branimir Sesar. A reinterpretation of the triangulum–andromeda stellar clouds: a population of halo stars kicked out of the galactic disc. *Monthly Notices of the Royal Astronomical Society*, 452(1):676–685, 2015, doi:10.1093/mnras/stv1324.

[427] Lawrence M. Widrow, Susan Gardner, Brian Yanny, Scott Dodelson, and Hsin-Yu Chen. Galactoseismology: Discovery of Vertical Waves in the Galactic Disk. ApJ, 750(2):L41, May 2012, doi:10.1088/2041-8205/750/2/L41, 1203.6861.

[428] Brian Yanny and Susan Gardner. The Stellar Number Density Distribution in the Local Solar Neighborhood is North-South Asymmetric. ApJ, 777(2):91, November 2013, doi:10.1088/0004-637X/777/2/91, 1309.2300.

[429] M. E. K. Williams, M. Steinmetz, J. Binney, A. Siebert, H. Enke, B. Famaey, I. Minchev, R. S. de Jong, C. Boeche, K. C. Freeman, O. Bienaymé, J. Bland-Hawthorn, B. K. Gibson, G. F. Gilmore, E. K. Grebel, A. Helmi, G. Kordopatis, U. Munari, J. F. Navarro, Q. A. Parker, W. Reid, G. M. Seabroke, S. Sharma, A. Siviero, F. G. Watson, R. F. G. Wyse, and T. Zwitter. The wobbly Galaxy: kinematics north and south with RAVE red-clump giants. MNRAS, 436(1):101–121, November 2013, doi:10.1093/mnras/stt1522, 1302.2468.

[430] Morgan Bennett and Jo Bovy. Vertical waves in the solar neighbourhood in Gaia DR2. MNRAS, 482(1):1417–1425, January 2019, doi:10.1093/mnras/sty2813, 1809.03507.

[431] Deokkeun An. Asymmetric Mean Metallicity Distribution of the Milky Way's Disk. ApJ, 878(2):L31, June 2019, doi:10.3847/2041-8213/ab2467, 1906.01244.

[432] Weishuang Linda Xu and Lisa Randall. Testing ΛCDM with Dwarf Galaxy Morphology. ApJ, 900(1):69, September 2020, doi:10.3847/1538-4357/aba51f, 1904.08949.

[433] Facundo A Gómez, Ivan Minchev, Brian W O'Shea, Timothy C Beers, James S Bullock, and Chris W Purcell. Vertical density waves in the milky way disc induced by the sagittarius dwarf galaxy. *Monthly Notices of the Royal Astronomical Society*, 429(1):159–164, 2013, doi:10.1093/mnras/sts327.

[434] Zhao-Yu Li. Vertical Phase Mixing across the Galactic Disk. ApJ, 911(2):107, April 2021, doi:10.3847/1538-4357/abea17, 2011.11250.

[435] Facundo A Gómez, Ivan Minchev, Álvaro Villalobos, Brian W O'Shea, and Mary EK Williams. Signatures of minor mergers in milky way like disc kinematics: ringing revisited. *Monthly Notices of the Royal Astronomical Society*, 419(3):2163–2172, 2012, doi:10.1111/j.1365-2966.2011.19867.x.

[436] E. D'Onghia, P. Madau, C. Vera-Ciro, A. Quillen, and L. Hernquist. Excitation of Coupled Stellar Motions in the Galactic Disk by Orbiting Satellites. ApJ, 823(1):4, May 2016, doi:10.3847/0004-637X/823/1/4, 1511.01503.

[437] Roger Fux. Order and chaos in the local disc stellar kinematics induced by the galactic bar. *Astronomy & Astrophysics*, 373(2):511–535, 2001, doi:10.1051/0004-6361:20010561.

[438] James Binney and Ralph Schönrich. The origin of the Gaia phase-plane spiral. MNRAS, 481(2):1501–1506, December 2018, doi:10.1093/mnras/sty2378, 1807.09819.

[439] Morgan Bennett and Jo Bovy. Did Sgr cause the vertical waves in the solar neighbourhood? MNRAS, 503(1):376–393, May 2021, doi:10.1093/mnras/stab524, 2010.04165.

[440] Helmer Koppelman, Amina Helmi, and Jovan Veljanoski. One Large Blob and Many Streams Frosting the nearby Stellar Halo in Gaia DR2. ApJ, 860(1):L11, June 2018, doi:10.3847/2041-8213/aac882, 1804.11347.

[441] S. E. Koposov, V. Belokurov, T. S. Li, C. Mateu, D. Erkal, C. J. Grillmair, D. Hendel, A. M. Price-Whelan, C. F. P. Laporte, K. Hawkins, et al. Piercing the milky way: an all-sky view of the orphan stream. *Monthly Notices of the Royal Astronomical Society*, 485(4):4726–4742, 2019, doi:10.1093/mnras/stz457.

[442] Ting S. Li, Sergey E. Koposov, Denis Erkal, Alexander P. Ji, Nora Shipp, Andrew B. Pace, Tariq Hilmi, Kyler Kuehn, Geraint F. Lewis, Dougal Mackey, Jeffrey D. Simpson, Zhen Wan, Daniel B. Zucker, Joss Bland-Hawthorn, Lara R. Cullinane, Gary S. Da Costa, Alex Drlica-Wagner, Kohei Hattori, Sarah L. Martell, and Sanjib Sharma. Broken into Pieces: ATLAS and Aliqa Uma as One Single Stream. *arXiv e-prints*, page arXiv:2006.10763, June 2020, doi:10.3847/1538-4357/abeb18, 2006.10763.

[443] Khyati Malhan, Rodrigo A. Ibata, Raymond G. Carlberg, Michele Bellazzini, Benoit Famaey, and Nicolas F. Martin. Phase-space Correlation in Stellar Streams of the Milky Way Halo: The Clash of Kshir and GD-1. ApJ, 886(1):L7, November 2019, doi:10.3847/2041-8213/ab530e, 1911.00009.

[444] Heidi Jo Newberg, Benjamin A. Willett, Brian Yanny, and Yan Xu. The Orbit of the Orphan Stream. ApJ, 711(1):32–49, March 2010, doi:10.1088/0004-637X/711/1/32, 1001.0576.

[445] Amina Helmi. Streams, Substructures, and the Early History of the Milky Way. ARA&A, 58:205–256, August 2020, doi:10.1146/annurev-astro-032620-021917, 2002.04340.

[446] G. C. Myeong, E. Vasiliev, G. Iorio, N. W. Evans, and V. Belokurov. Evidence for two early accretion events that built the Milky Way stellar halo. MNRAS, 488(1):1235–1247, September 2019, doi:10.1093/mnras/stz1770, 1904.03185.

[447] N. Wyn Evans. The early merger that made the galaxy's stellar halo. 353:113–120, January 2020, doi:10.1017/S1743921319009700, 2002.05740.

[448] B. Ostdiek, L. Necib, T. Cohen, M. Freytsis, M. Lisanti, S. Garrison-Kimmmel, A. Wetzel, R. E. Sanderson, and P. F. Hopkins. Cataloging accreted stars within Gaia DR2 using deep learning. A&A, 636:A75, April 2020, doi:10.1051/0004-6361/201936866, 1907.06652.

[449] Lina Necib, Bryan Ostdiek, Mariangela Lisanti, Timothy Cohen, Marat Freytsis, and Shea Garrison-Kimmel. Chasing Accreted Structures within Gaia DR2 Using Deep Learning. ApJ, 903(1):25, November 2020, doi:10.3847/1538-4357/abb814, 1907.07681.

[450] Khyati Malhan and Rodrigo A. Ibata. STREAMFINDER - I. A new algorithm for detecting stellar streams. MNRAS, 477(3):4063–4076, July 2018, doi:10.1093/mnras/sty912, 1804.11338.

[451] Daniel B. Zucker, Jeffrey D. Simpson, Sarah L. Martell, Geraint F. Lewis, Andrew R. Casey, Yuan-Sen Ting, Jonathan Horner, Thomas Nordlander, Rosemary F. G. Wyse, Tomaž Zwitter, Joss Bland-Hawthorn, Sven Buder, Martin Asplund, Gayandhi M. De Silva, Valentina D'Orazi, Ken C. Freeman, Michael R. Hayden, Janez Kos, Jane Lin, Karin Lind, Katharine J. Schlesinger, Sanjib Sharma, and Dennis Stello. The GALAH Survey: No Chemical Evidence of an Extragalactic Origin for the Nyx Stream. ApJ, 912(2):L30, May 2021, doi:10.3847/2041-8213/abf7cd, 2104.08684.

[452] S. Sivertsson, H. Silverwood, J. I. Read, G. Bertone, and P. Steger. The local dark matter density from SDSS-SEGUE G-dwarfs. MNRAS, 478(2):1677–1693, August 2018, doi:10.1093/mnras/sty977, 1708.07836.

[453] Jacobus Cornelius Kapteyn. First attempt at a theory of the arrangement and motion of the sidereal system. *The Astrophysical Journal*, 55:302, 1922, doi:10.1086/142670.

[454] Jan H Oort et al. The force exerted by the stellar system in the direction perpendicular to the galactic plane and some related problems. *Bulletin of the Astronomical Institutes of the Netherlands*, 6:249, 1932.

[455] J. I. Read. The local dark matter density. *Journal of Physics G Nuclear Physics*, 41(6):063101, June 2014, doi:10.1088/0954-3899/41/6/063101, 1404.1938.

[456] J. N. Bahcall. Self-consistent determinations of the total amount of matter near the sun. ApJ, 276:169–181, January 1984, doi:10.1086/161601.

[457] Christopher F. McKee, Antonio Parravano, and David J. Hollenbach. Stars, Gas, and Dark Matter in the Solar Neighborhood. ApJ, 814(1):13, November 2015, doi:10.1088/0004-637X/814/1/13, 1509.05334.

[458] Nilanjan Banik, Lawrence M. Widrow, and Scott Dodelson. Galactoseismology and the local density of dark matter. MNRAS, 464(4):3775–3783, February 2017, doi:10.1093/mnras/stw2603, 1608.03338.

[459] N. Wyn Evans, Ciaran A. J. O'Hare, and Christopher McCabe. SHM^{++}: A Refinement of the Standard Halo Model for Dark Matter Searches in Light of the Gaia Sausage. *arXiv e-prints*, page arXiv:1810.11468, October 2018, doi:10.1103/PhysRevD.99.023012, 1810.11468.

[460] Pablo F. de Salas and Axel Widmark. Dark matter local density determination: recent observations and future prospects. *arXiv e-prints*, page arXiv:2012.11477, December 2020, 2012.11477.

[461] Adam J. Anderson, Patrick J. Fox, Yonatan Kahn, and Matthew McCullough. Halo-independent direct detection analyses without mass assumptions. J. Cosmology Astropart. Phys., 2015(10):012, October 2015, doi:10.1088/1475-7516/2015/10/012, 1504.03333.

[462] Mark Vogelsberger, Amina Helmi, Volker Springel, Simon D. M. White, Jie Wang, Carlos S. Frenk, Adrian Jenkins, Aaron Ludlow, and Julio F. Navarro. Phase-space structure in the local dark matter distribution and its signature in direct detection experiments. MNRAS, 395(2):797–811, May 2009, doi:10.1111/j.1365-2966.2009.14630.x, 0812.0362.

[463] F. S. Ling, E. Nezri, E. Athanassoula, and R. Teyssier. Dark matter direct detection signals inferred from a cosmological N-body simulation with baryons. J. Cosmology Astropart. Phys., 2010(2):012, February 2010, doi:10.1088/1475-7516/2010/02/012, 0909.2028.

[464] Michael Kuhlen, Neal Weiner, Jürg Diemand, Piero Madau, Ben Moore, Doug Potter, Joachim Stadel, and Marcel Zemp. Dark matter direct detection with non-Maxwellian velocity structure. J. Cosmology Astropart. Phys., 2010(2):030, February 2010, doi:10.1088/1475-7516/2010/02/030, 0912.2358.

[465] Yao-Yuan Mao, Louis E. Strigari, Risa H. Wechsler, Hao-Yi Wu, and Oliver Hahn. Halo-to-halo Similarity and Scatter in the Velocity Distribution of Dark Matter. ApJ, 764(1):35, February 2013, doi:10.1088/0004-637X/764/1/35, 1210.2721.

[466] Iryna Butsky, Andrea V. Macciò, Aaron A. Dutton, Liang Wang, Aura Obreja, Greg S. Stinson, Camilla Penzo, Xi Kang, Ben W. Keller, and James Wadsley. NIHAO project II: halo shape, phase-space density and velocity distribution of dark matter in galaxy formation simulations. MNRAS, 462(1):663–680, October 2016, doi:10.1093/mnras/stw1688, 1503.04814.

[467] Nassim Bozorgnia, Francesca Calore, Matthieu Schaller, Mark Lovell, Gianfranco Bertone, Carlos S. Frenk, Robert A. Crain, Julio F. Navarro, Joop Schaye, and Tom Theuns. Simulated Milky Way analogues: implications for dark matter direct searches. J. Cosmology Astropart. Phys., 2016(5):024, May 2016, doi:10.1088/1475-7516/2016/05/024, 1601.04707.

[468] Chris W. Purcell, Andrew R. Zentner, and Mei-Yu Wang. Dark matter direct search rates in simulations of the Milky Way and Sagittarius stream. J. Cosmology Astropart. Phys., 2012(8):027, August 2012, doi:10.1088/1475-7516/2012/08/027, 1203.6617.

[469] Bradley J. Kavanagh and Ciaran A. J. O'Hare. Reconstructing the three-dimensional local dark matter velocity distribution. Phys. Rev. D, 94(12):123009, December 2016, doi:10.1103/PhysRevD.94.123009, 1609.08630.

[470] Jonah Herzog-Arbeitman, Mariangela Lisanti, and Lina Necib. The metal-poor stellar halo in RAVE-TGAS and its implications for the velocity distribution of dark matter. J. Cosmology Astropart. Phys., 2018(4):052, April 2018, doi:10.1088/1475-7516/2018/04/052, 1708.03635.

[471] Nassim Bozorgnia, Azadeh Fattahi, David G. Cerdeño, Carlos S. Frenk, Facundo A. Gómez, Robert J. J. Grand, Federico Marinacci, and Rüdiger Pakmor. On the correlation between the local dark matter and stellar velocities. J. Cosmology Astropart. Phys., 2019(6):045, June 2019, doi:10.1088/1475-7516/2019/06/045, 1811.11763.

[472] Ciaran A. J. O'Hare, Christopher McCabe, N. Wyn Evans, GyuChul Myeong, and Vasily Belokurov. Dark matter hurricane: Measuring the S1 stream with dark matter detectors. Phys. Rev. D, 98(10):103006, November 2018, doi:10.1103/PhysRevD.98.103006, 1807.09004.

[473] Lina Necib, Mariangela Lisanti, and Vasily Belokurov. Inferred Evidence for Dark Matter Kinematic Substructure with SDSS-Gaia. ApJ, 874(1):3, March 2019, doi:10.3847/1538-4357/ab095b, 1807.02519.

[474] Lina Necib, Mariangela Lisanti, Shea Garrison-Kimmel, Andrew Wetzel, Robyn Sanderson, Philip F. Hopkins, Claude-André Faucher-Giguère, and Dušan Kereš. Under the FIRElight: Stellar Tracers of the Local Dark Matter Velocity Distribution in the Milky Way. ApJ, 883(1):27, September 2019, doi:10.3847/1538-4357/ab3afc, 1810.12301.

[475] Ciaran A. J. O'Hare, N. Wyn Evans, Christopher McCabe, GyuChul Myeong, and Vasily Belokurov. Velocity substructure from Gaia and direct searches for dark matter. Phys. Rev. D, 101(2):023006, January 2020, doi:10.1103/PhysRevD.101.023006, 1909.04684.

[476] GC Myeong, NW Evans, V Belokurov, JL Sanders, and SE Koposov. The sausage globular clusters. *The Astrophysical Journal Letters*, 863(2):L28, 2018, doi:10.3847/2041-8213/aad7f7.

[477] Nassim Bozorgnia, Azadeh Fattahi, Carlos S. Frenk, Andrew Cheek, David G. Cerdeño, Facundo A. Gómez, Robert J. J. Grand, and Federico Marinacci. The dark matter component of the Gaia radially anisotropic substructure. J. Cosmology Astropart. Phys., 2020(7):036, July 2020, doi:10.1088/1475-7516/2020/07/036, 1910.07536.

[478] Thomas M. Callingham, Marius Cautun, Alis J. Deason, Carlos S. Frenk, Robert J. J. Grand, Federico Marinacci, and Ruediger Pakmor. The orbital phase space of contracted dark matter haloes. MNRAS, 495(1):12–28, June 2020, doi:10.1093/mnras/staa1089, 2001.07742.

[479] Alejandro Ibarra, Bradley J. Kavanagh, and Andreas Rappelt. Impact of substructure on local dark matter searches. J. Cosmology Astropart. Phys., 2019(12):013, December 2019, doi:10.1088/1475-7516/2019/12/013, 1908.00747.